MEASUREMENT OF THERMAL CONDUCTIVITY OF PAN BASED CARBON FIBER

A THESIS

Presented to

The Faculty of the Division of Graduate Studies

By

William Marshall Moses, Jr.

In Partial Fulfillment

of the Requirements for the Degree

Master of Science in Mechanical Engineering

Georgia Institute of Technology

March, 1978

MEASUREMENT OF THERMAL CONDUCTIVITY

OF PAN BASED CARBON FIBER

Approved:

W. Z. Black, Chairman

P. V. Kadaba

D. S. Brookstein

Date approved by Chairman: 4/20/78

ACKNOWLEDGMENTS

The author would like to express his sincere appreciation to the following people and organizations for their assistance in the completion of this thesis:

-- the Hercules Chemical Company and the United States Air Force Materials Laboratory, for their financial support of this research;

-- Dr. P. V. Kadaba and Dr. D. S. Brookstein, for their conscientious service as members of the thesis reading committee;

-- Dr. W. Z. Black, for the sound advice and guidance which made this thesis possible;

-- my parents, for their continued interest and encouragement in my academic endeavors;

-- Sherie, for her continued support, patience, and understanding throughout the preparation of this thesis.

TABLE OF CONTENTS

TABLE OF CONTENTS (Continuation)

LIST OF TABLES

LIST OF ILLUSTRATIONS

LIST OF ILLUSTRATIONS (Continued)

SUMMARY

The objective of this thesis was to measure the axial thermal conductivity of individual polyacrylonitrile (PAN) based carbon fibers. To achieve this objective the thesis was sub-divided into three areas with the following goals:

1. Devise a test procedure which could be used to determine the value of carbon fiber thermal conductivity.
2. Design and construct the appropriate testing device and supporting equipment.
3. Verify the accuracy, repeatability, and suitability of the completed device for the measurement of the thermal conductivity of carbon fibers.

The test method selected employed the use of a guarded hot plate device to measure the mean thermal conductivity of a carbon fiber/epoxy resin composite specimen as a function of the volume fraction of carbon fiber. The thermal conductivity of the pure carbon fiber was then determined by the rule of mixtures.

The test procedure provided results for the thermal conductivity of the carbon fibers which were in good agreement with published results for carbon fibers with a comparable modulus of elasticity.

The accuracy of the guarded hot plate device was predicted by a theoretical error analysis and by a comparison of experimental data from the guarded hot plate device and other sources for the same test material. These results have shown that the accuracy of the device was within 10.9

percent for the measurements completed in this thesis. Repeatability tests have shown that the results for materials with low thermal conductivity were repeatable to within 4.0 percent.

CHAPTER I

INTRODUCTION AND BACKGROUND OF CARBON FIBER THERMAL CONDUCTIVITY MEASUREMENT

1.1. Introduction

Carbon fiber composites have been used since the late 1950's as reinforcing agents in a variety of systems. In this capacity strength and elasticity were the properties of primary importance. Typical uses of carbon fiber composites at this stage of development include the development of lightweight aircraft structural elements, reinforcement in rocket nozzle throats, and various types of sporting equipment [1].*

Because of the need for greater elongation and a balance of tension and elongation in the composite matrix, the development of production processes eventually led to fabrication by the pyrolysis of polyacrylonitrile (PAN) in 1969. The uniformity of property performance and balance of strength and modulus of this fiber have made it widely accepted in the aerospace field [1].

The United States Air Force Materials Laboratory is supporting a study to determine the thermal conductivity of carbon fibers for use on re-entry nose cones. For this application, it is desired to have a low thermal conductivity fiber for superior ablative performance. As a result of the experimental nature of this problem, only small amounts of carbon fiber are available for evaluation of the thermal conductivity of the fibers.

*References are listed following the appendices.

Macroscopically, the thermal conductivity has been defined by the Fourier law, the basic law of heat conduction, which may be expressed as [2,3]

$$q = - k \frac{\partial T}{\partial \eta} \qquad (1)$$

where q = rate at which heat crosses from the inside to the outside of an isothermal surface per unit area per unit time

k = thermal conductivity

T = temperature

$\frac{\partial}{\partial \eta}$ = differentiation along the outward drawn normal to the surface.

In general, the thermal conductivity, k, can be assumed to be a linear function of the temperature, such that,

$$k = k_o(1 + \beta T) \qquad (2)$$

where β is small, and in fact, negative for most non-metallic substances [4]. If β is assumed to be zero, then the thermal conductivity of a material is independent of temperature.

For the case of steady state, one-dimensional heat conduction with no internal heat generation and with the thermal conductivity independent of temperature, Equation (1) reduces to

$$q = \frac{kA\Delta T}{L} \qquad (3)$$

where q = time rate of heat flow

A = cross-sectional area perpendicular to the direction of heat flow

L = distance between two isothermal planes

k = thermal conductivity

ΔT = temperature difference between isothermal planes across thickness, L ($\Delta T = T_h - T_c$)

T_h = temperature of the hot surface

T_c = temperature of the cold surface

Kreith [5] has shown that, if the thermal conductivity varies linearly with the temperature, the k term in Equation (3) represents a mean value of thermal conductivity over the temperature range involved. Thus, for the thermal conductivity as a linear function of temperature:

$$k(\bar{T}) = \frac{qL}{(T_h - T_c)A} \tag{4}$$

where

$$\bar{T} = \frac{T_h + T_c}{2} .$$

Equation (4) forms the basis for the experimental determination of thermal conductivity.

1.2. Kohlrausch Method

There are several measurement techniques available for determining the thermal conductivity of textile fibers. I. L. Kalnin [6] has utilized the techniques developed by Kohlrausch. A diagram of the test assembly is shown in Figure 1. Following this procedure, a long, straight test specimen is heated by an electrical current until a steady state condition is reached with heat flowing axially from the center of the

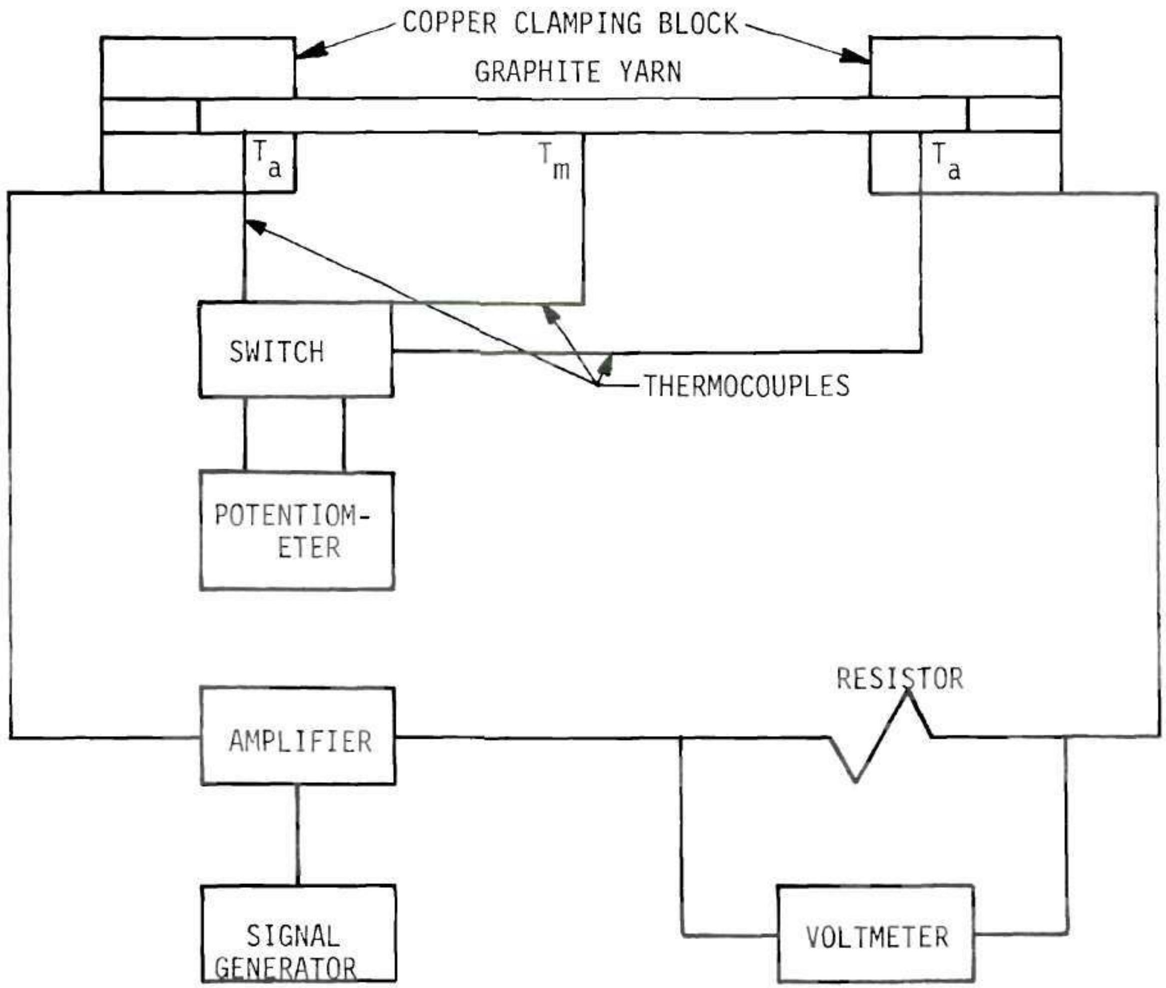

Figure 1. Experimental Arrangement for Kohlrausch Method [6].

test specimen, at temperature T_m, to the ends of the sample, which are maintained at a temperature T_a. Knowing the potential drop across the specimen and the electrical resistivity, the thermal conductivity may be calculated from [6]:

$$k = \frac{\Delta e^2}{8R_e(T_m - T_a)} \tag{5}$$

where

k = thermal conductivity

Δe = potential drop across the specimen

R_e = electrical resistivity

T_m = temperature at center of test specimen

T_a = temperature at ends of test specimen

Equation (5) is exact only for very long thin test specimens having a temperature-independent electrical resistivity and negligible lateral heat loss. Thus, for carbon fiber bundles, Kalnin [6] has determined that, if the temperature difference, $\Delta T = T_m - T_a$, is not large, the geometrical and electrical resistivity constraints may be essentially fulfilled. Experimental measurements of the electrical resistance of two typical graphite fibers has shown that the resistivity of these fibers varies from 2.5 to 11 percent over a temperature difference of 75 C. Consequently, for accurate determination of thermal conductivity or large values of ΔT, a resistivity correction would have to be applied.

The condition of no lateral heat losses can not be achieved because of the extremely large fiber surface to volume ratio and the high emissivity of graphite contributing to radiative heat losses that might greatly exceed the conductive heat flux rate along the fiber bundle [6]. Additionally, the Kohlrausch method for measuring thermal conductivity is an indirect method because the electrical resistivity and the surface emissivity must be known prior to making the thermal conductivity calculations. Further, this technique is not useful for low resistance fibers.

1.3. Schroeder Method

Kalnin [6] has also attempted to measure thermal conductivity of carbon fibers by way of the Colora or Schroeder method. The Colora method uses pairs of liquids which have boiling points separated by 10 - 20 C. The fluid with the higher boiling point is used to heat one surface of the sample while the second fluid is placed in contact with the other end of the specimen. The quantity of heat passing through the specimen is determined by measuring the time required to condense a fixed volume of the liquid with the lower boiling point.

Figure 2 shows the principles of the Colora method. Fluid A is caused to boil and the vapor is directed to a high thermal conductivity plate, s_1, causing the temperature of this plate to be maintained at the boiling point of liquid A. Fluid B, with a boiling point below that of fluid A, is contained in the upper chamber. The base of the upper chamber is a high conductivity plate, s_2 [7].

The test sample is fitted between s_1 and s_2. Heat flowing through

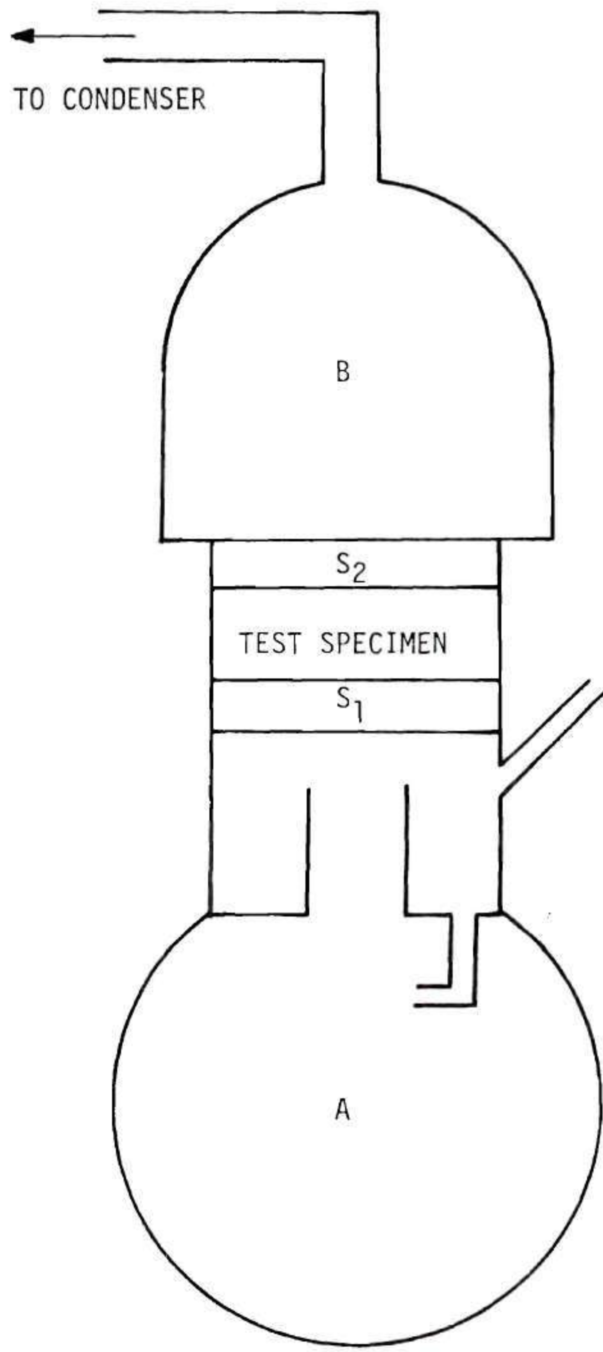

Figure 2. Basic Apparatus for Colora Test Method [7].

the sample from s_1 to s_2 causes liquid B to boil. The boiling liquid at either end of the test specimen creates a constant temperature difference across the sample. The vapor from liquid B is condensed, and the time required to collect a specified amount of condensate is recorded. The thermal conductivity of the test specimen is given by [7]

$$k = [Q/t(T_H - T_C)]\ L/A \qquad (6)$$

where

- Q = heat of vaporization for a volume of liquid B
- t = time to distill a given volume of liquid B
- T_H = boiling point of liquid A
- T_C = boiling point of liquid B
- L = length of test specimen
- A = cross-sectional area of test specimen
- k = thermal conductivity

Kalnin has established that the large contribution of radiative heat losses from the perimeter of the heated fiber bundle, even near room temperature, interferes with the direct determination of the thermal conductivity by the Colora method. An attempt to correct for radiative losses is complex because the radiative heat transfer from the sample is a function of a number of factors. Among these factors are: fiber emissivity which depends on surface composition and morphology; the emissivity of the surrounding medium; the effective radiating bundle perimeter which changes with the shape and size of the mounted test yarn, and the geometry of the test fixture into which the fiber bundle radiates [6].

This correction factor would introduce as much uncertainty into the Colora method as is present in the Kohlrausch method and would also raise doubts as to its applicability for the direct determination of carbon fiber thermal conductivity.

1.4. Flash Diffusivity Method

The flash diffusivity method is a technique by which the front surface of a homogeneous sample is subjected to a short radiant energy pulse and the resulting temperature history of the rear surface is recorded. From this temperature history the thermal diffusivity of the material may be determined. This technique has been used to measure the thermal diffusivity of metals, alloys, ceramics, semiconductors, liquid metals, rock, composites, and amoeba [8].

Once the thermal diffusivity of the material has been established, it is still necessary to obtain measurements of specific heat and density before the thermal conductivity may be determined from the relation:

$$k = \alpha\rho c \tag{7}$$

where

α = thermal diffusivity,

ρ = volumetric density,

c = specific heat.

Lee and Taylor [8] have used the flash diffusivity technique to measure the thermal conductivity of carbon/graphite fibers. Results of these measurements have revealed errors of up to 40 percent in the thermal conductivity of Morganite II carbon fiber -- attributed partially to difficulties in sample fabrication [8]. Thus, while the flash technique is an accurate and well-accepted technique for measuring thermal diffusivity, difficulties in sample preparation and other property measurements render the method unsuitable for the indirect determination of thermal conductivity of carbon fibers.

1.5. Guarded Hot Plate Method

1.5.1. Guarded Hot Plate

In addition to the test methods described above, the guarded hot plate method may also be used to measure thermal conductivity. This method is based on a device which transfers a measurable amount of heat through a specimen while imposing a known temperature difference across the test specimen of known thickness. The guarded hot plate method is specially designed for materials of low thermal conductivity.

The apparatus uses two identical specimens and is constructed symmetrically about the hot-side (central) heater of known surface area. The symmetry of the device is required to insure the equal and uniform flow of heat through the apparatus. The central heater is sandwiched between the two test specimens and an additional cold-side heater plate is placed against the exposed surface of each sample. Each cold-side heater plate is maintained at a constant temperature by a separate automatically controlled power supply and heat is removed by a circulating fluid bath. A regulated power supply is used to provide power to the central heater. An annular guard heater, separated from the central heater by a narrow air gap, encloses the central heater to eliminate radial heat losses by preventing a temperature drop across the air gap. This reduces the problem to one of one-dimensional heat flow. The basic components of the guarded hot plate device are shown in Figure 3.

In terms of the measured quantities the thermal conductivity of the test specimen is:

$$k = \frac{\frac{1}{2} ViL}{A(T_H - T_C)} \tag{8}$$

where

- k = specimen thermal conductivity
- V = voltage drop across central heater
- i = current through central heater
- A = metered area of central heater
- L = thickness of test specimen
- T_H = temperature of specimen surface adjacent to central heater
- T_C = temperature of specimen surface adjacent to cold-side heater

K. W. Jackson [9] designed and utilized a guarded hot plate device for the measurement of the thermal conductivity of thermoplastic materials. This particular device is in compliance with the ASTM C-177

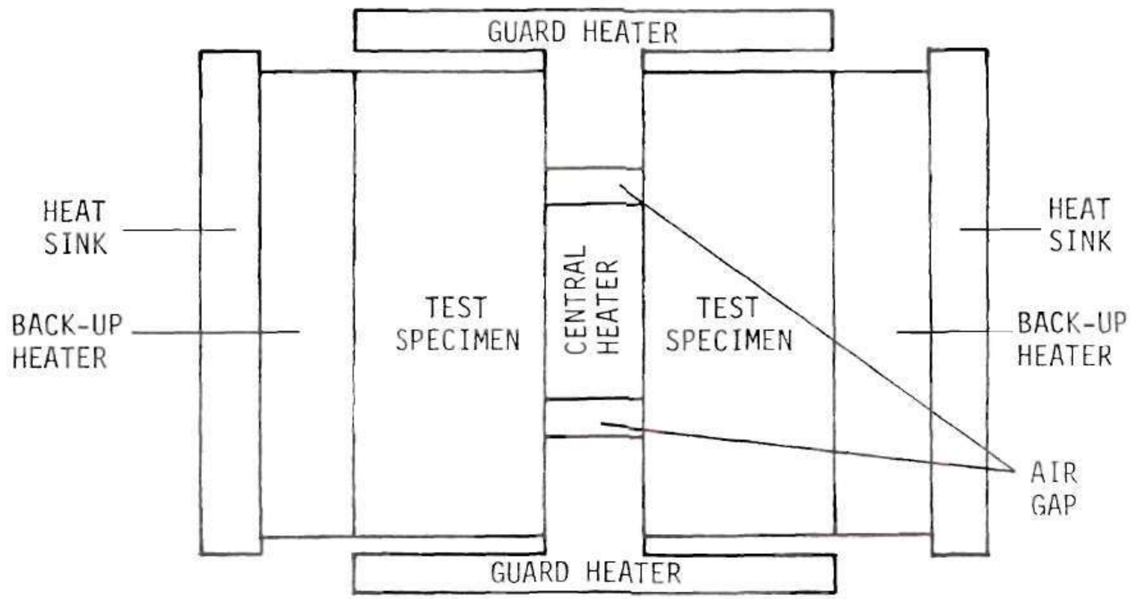

Figure 3. Major Components of the Guarded Hot Plate Device.

"Standard Test Method for Thermal Conductivity of Materials by Means of the Guarded Hot Plate" [10]. The results obtained by Jackson in these tests have indicated that measurements by this device on polytetraflouroethylene (Teflon*) specimens are within 20 percent of other experimentally derived data and are repeatable to within 0.5 percent.

Due to the simplicity, accuracy, and directness of the method, the thermal conductivity of the fibers analyzed in this thesis was measured by use of a guarded hot plate apparatus. Because of the limited amounts of carbon fibers that could be supplied for use in sample preparation, it was impractical to use the large guarded hot plate device designed by Jackson [9]. Therefore, a second, smaller device was designed and built to accommodate the smaller test specimens which were supplied by the fiber manufacturer. The particular device used was patterned after the device developed by Jackson [9]. Since the design of the smaller device was similar to that previously carried out by Jackson [9], the success and accuracy of the test method was reasonably well assured.

1.5.2. Carbon Fiber Test Specimens

There are two types of test specimens available to use with the guarded hot plate test method -- either a pure fiber specimen or a composite specimen in which the fibers are aligned in a base matrix. The primary advantage of the pure fiber specimen is that measurement of such a specimen yields direct results for the thermal conductivity. Such a specimen, however, would lead to significant difficult in specimen preparation.

*Teflon is a registered trademark of the E.I. Du Pont de Nemours and Company.

Firstly, the specimen must be fabricated so that it is void of air, since the thermal conductivity of air is much less than the thermal conductivity of the carbon fibers. Otherwise, the air-fiber composite system would yield an apparent thermal conductivity which is lower than the conductivity of the actual fibers. Secondly, carbon fibers are anisotropic, with the transverse thermal conductivity of the fiber being much lower than the axial conductivity. Consequently, the fiber bundle must be kept in relatively perfect alignment in order to prevent the introduction of a large thermal resistance at each end of the specimen.

Composite specimens present neither of the major difficulties encountered in the pure fiber specimens. Specimen fabrication techniques [Section 4.1] have been developed which maintain the fiber alignment and remove air voids from the test specimen by imbedding the carbon fibers in an epoxy resin base material.

Further, Springer and Tsai [11], by way of a shear stress analogy, and Behrens [12], by way of an analogy with the diffusion equation, have shown that the axial thermal conductivity of a fiber may be determined from the thermal conductivity of a unidirectionally reinforced bulk composite by means of a rule of mixture, such that

$$k_m = k_g v_f + k_e(1 - v_f) \tag{9}$$

where

k_m = thermal conductivity of the composite material

k_g = thermal conductivity of the carbon fiber

k_e = thermal conductivity of the base material

v_f = volume fraction of carbon fiber

Finally, composite test specimens require a great deal less carbon fiber than the pure specimen. Since the basic test methods are to be applied to experimental fibers, the amount of material available for the fabrication of test specimens is very limited. Consequently, in light of all of the factors present, composite test specimens have shown the best test specimen qualities available.

CHAPTER II

ANALYSIS OF THERMAL CONDUCTIVITY IN COMPOSITE ARRAYS

Before proceeding directly with the rule of mixtures [Equation (9)], it was decided to develop independently an expression relating the mean thermal conductivity of the test specimen with the geometry of the specimen and the thermal conductivity of the component parts. A literature survey revealed several mathematical solutions for the problem of spherical inclusions in a cubic array [13, 14, 15].

The complexity of these solutions made it desirable to approach the problem of cylinders in a cubic array (which represented the geometry of the test specimen) from the standpoint of an approximate solution. For this purpose the electrical-thermal resistance analog was chosen. This analog model was developed by comparing solutions for a sphere and a cube in a cubic matrix with the mathematical solutions available for spheres in a cubic array. Once the similarity of the analog procedure was developed for the case of spherical inclusions, the analog relationship for cylinders in a cubic matrix was determined.

2.1. Exact Analysis -- Spherical Inclusions

Several references appear in the literature concerning composite materials wherein one material is included within another. The principal focus of these results lies in the area of uniform spherical inclusions in a cubic matrix (see geometry insert in Figure 3), an idea advanced by Lord Rayleigh [13]. Rayleigh's development, which is mathematical in nature, accounts for interaction of the particles within the matrix, or "when the dimensions of the obstacles are no longer very small in comparison with the distances between them" [13]. Rayleigh's results, with corrections introduced by I. Runge are given in reference [14] as:

$$K_m = \frac{\left[\frac{2 + K_g}{1 - K_g} - 2\, v_f - (0.525\, v_f^{10/3}) \frac{3 - 3\, K_g}{4 + 3\, K_g}\right]}{\left[\frac{2 + K_g}{1 - K_g} + v_f - (0.525\, v_f^{10/3}) \frac{3 - 3\, K_g}{4 + 3\, K_g}\right]} \tag{10}$$

where

v_f = volume fraction of the included material

k_m = effective thermal conductivity of the composite material

k_g = conductivity of the included material (carbon fibers)

k_e = conductivity of the base material surrounding the included material (epoxy resin)

$$K_m = k_m/k_e$$

$$K_g = k_g/k_e$$

J. C. Maxwell [15] also developed a similar relationship for the same geometry, but with no interaction among inclusions, that is, for dilute dispersions of included material. Maxwell's result is [14]

$$K_m = \frac{K_g + 2 - 2\, v_f\, (1 - K_g)}{K_g + 2 + v_f\, (1 - K_g)} \quad . \tag{11}$$

It may be observed at this point, that Equation (11) is the limiting case of Equation (10) as the volume fraction, v_f, approaches zero.

A further definitive work for spheres arranged in a cubic matrix has been carried out by Meredith and Tobias [14]. This work, which is essentially based on Rayleigh's solution, examines the case where the volume fraction approaches $\pi/6$ (the point where the spheres come into point contact). These authors have utilized a modified derivation of Rayleigh's equation and obtained the result:

$$K_m = \frac{\left[\dfrac{2 + K_g}{1 - K_g} - 2v_f + 0.409v_f^{7/3}\left(\dfrac{6 + 3K_g}{4 + 3K_g}\right) - 2.133v_f^{10/3}\left(\dfrac{3 - 3K_g}{4 + 3K_g}\right)\right]}{\left[\dfrac{2 + K_g}{1 - K_g} + v_f + 0.409v_f^{7/3}\left(\dfrac{6 + 3K_g}{4 + 3K_g}\right) - 0.906v_f^{10/3}\left(\dfrac{3 - 3K_g}{4 + 3K_g}\right)\right]} \qquad (12)$$

Further experimental work conducted by Meredith and Tobias indicates that Equation (12) more nearly predicts the actual behavior of the system geometry than either the Maxwell or Rayleigh solutions [14].

Other authors, for example Garrett and Rosenburg [16], Kingery [17], Gorring and Churchill [18], Godbee and Ziegler [19], Schumann and Voss [20], and Fricke [21], have used a similar analysis to obtain thoeretical results for a variety of composite structures; ranging from powders [16,19], to granulated materials [20], to other generally spherical distributions of material [16, 17, 18, 21]. From the literature, it appears that equations of the Rayleigh-Maxwell type, which represent the thermal conductivity of the composite material as a function of the conductivities of each phase, the geometry of the included phase, and the volume fraction of the included phase, give results which correspond relatively well with experimental findings.

Figures 4 and 5 compare Equations (10), (11) and (12). In Figure 4 both Equations (10) and (12) predict results which are higher than Equation (11) due to the inclusion of terms involving the interaction among particles in the matrix. Equation (12), which is an expanded form of Equation (10), contains more of these interaction terms and predicts the greatest values of thermal conductivity for the case in Figure 4.

Figure 5 shows the reverse trend of Figure 4, with Equation (11) predicting higher values than either Equation (10) or (12). Here again, this is due to the exclusion of the particle interaction terms in Equation (11), which cause a more conservative prediction of the thermal conductivity by Equation (9) as opposed to the values predicted by Equation (10) or Equation (12).

2.2. Analog Analysis of Inclusions in a Cubic Array

2.2.1. Analog Analysis

Resistance analog models have been developed for comparison with the analytical models developed earlier. These models are based on the analogy which exists between thermal and electrical resistance.

Ohm's law may be represented by the expression

$$i = \frac{\Delta e}{R_e} \tag{13}$$

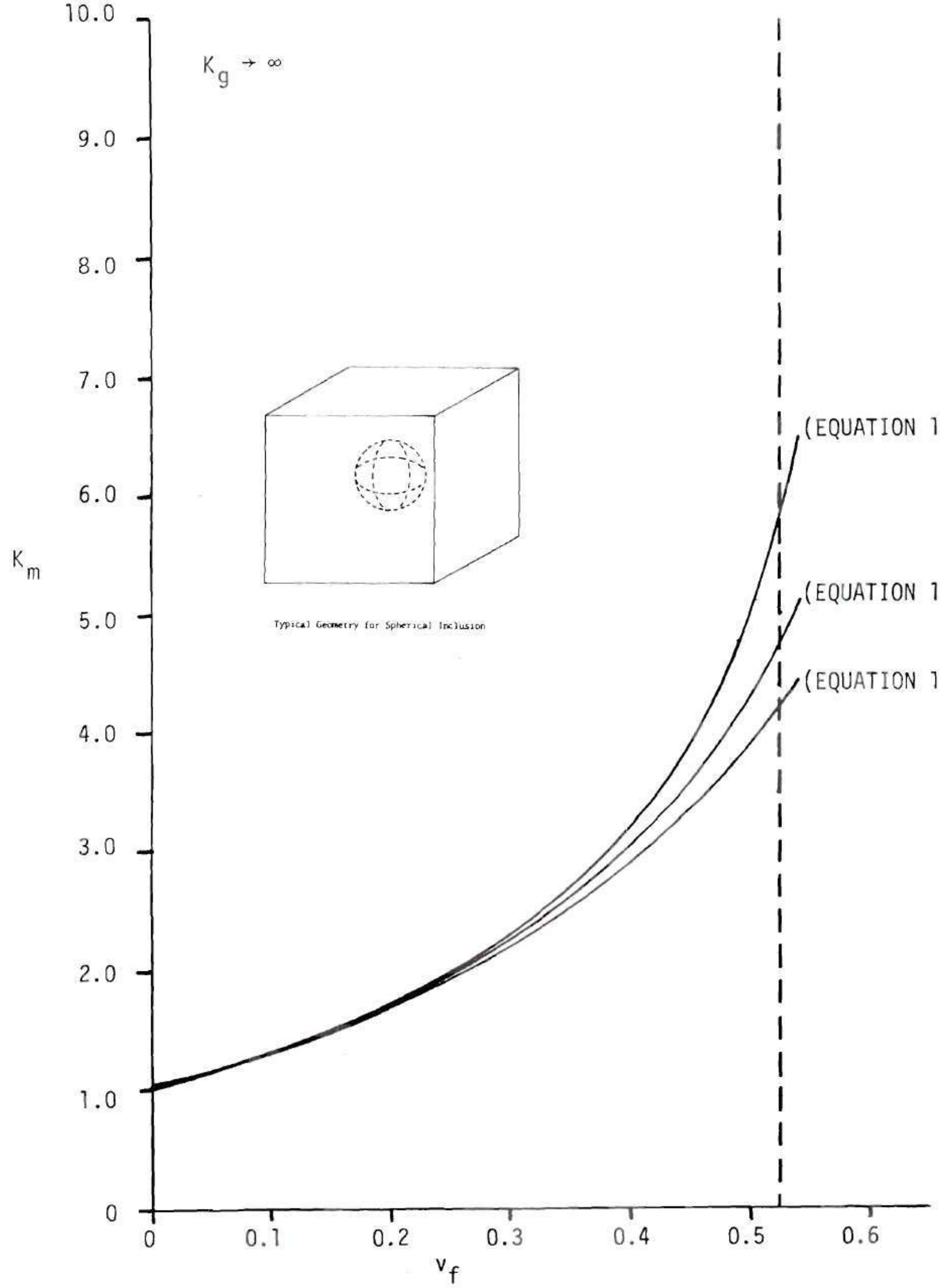

Figure 4. Spheres in a Cubic Array -- Exact Analysis ($K_g \to \infty$).

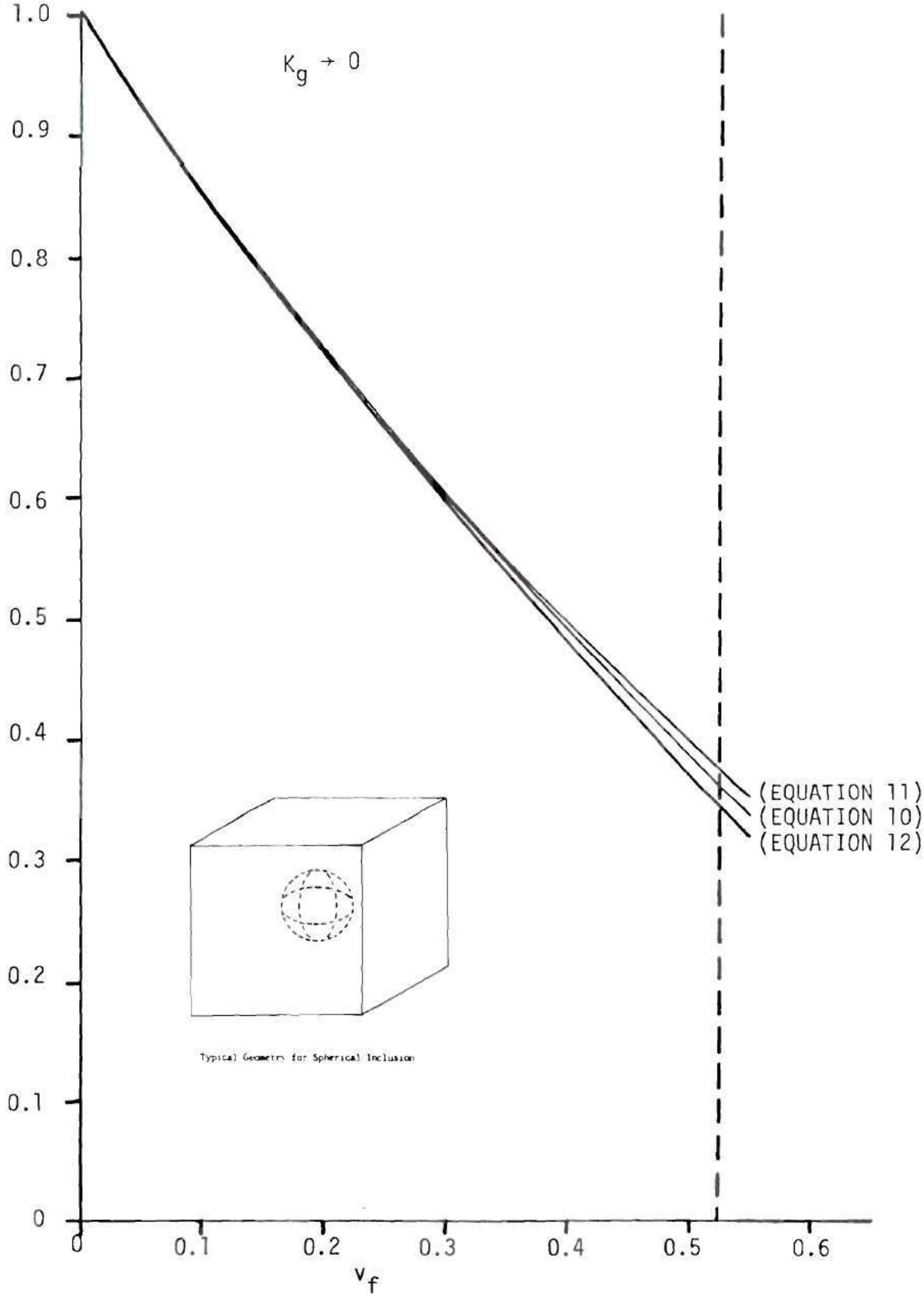

Figure 5. Spheres in a Cubic Array -- Exact Analysis ($K_g \to 0$).

where

Δe = electrical potential difference,

i = current,

R_e = electrical resistance.

Further, the electrical current, i, may be expressed as [4]

$$i = \frac{k_i \; A\Delta e}{\ell} \tag{14}$$

where k_i is the electrical conductivity for a conductor of area A and length ℓ.

Therefore the electrical resistance is of the form

$$R_e = \ell/k_i A \; . \tag{15}$$

From the Fourier law for heat conduction [Equation (3)],

$$q = \frac{kA\Delta T}{L} \; . \tag{3}$$

If the thermal resistance is defined by

$$R = L/kA \tag{16}$$

then Equation (7) may be written as:

$$q = \frac{\Delta T}{R} \; . \tag{17}$$

Comparison of Equations (13) and (17) shows the analogy which exists between thermal and electrical systems. The left hand side of each equation represents energy per unit time, while the right hand side of the equation represents a potential difference divided by an appropriately defined resistance.

By way of this analogy, thermal resistances may be manipulated in the same manner as electrical resistances, that is, for n bodies connected in series,

$$R_{1n} = R_1 + R_2 + R_3 + \cdots + R_{n-1} + R_n \tag{18}$$

and, for n bodies connected in parallel,

$$R_{1n} = \frac{1}{\left(\frac{1}{R_1}\right) + \left(\frac{1}{R_2}\right) + \cdots + \left(\frac{1}{R_n}\right)} \tag{19}$$

2.2.2. Analog Methods

The parallel-series method of analysis is one of two methods by which the thermal-electrical resistance model may be analyzed. This approach consists of evaluating regularly ordered inclusions in a matrix by means of a number of parallel circuits joined in series. The series-parallel method of analysis consists of the evaluation of a number of series circuits joined in parallel.

For example, consider the two-dimensional case of square inclusions in a square array, shown in Figure 6, and an element of this system, shown in Figure 7. The parallel-series circuit for this system is shown in Figure 8, and has a total resistance given by [22]

$$R_{PS} = \left[\frac{\frac{1}{K_g} + \left(1 - \frac{1}{K_g}\right)\left(\frac{d}{x} - \frac{d^2}{x^2}\right)}{\frac{1}{K_g} + \left(1 - \frac{1}{K_g}\right)\frac{d}{x}}\right] \tag{20}$$

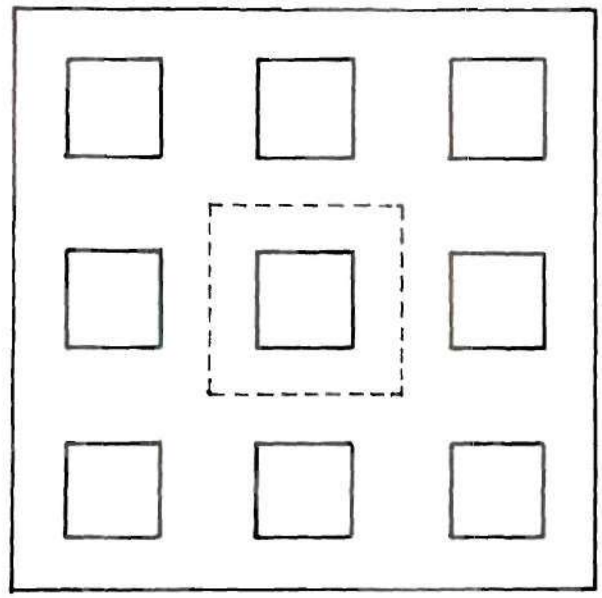

Figure 6. Two-Dimensional Composite Matrix.

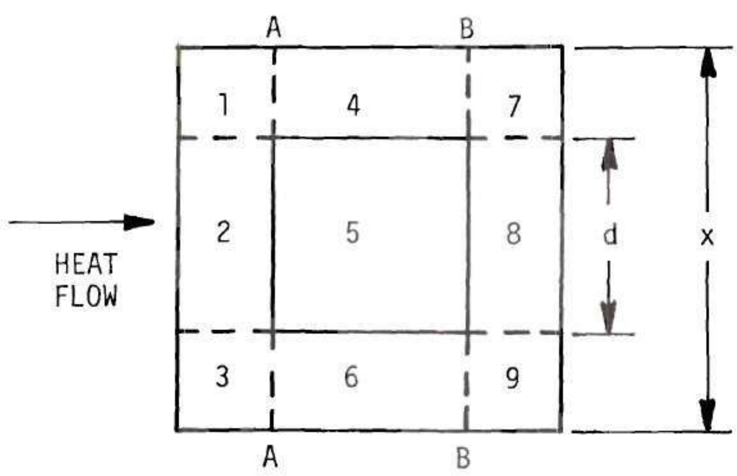

Figure 7. Typical Element of Composite Matrix.

and the total resistance of the series-parallel circuit of Figure 9 is

$$R_{SP} = \left[\frac{1 - \left(1 - \frac{1}{K_g}\right)\frac{d}{x}}{1 - \left(1 - \frac{1}{K_g}\right)\left(\frac{d}{x} - \frac{d^2}{x^2}\right)}\right] \qquad (21)$$

In general, $R_{PS} \neq R_{SP}$, and, in fact, for non-trivial cases $R_{SP} > R_{PS}$ [22], as shown in Figures 10 and 11.

A further requirement of the parallel-series solution is that the potential along the planes AA and BB in Figure 7 be uniform. The series-parallel circuit, on the other hand, is not restricted by this requirement; it requires only a uniform potential along each outer surface. Since the guarded hot plate apparatus imposes a uniform temperature distribution only along the surfaces of the sample, while the internal temperature distribution remains essentially unknown, the series-parallel approach seems to be more applicable to the nature of the problem of measuring thermal conductivity of composite media. Consequently, it will be the one used in this study.

2.2.3. Spherical Inclusions

Utilizing the analog approach, Duga modeled the problem of a sphere with radius b in a cubic matrix with a side of length a by the parallel-series method. This analog method of approach also follows the Maxwell assumption of no interaction among neighboring cells. The general result, which corresponds to Equation (10), (11) and (12) of section 2.1, obtained under these conditions for the arrangement in Figure 12 is [22]:

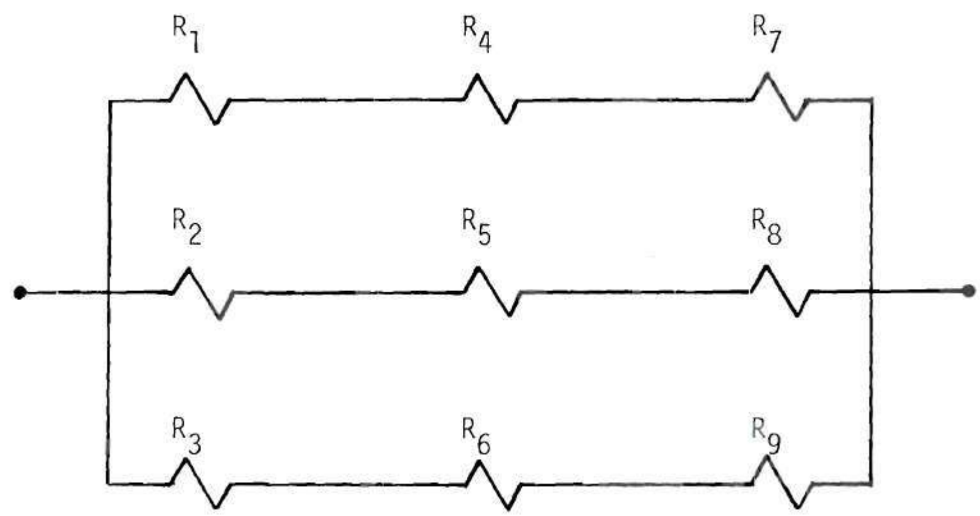

Figure 8. Parallel-Series Circuit.

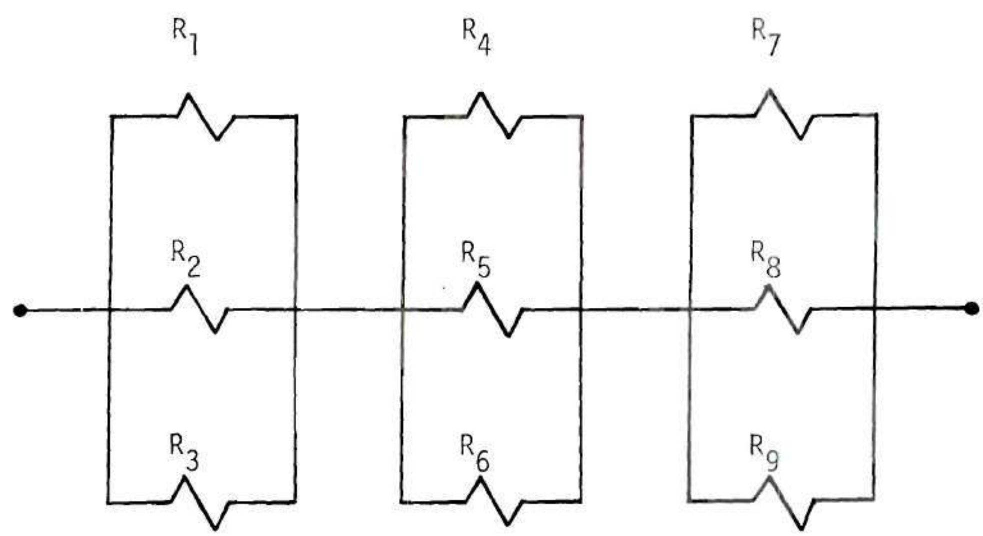

Figure 9. Series-Parallel Circuit.

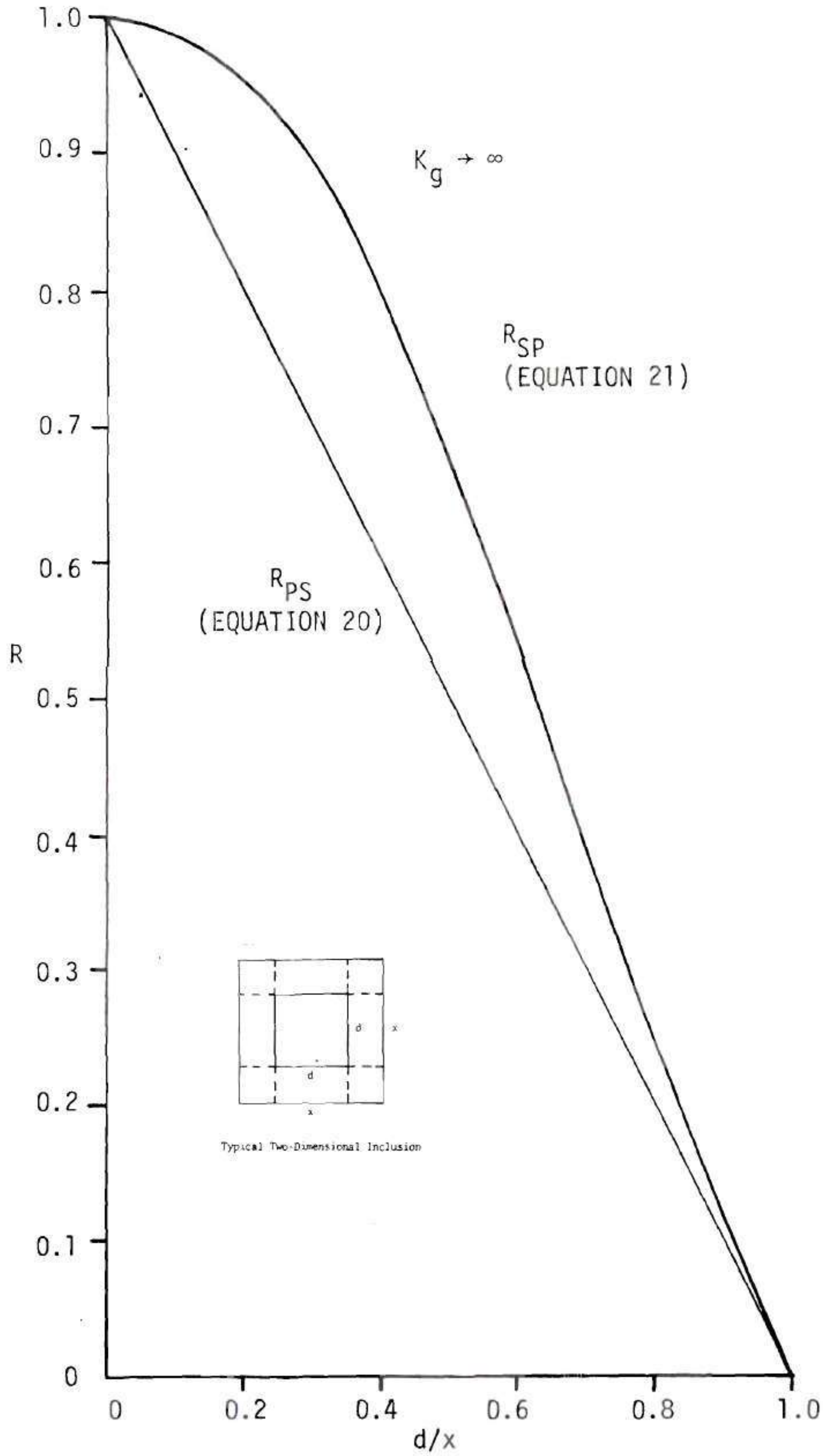

Figure 10. Comparison of R_{SP} and R_{PS} for Equations (20) and (21) with $K_g \rightarrow \infty$.

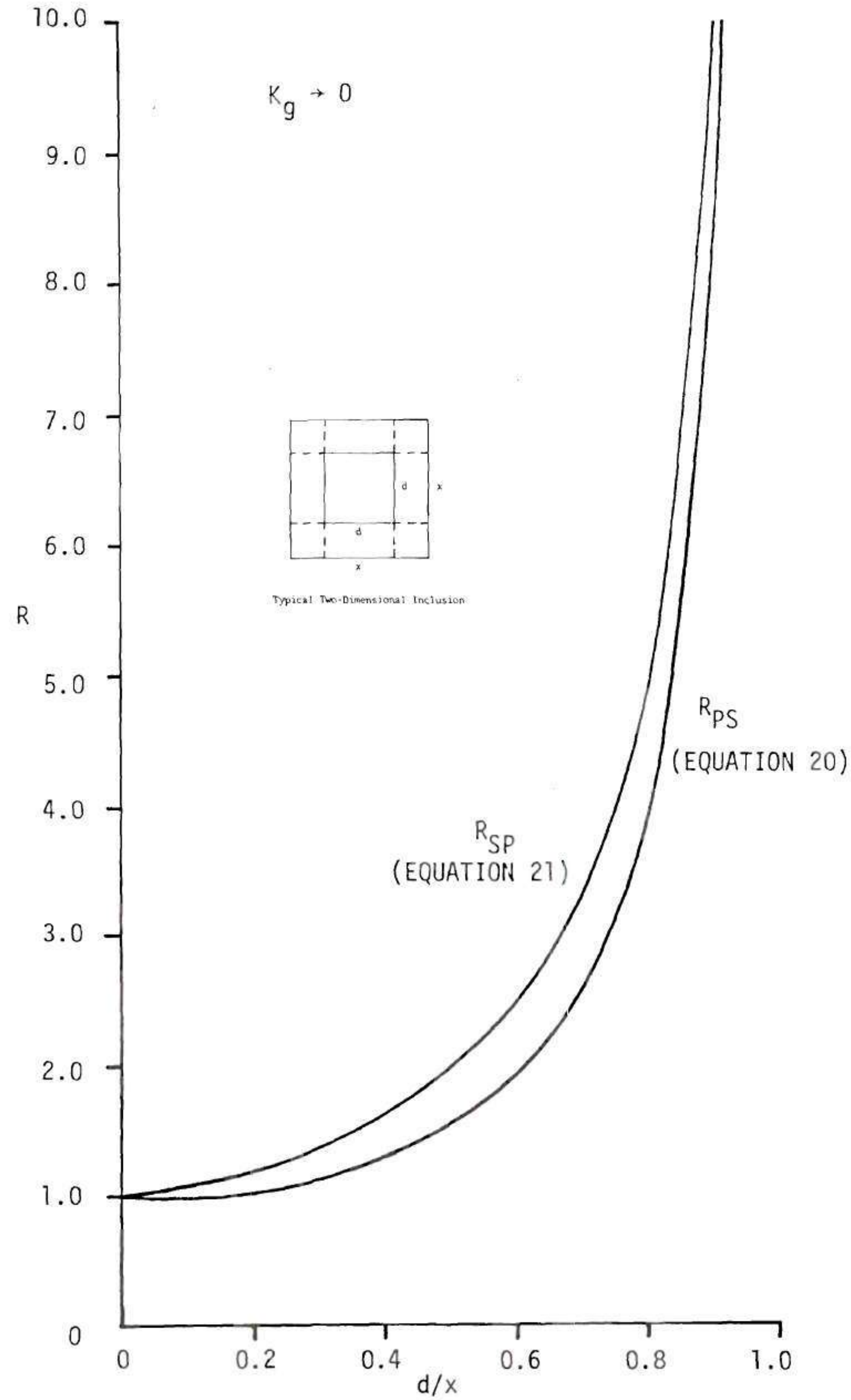

Figure 11. Comparison of R_{SP} and R_{PS} for Equations (20) and (21) with $K_g \to 0$.

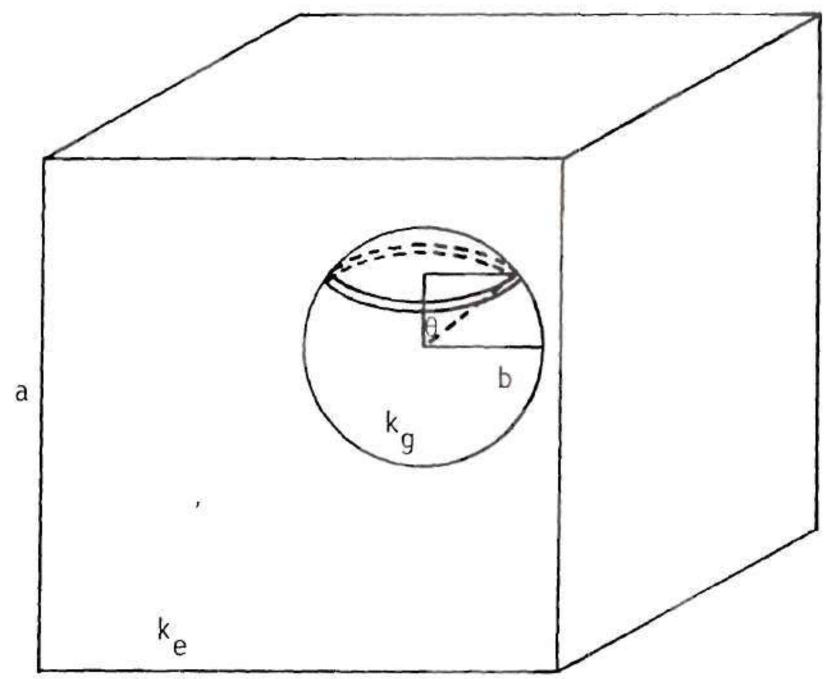

Figure 12. Single Cell Model for a Cubic Array of Sperical Inclusions [21].

$$K_m = \left[1 - \left(\frac{6v_f}{\pi}\right)^{1/3} \left(1 - \gamma\int_o^{\pi/2} \frac{\sin\theta d\theta}{r + \sin^2\theta}\right)\right]^{-1} \tag{22}$$

where

$$v_f = \frac{\frac{4}{3}\pi b^3}{a^3}$$

$$\gamma = \frac{1}{K_g - 1}\left(\frac{4\pi}{3v_f}\right)^{2/3} \frac{1}{\pi} .$$

If $1 > K_g$, Equation (21) becomes

$$K_m = \left\{1 - \left(\frac{6v_f}{\pi}\right)^{1/3} \left[1 + \frac{\gamma}{\sqrt{-(\gamma+1)}} \mathrm{TAN}^{-1} \frac{1}{\sqrt{-(\gamma+1)}}\right]\right\}^{-1} \tag{23}$$

and, for $1 < K_g$,

$$K_m = \left\{1 - \left(\frac{6v_f}{\pi}\right)^{1/3} \left[1 - \frac{\gamma}{2\sqrt{\gamma+1}} \ln \frac{\sqrt{\gamma+1} + 1}{\sqrt{\gamma+1} - 1}\right]\right\}^{-1} . \tag{24}$$

A comparison of these results with those expressed previously is shown in Figure 13 for the case of the thermal conductivity of the included spheres approaching infinity, and in Figure 14 for the case of the thermal conductivity of the included material approaching zero.

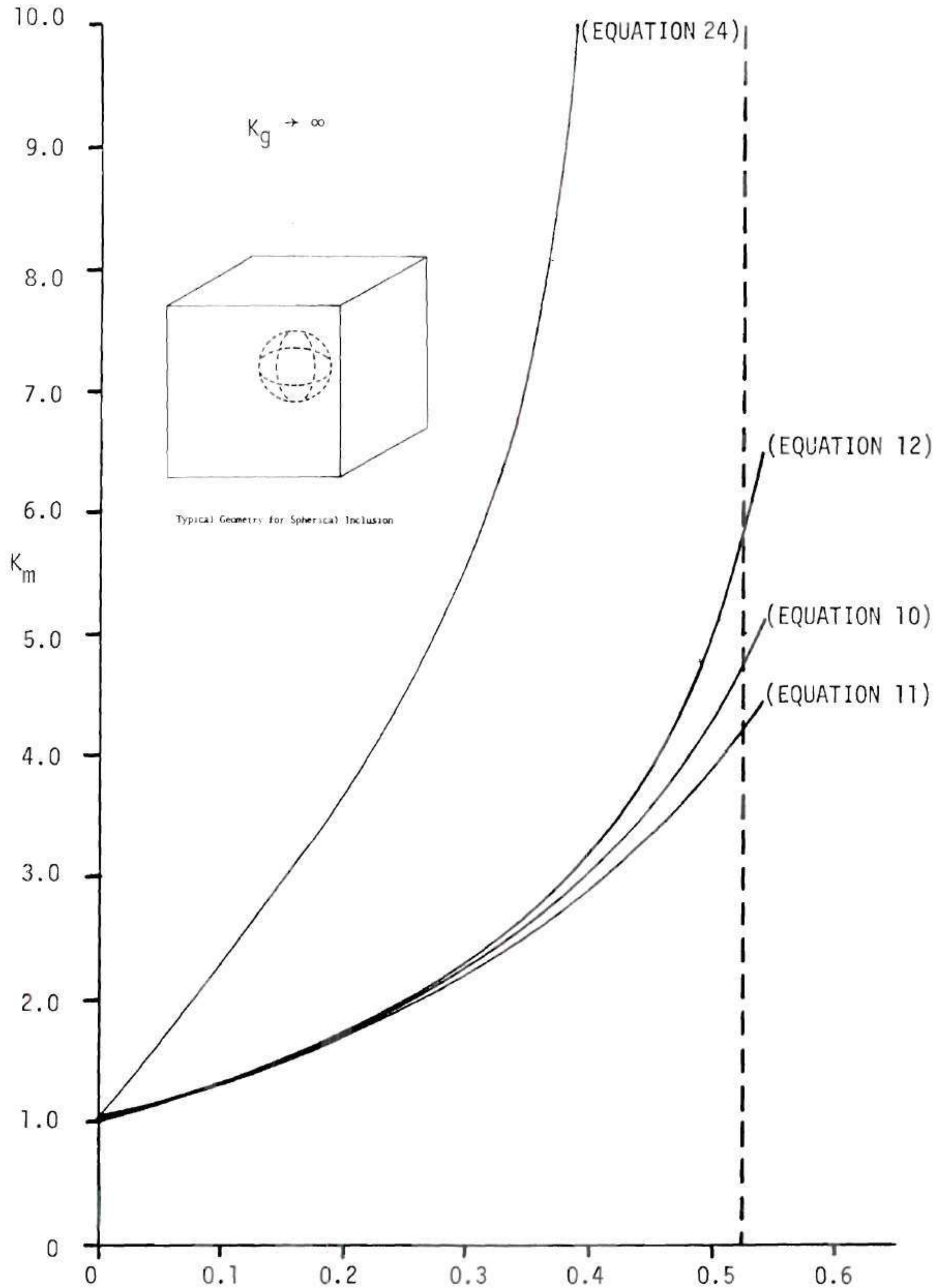

Figure 13. Spheres in a Cubic Array -- Analog and Exact Analysis ($K_g \to \infty$).

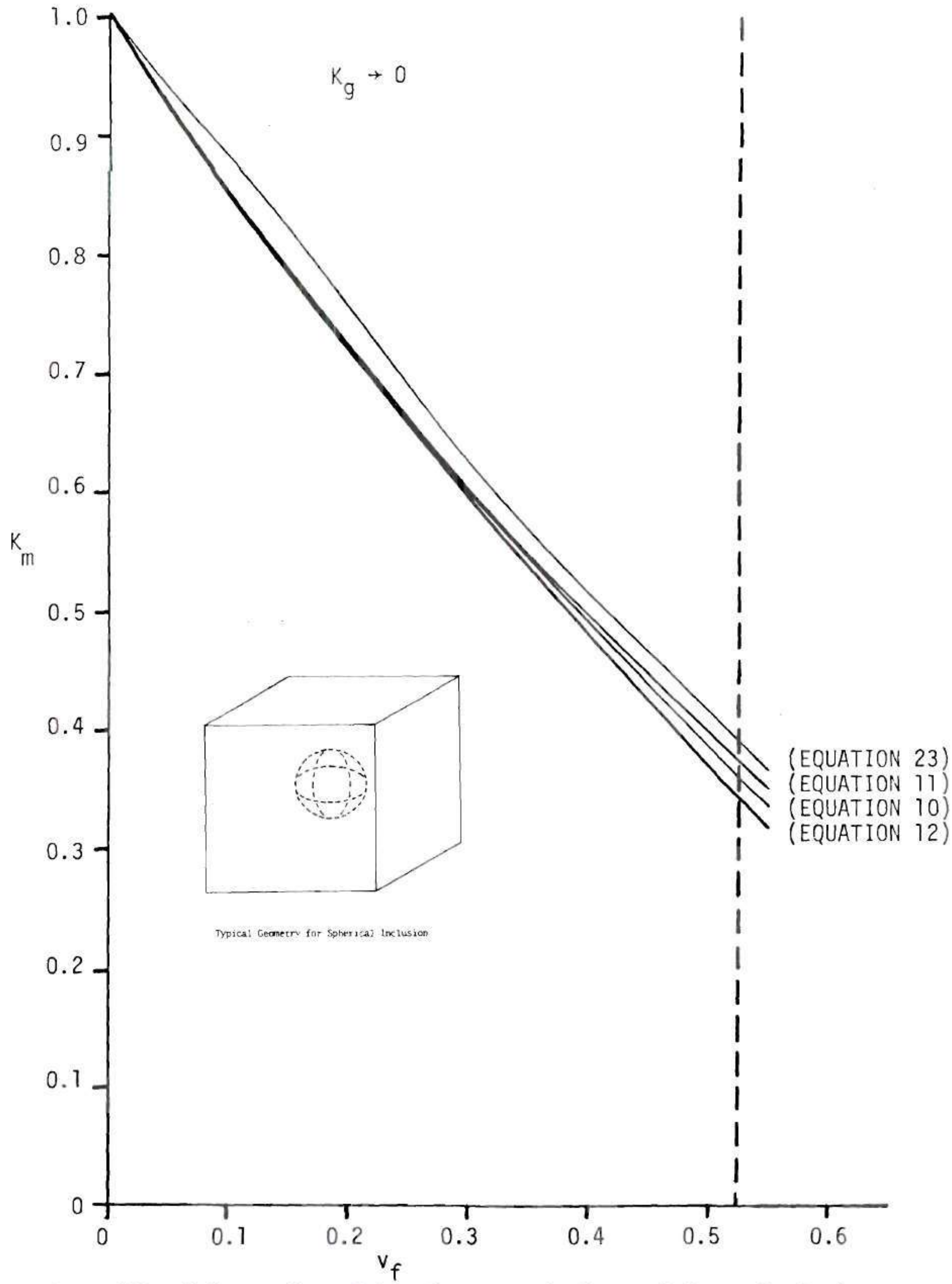

Figure 14. Spheres in a Cubic Array -- Analog and Exact Analysis ($K_g \rightarrow 0$).

2.2.4. Cubes in a Cubic Array

In order to predict the influence of geometry on the thermal conductivity of a composite material, the relatively simple case of a cubic inclusion in a spherical array may be analyzed for comparative purposes with the results of sections 2.1 and 2.2.3. Duga [22] has developed the following expression for the series-parallel resistance of this geometry:

$$R_{Sp} = \left[\frac{1 - \left(1 - \frac{k_e}{k_g}\right) v_f^{1/3}}{1 - \left(1 - \frac{k_e}{k_g}\right) v_f^{1/3} (1 - v_f^{2/3})} \right] \frac{1}{k_e} \quad . \tag{25}$$

When transformed from an expression for the thermal resistance into an expression for the thermal conductivity, the result is the same as that derived in Appendix A:

$$K_m = 1 + \frac{v_f (K_g - 1)}{K_g + v_f^{1/3} (1 - K_g)} \quad . \tag{26}$$

A comparison of these results with those obtained earlier is given in Figures 15 and 16.

2.2.5. Cylinders in a Cubic Array

Since the analog analysis for both the spherical inclusions and the approximation of spherical inclusions by cubic inclusions yields results which are compatable with the results of the mathematical analysis, the thermal-electrical analog procedure will be used to predict

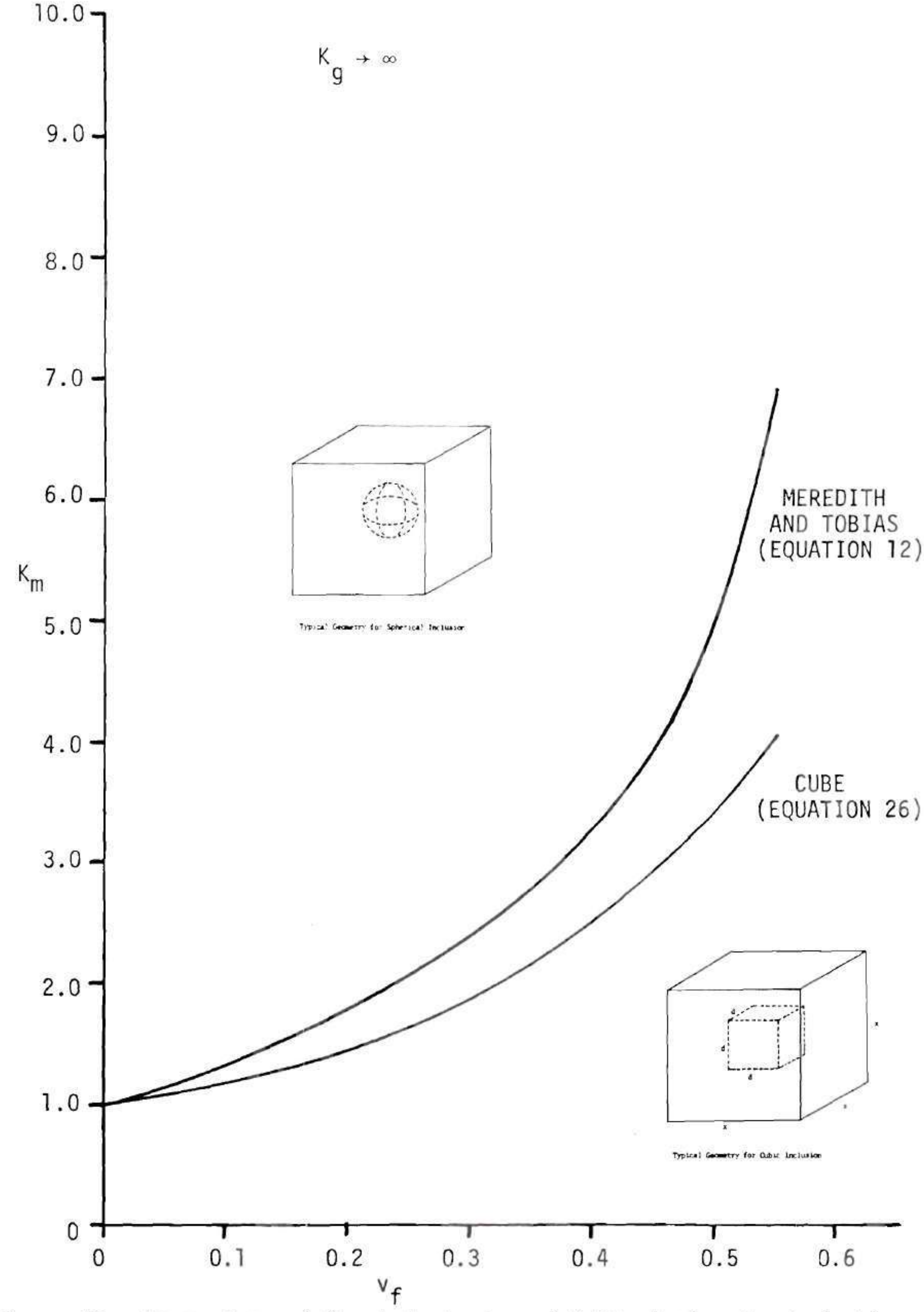

Figure 15. Comparison of Exact Analysis and Cubic Analog Approximation ($K_g \to \infty$).

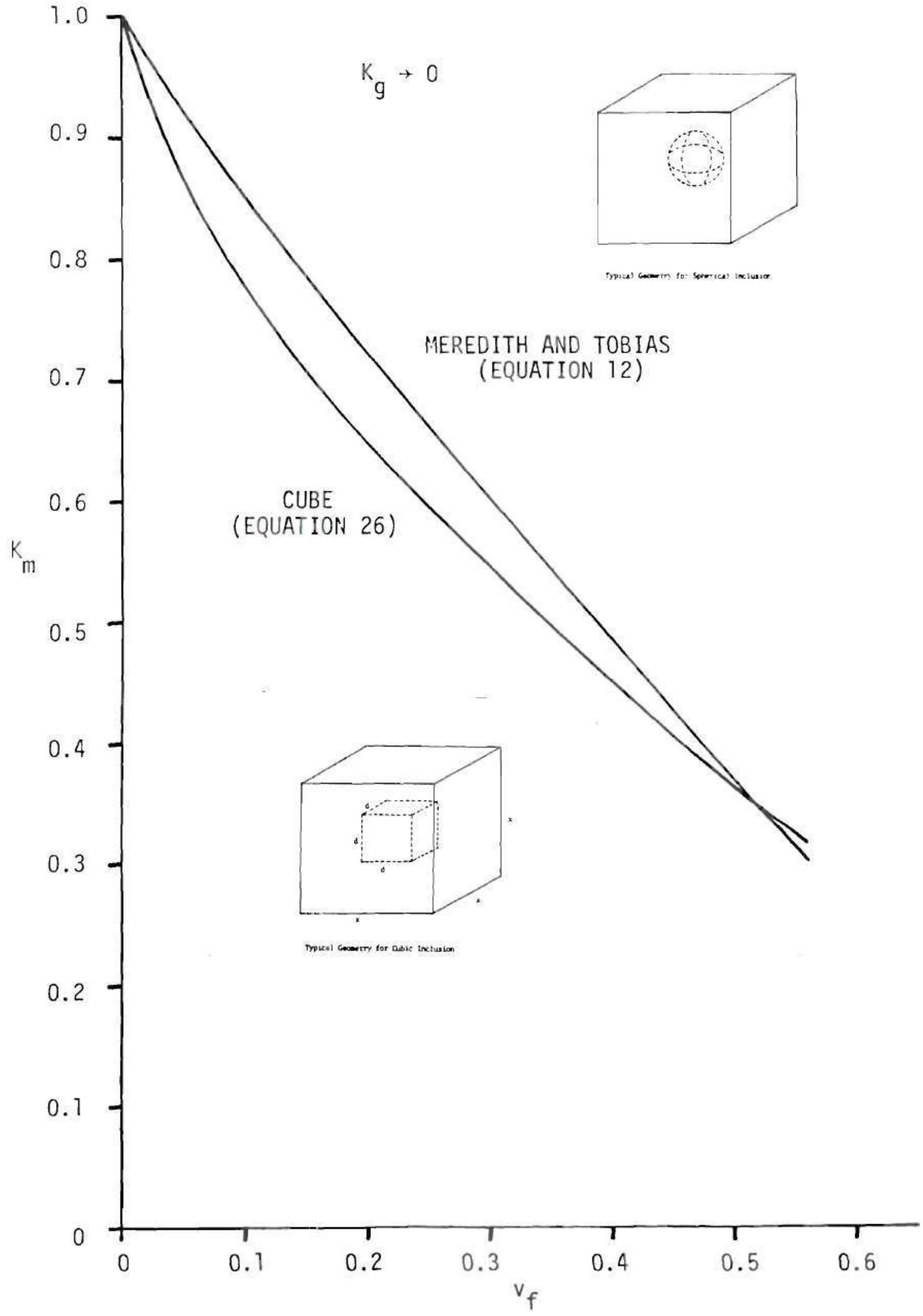

Figure 16. Comparison of Exact Analysis and Cubic Analog Approximation ($K_g \to 0$).

the behavior of included cylinders in a cubic matrix (Figure 17). The results will then be used for comparison with previous analyses and with the experimental results associated with this thesis.

Appendix B shows the series-parallel analog derivation of the cylinder in a cubic matrix. The general result for the analog model is:

$$K_m = 1 + \frac{v_f(K_g - 1)}{K_g + \frac{\ell}{x}(1 - K_g)} \qquad (27)$$

where ℓ is the length of the cylinder and x is the length of one side of the cube. For the limiting case of $\ell/x = 1$, equation (27) becomes:

$$K_m = 1 + v_f(K_g - 1) \qquad (28)$$

which is the rule of mixtures.

Equation (28) will be used to determine the thermal conductivity of the pure carbon fiber from experimental data collected on the guarded hot plate device at several different volume fractions.

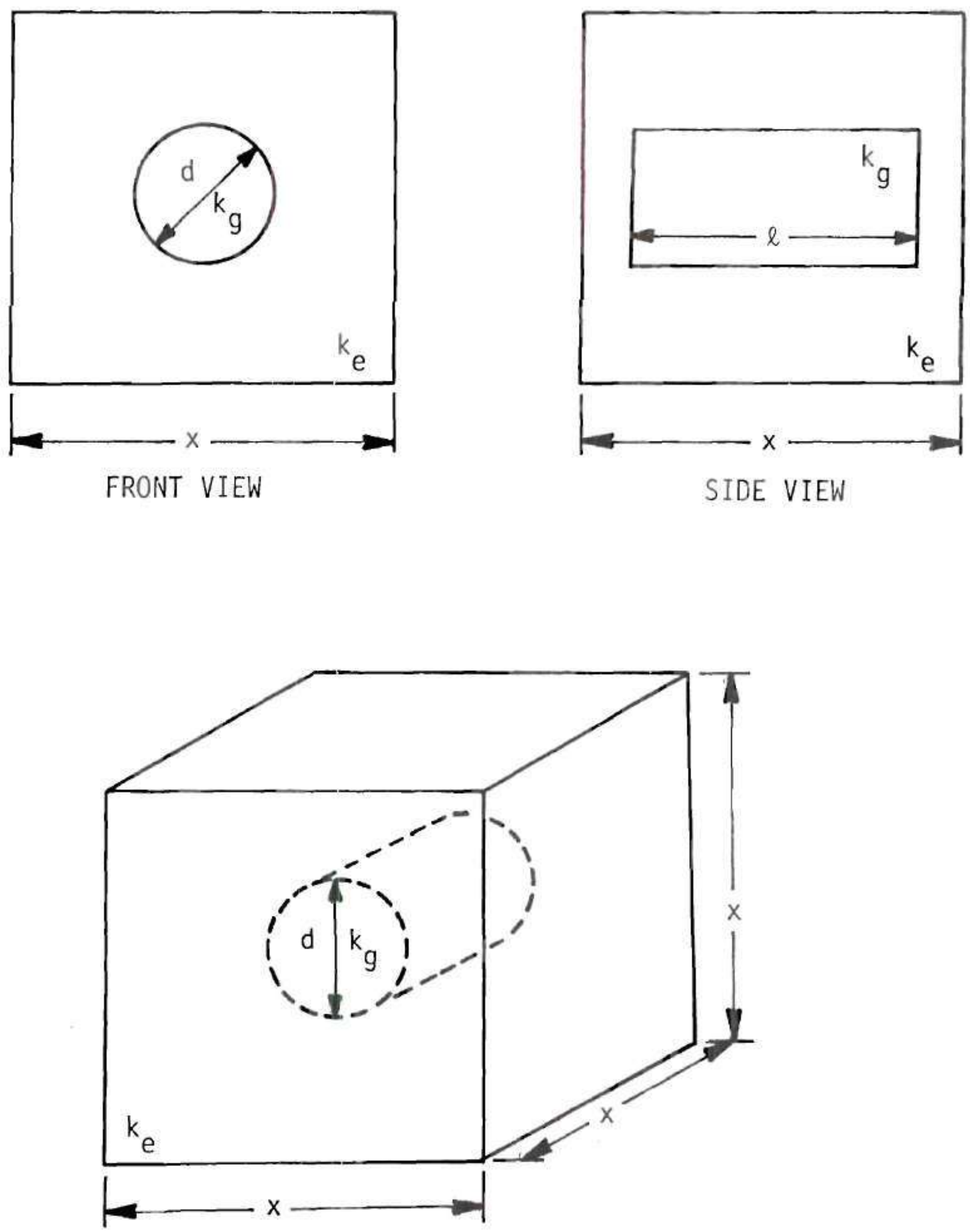

Figure 17. Geometry for a Cylinder in a Cubic Matrix.

CHAPTER III

EXPERIMENTAL APPARATUS

A guarded hot plate device was constructed as outlined in Section 1.5.1. With a few exceptions, the apparatus conformed to the ASTM C177 specifications. These exceptions were due to the size limitations imposed on the device by the limited amount of carbon fibers available for thermal conductivity measurements.

The assembled guarded hot plate is shown in Figure 18. The basic components of the experiment apparatus are identified in the figure. This chapter will describe the details of the design and function of the major components of the guarded hot plate device.

The electronics package used in conjunction with the guarded hot plate is shown in Figure 19 with the individual instruments identified. This package was a portable unit that was used to power, monitor, and regulate not only the guarded hot plate device designed to measure the thermal conductivity of carbon fibers but also the larger guarded hot plate device designed by Jackson [9].

3.1. Power Input Components

Several devices were required to provide and measure the power input to the central heater. The voltage was supplied by a constant voltage source. The magnitude of this input was monitored by a voltmeter located on the instrument panel.

The current input to the central heater was measured by using a

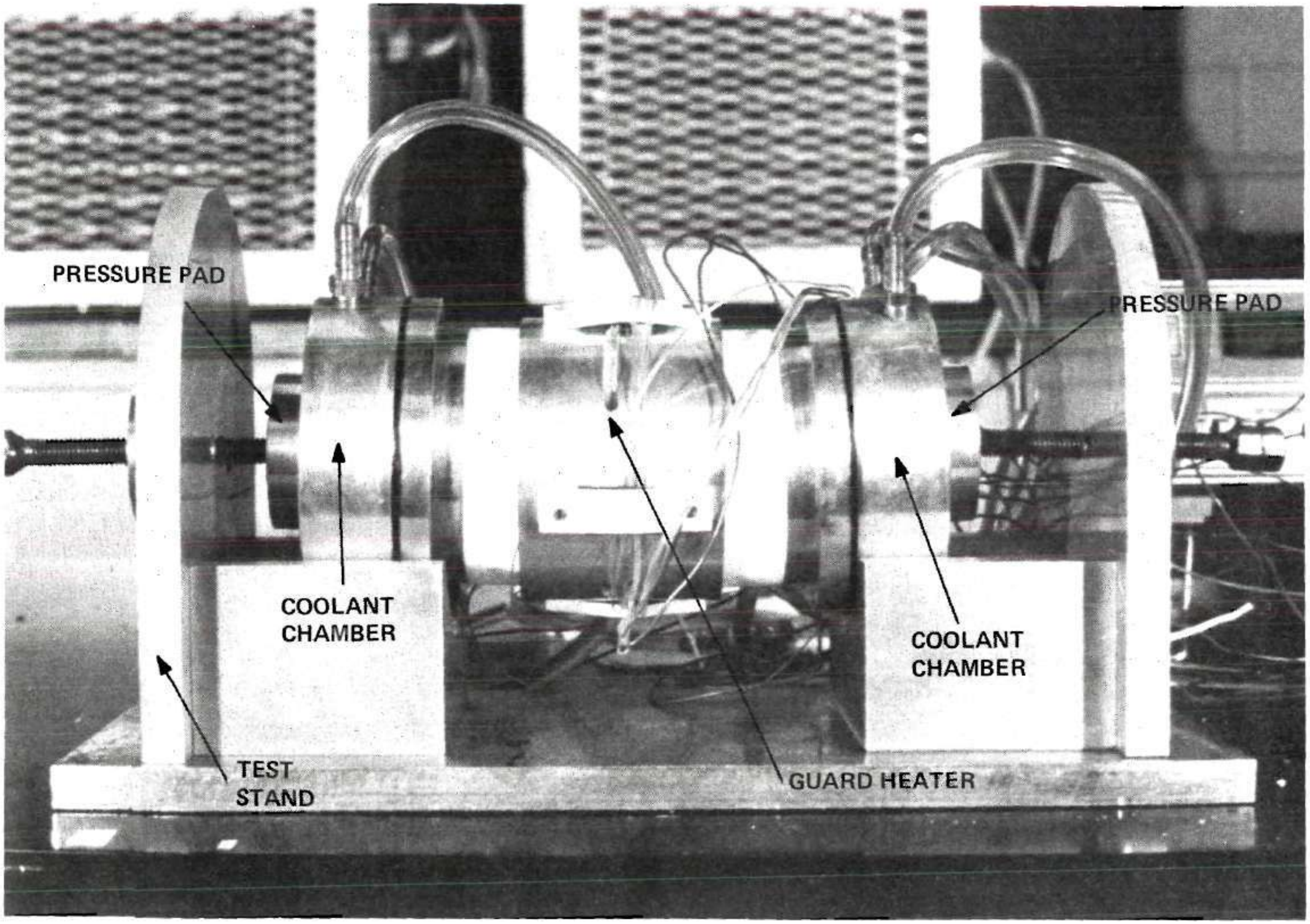

Figure 18. Guarded Hot Plate Apparatus

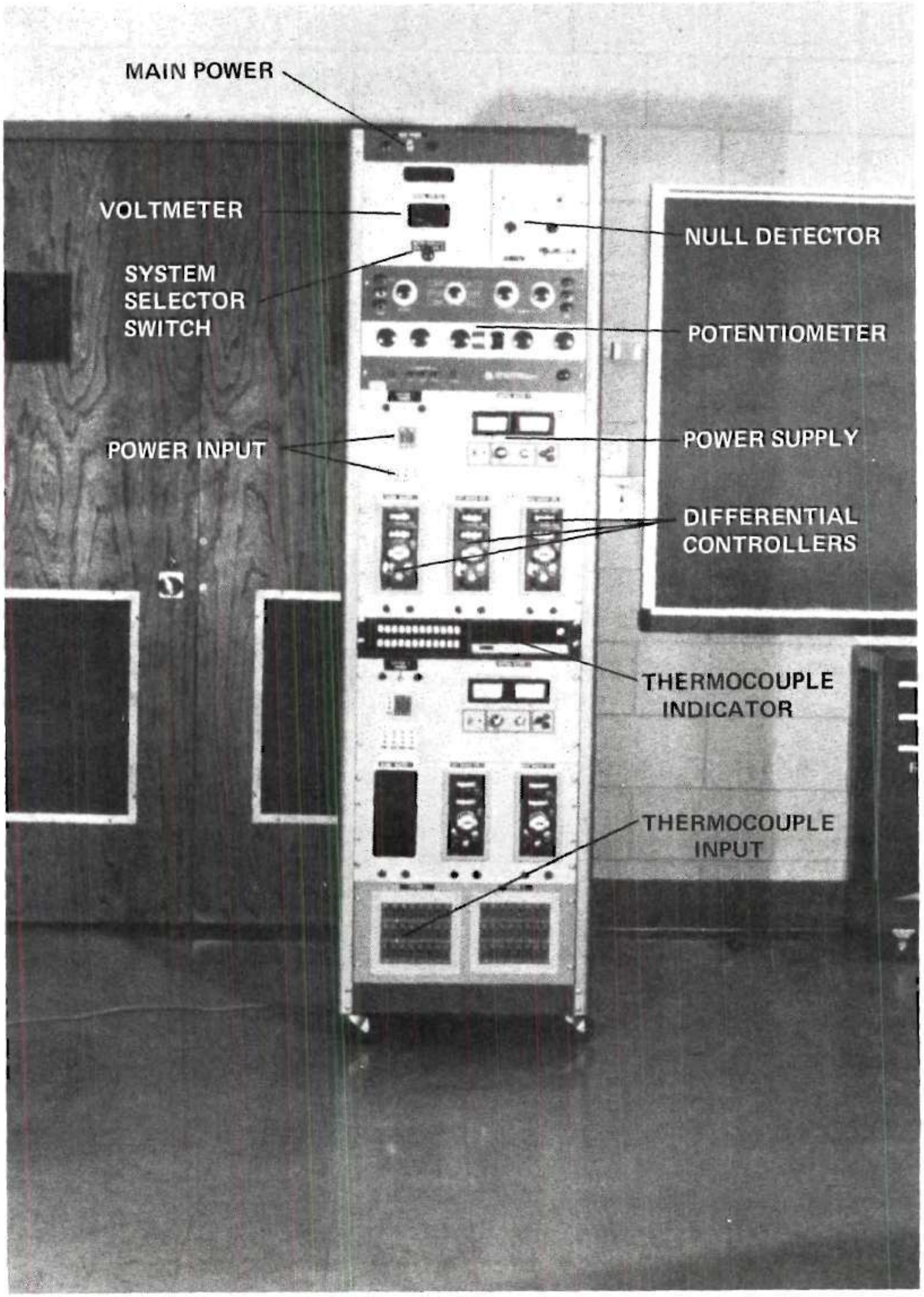

Figure 19. Electronic Support Package

potentiometer to determine the voltage drop across a standard resistor.

The specifications of the power system input components are given in this section.

3.1.1. Regulated Power Supply

The regulated power supply used in this experimental set-up was a Power/Mate Corporation Model BPA-E-40. With this particular device, the input power to the central heater could be regulated to a stability of ± 0.1 percent. The Model BPA-E-40 power supply was rated at 40 volts and 2.5 amperes of direct current.

3.1.2. Potentiometer

The potentiometer used in these experiments to monitor the current across the standard resistor was a Leeds and Northrup Type K-5 potentiometer. The error limitations of this device were ± (0.003 percent of reading + 3 microvolts).

3.1.3. Null Detector

The null detector used in conjunction with the potentiometer for the determination of the current flow across the standard resistor was a Leeds and Northrup Catalog 9834 D-C null detector.

3.1.4. Standard Resistor

The standard resistor used in these measurements was a Leeds and Northrup Model 4360. This resistor consisted of a continuous strip of manganin mounted on a wooden panel. Operational specifications of this resistor were as follows:

resistance: 0.1 ohm

current rating: 15 amperes

potential drop with maximum current: 1.5 volts

accuracy: ± 0.04 percent with air cooling at room
temperature for any current

corrections: four-terminal, current/potential type.

3.2. Temperature Measurement

3.2.1. Thermocouples

All thermocouples used in the guarded hot plate apparatus were type T (copper-constantan) thermocouples. With the exception of those thermocouples used to measure the temperature of the circulator fluid and the ambient air temperature, the thermocouple wire used was Omega Engineering, Incorporated TT-T-36 (36 gage) wire. The thermocouples for the ambient air and coolant temperatures utilized 24 gage thermocouple wire.

Thermocouple locations are shown in Figure 20.

3.2.2. Thermocouple Recorder

Temperature measurement for the apparatus was achieved with a Doric Scientific Model DS-350-T3, 24 channel, digital thermocouple indicator. The digital recorder was used to monitor the temperature of each sample surface as well as the temperature differential between the central heater and the guard ring.

This device had an accuracy of ± 0.1 percent and a sensitivity of one microvolt. The accuracy of this thermocouple indicator was established by the use of a constant temperature bath arrangement, outlined in reference [9].

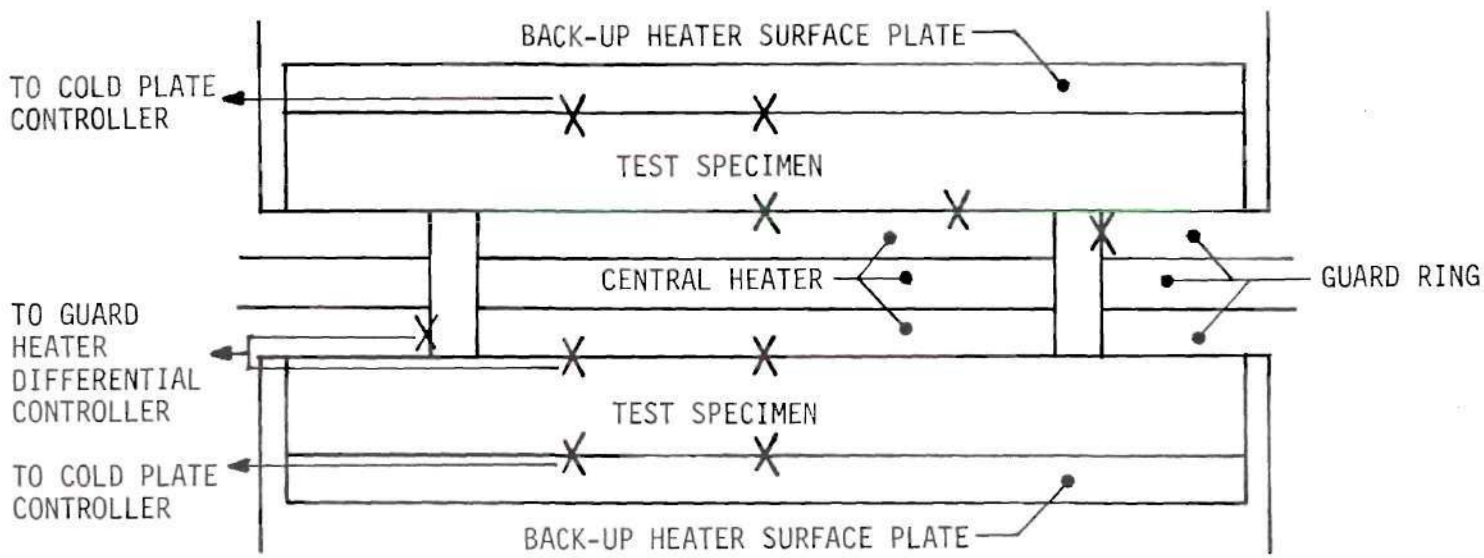

Figure 20. Thermocouple Locations.

3.3. Circulator

The circulator used in this assembly was a Haake Constant Temperature Circulator Model KT33. This circulator was designed for use in the temperature range -30C to 100C. The unit contains a 186 watt (0.25 horsepower) cooling compressor. Internal temperature control in the circulator was maintained through the use of an electronic triac relay.

A mixture of ethylene glycol and water (approximately 60 percent ethylene glycol by volume) was used as a coolant. By utilizing the Doric DS-350 thermocouple indicator in conjunction with the thermoregulator on the circulator, the temperature of the fluid in the circulator reservoir could be controlled to within $\pm$ 0.05C.

3.4. Differential Controllers

Temperature control for the guard and back-up heaters (Section 3.6 and 3.7) was achieved through the use of three Electronic Control Systems Corporation Model 6823 controllers. Each controller was equipped with a 120 volt/25 ampere power output.

For the back-up heaters, temperature sensing was accomplished by a copper-constantan thermocouple mounted on the surface of each heater. Each of the back-up heater controllers operated independently of the other, zeroing on an individually established, arbitrary set point.

The controller for the guard heater assembly was wired for differential control. Under this experimental set-up, the guard controller received an electromotive force from each of two thermocouples;

one located on the guard heater at the air gap between the guard and central heaters, and the other located near the edge of the central heater. It was the basic purpose of the controller to maintain power to the guard heater such that the temperature of the guard assembly was the same as that of the central heater.

Each controller was a three-mode controller, utilizing proportional, rate, and reset controls. A typical electrical schematic for the feedback control system of the controllers is shown in Figure 21 [23].

For the proportional-rate-reset controller, the controller output, M(s), is proportional to the error signal, E(s), the time rate of change (derivative) of the error, and the time integral of the error. The transfer function of the proportional-derivative-integral feedback network of Figure 21 is [23]:

$$\frac{M(s)}{E(s)} = k_c \left(1 + T_D s + \frac{1}{T_I s}\right) \tag{29}$$

where

k_c = proportional sensitivity

T_D = rate time

$\frac{1}{T_I}$ = reset

s = any selected complex variable (s = a + ib)

E(s) = error signal

M(s) = controller output signal

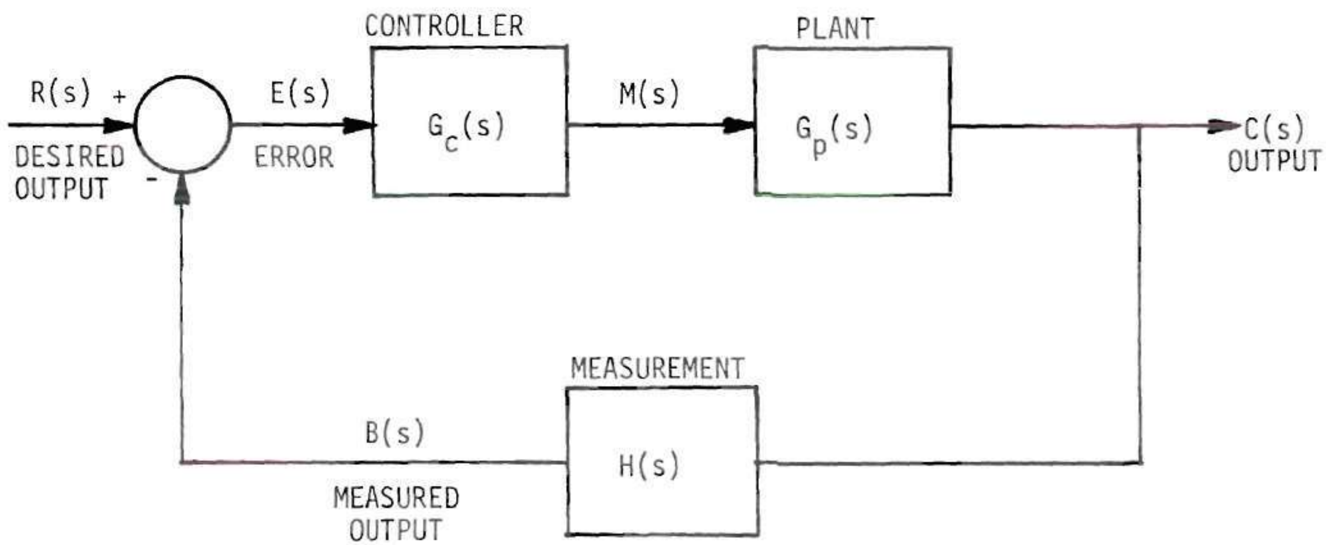

Figure 21. Feedback Control Loop.

From Equation (29) it is seen that the output signal is linearly related to the error signal by the proportional sensitivity during the period in which the controlled variable is within the proportional band. The proportional band is expressed as a percentage of the full-scale range of the controller. For example, if a controller has a bandwidth of 200 C, but proportional action occurs only in a 50 C range, then the proportional band setting is 25 percent [24, 25].

The proportional bandwidth also controls the rate at which the system responds to a change in the controlled variable. For a given change, a controller with a proportional bandwidth of 50 percent will respond twice as rapidly as a controller width a 100 percent proportional band, and half as quickly as a controller with a 25 percent proportional band. Thus, the larger the proportional band, the smaller the change in control position for a given change in the controlled variable. The narrower the proportional band, the faster the response, the smaller the offset, but the greater the tendency to oscillate [24, 26].

Further, from Equation (29), it is seen that the output signal is also proportional to the rate setting. The rate action provides a continuous relationship between the rate of change of the controlled variable and the position of the final control element, so that the controller output signal changes with the rate of the error signal [24, 26]. Thus, the rate function of the controller operates on the derivative of the error signal.

The reset mode of control adds stability to the proportional control mechanism by creating a response which is additionally dependent on the duration of the error signal [24]. Since the reset mode is acting upon the integral of the error signal, the reset control process will be terminated only when the process reaches the set point of the controller, at which time the error signal is zero.

The response for a typical proportional-rate-reset controller is shown in Figure 22 [26]. At t_1 the input signal, E, begins to decrease. The controller output signal rises correspondingly, but at a faster rate. At t_2 the input signal stops decreasing and remains constant at a new level. The effect of the rate action subsides immediately to a point which is determined by the proportional band. The action of the reset mechanism, however, continues to increase the controller output signal, though at a slower rate. From time t_3 to t_4, the input signal increases at a faster rate and with a greater magnitude of change. The action is correspondingly reflected in the controller output signal [26].

A further approximate control characteristic for the proportional-derivative-integral controller may be obtained from Figure 23 [27,28]. The transfer function for this network is [29]:

$$\frac{E_o}{E_i}(s) = \frac{(1 + \alpha\tau_1 s)(1 + \beta\tau_2 s)}{(1 + \tau_1 s)(1 + \tau_2 s)} \qquad (30)$$

where

$$\alpha\tau_1 = R_1 C_1$$

$$\beta\tau_2 = R_2 C_2$$

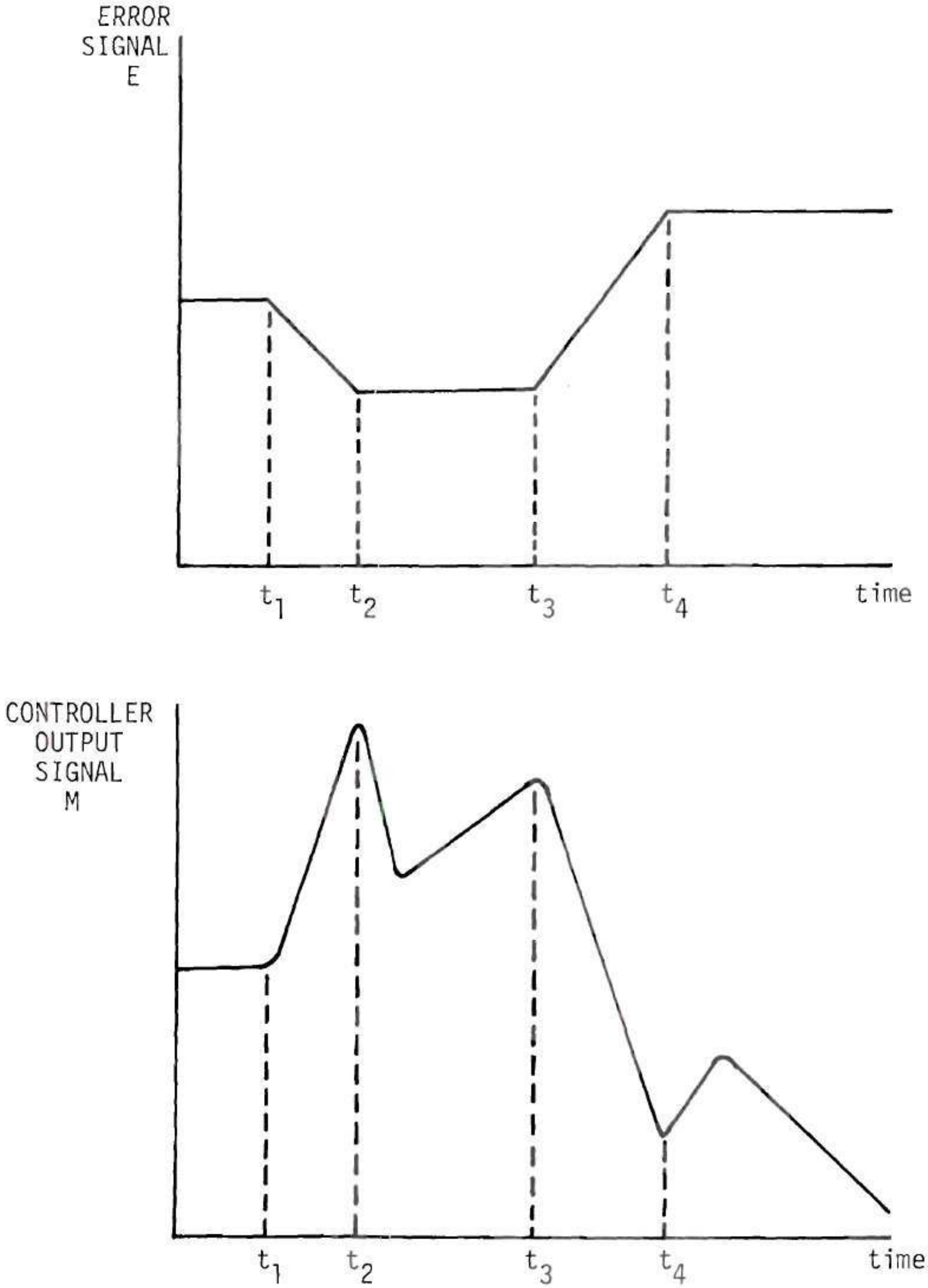

Figure 22. Response of a Three-Mode Controller [26].

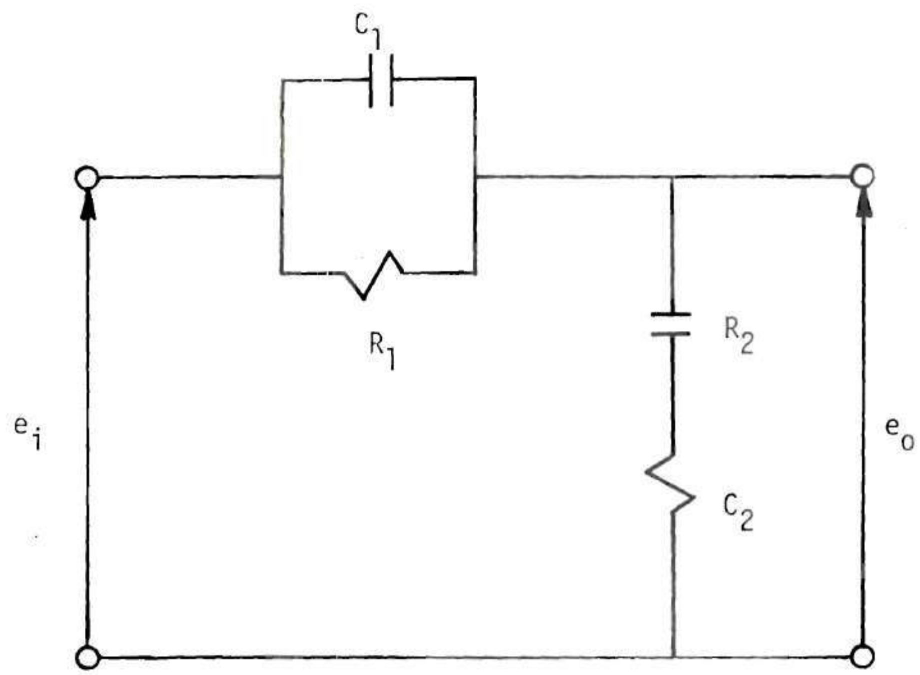

Figure 23. Resistance-Capacitance Network for a Three-Mode Controller.

$$\tau_1\tau_2 = R_1R_2C_1C_2$$

$$\alpha\beta = 1 \quad \text{and} \quad \alpha > 1 \ , \ \beta < 1 \ .$$

For a forward feedback loop, the rate action is provided by the lead portion of the network, denoted in the transfer function by those terms which are a function of τ_1. The terms which are a function of τ_2 provide the reset control, or lag portion of the feedback loop [26,29].

For the particular controllers utilized for the thermal conductivity measurements, the initial control settings were: proportional band = 100 percent, rate = 0, and reset = 0. As the system approached equilibrium, the proportional band was turned down in order to narrow the range of operation of the controller. At the same time, both the rate and reset controls were increased in order to stabilize the control system.

Various combinations of proportional band, rate, and reset control setting could be used to achieve a stable system response for any single thermal conductivity measurement. Typical control settings at equilibrium conditions were: proportional band = 40 percent, rate = 3, and reset = 2 for the guard heater controller; and proportional band = 40 percent, rate = 1, and reset = 0.1 for the back-up heater controllers.

3.5. Central Heater

The central heater assembly for the guarded hot plate apparatus consisted of three pieces; two cover plates and a central section containing the heater wire. All three pieces were cylindrical and 0.02423 m (0.954 inches) in diameter. This diameter gave the central heater a metering diameter of 0.0005 m^2 (0.775 in^2).

The central section of the heater consisted of a copper plate which contained concentric grooves machined into each surface for insertion of the heater wire. In addition, each surface contained a radial groove to facilitate the passage of the heater wire between each of the concentric grooves.

The cover plates were machined from copper, and had their surfaces machined flat to within $\pm$ 0.125 mm/m. These two plates also had two grooves cut into each surface for the purpose of mounting thermocouples flush with the surface of each heater plate. The cover plates were secured to the central section of the heater by means of a threaded steel post anchored in the central section. To prevent the stripping of threads in the cover plates, each of these components contained a "Heli-coil" threaded spring steel insert.

The heater wire used in the central heater was made from 36 gage Teflon insulated constantan thermocouple wire, with a resistance of 39.9 Ω/m. The wire was doubled and twisted together, wound into the central containment section, and then covered with a high conductivity copper flake grease to insure good thermal contact between all parts of the heater assembly. Each side of the central heater contained approximately 0.30 m (11.8 in.) of constantan wire, giving the heater a total resistance of 23.9 ohms.

To insure that the power input into the guarded hot plate was dissipated in the central heater, the connection between the constantan heater wire and the copper lead wire was made in the heater itself. Due to the small size of the constantan heater wire, it was found necessary to make the transition in two stages. First, 30 gage copper wire in a length of 0.076 m (3.0 in.) was silver-soldered to each constantan connection. Then, 24 gage copper leads were silver-soldered to the connectors for plug-in to the regulated power supply. The resistance of the copper transition wire was 0.98 Ω/m and the copper lead wire had a resistance of 0.58 Ω/m. Since the resistance of both copper transition wires was low when compared to the resistance of the constantan heater wire, the copper lead and transition wires had a negligible effect on the power dissipation of the central heater.

Thermocouples were located on each heater plate as shown in Figure 24. Thermocouples in position A were used to measure the surface temperature of each plate. One thermocouple at position B was used to measure the central heater edge temperature. The other position B thermocouple was utilized in the transfer of information to the guard heater differential control device. Due to the nature of the heater and the heater material, the error induced by locating the central heater edge thermocouple in the B position was negligible.

Power to the central heater was provided by the regulated power supply and control system described in Section 4.4.

3.6. Guard Heater

The purpose of the guard heater was to previent radial heat

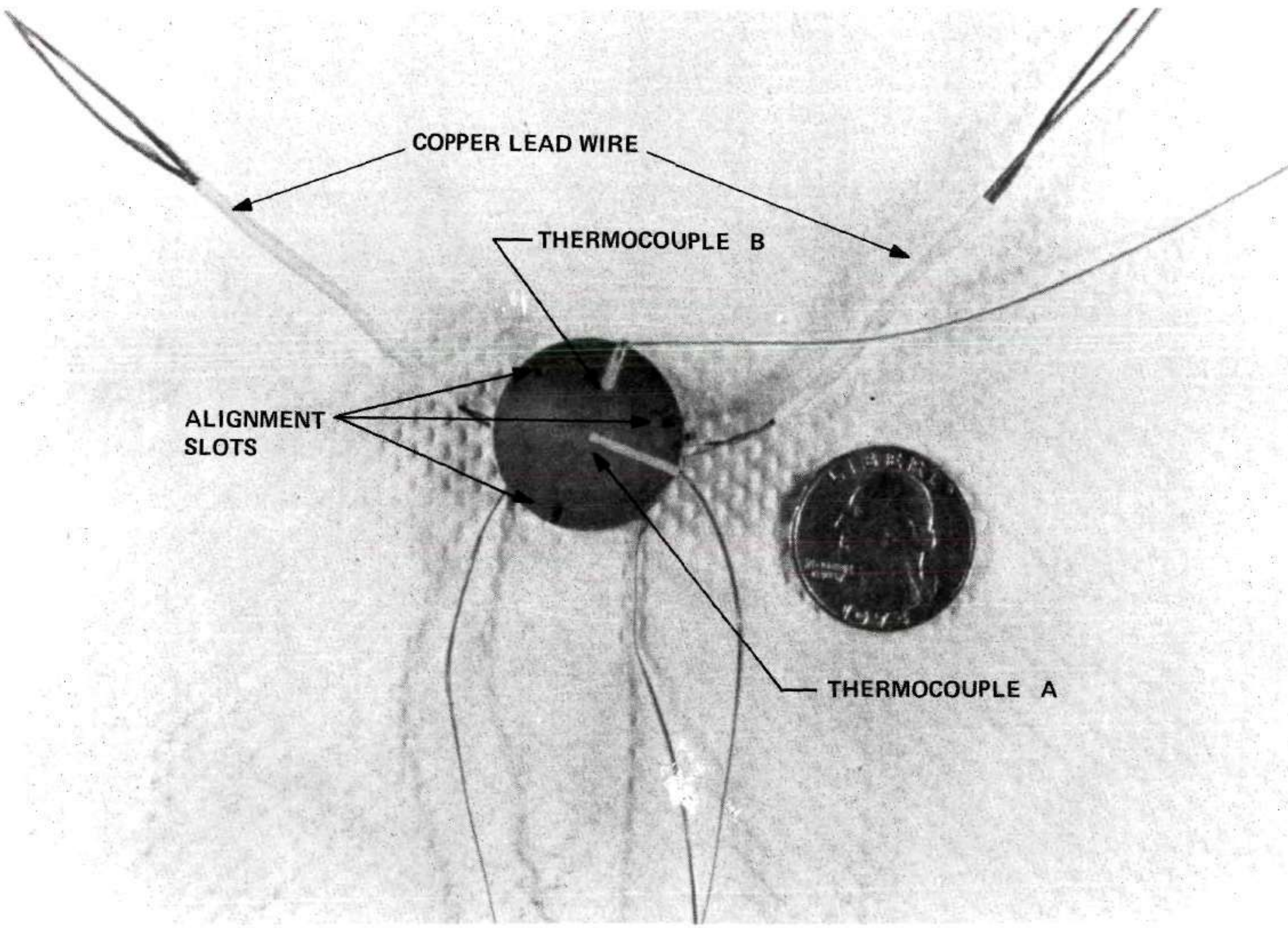

Figure 24. Central Heater

losses from the edges of the central heater and the test specimen. The guard heater assembly was constructed from five pieces -- two copper heater plates, two copper retaining rings, and a central aluminum guard.

During the actual test measurements, the temperature difference across the air gap between the guard and central heaters was not greater than 0.1 C. Based on this temperature difference, the errors associated with radial heat flow as given by the thermal imbalance error were estimated as 1.728 percent. (Details are given in Appendix C.) In addition to the small temperature differences across the guard gap, the guard shell, which enclosed the edge of both test specimens, further reduced the radial heat flow between the guard and central heaters. The temperature of the guard shell (shown in Figure 25) was approximately the same as that of the guard heater surface. The design of the guard heater assembly effectively prevented significant radial heat flow during the conduction of the test measurements.

The copper heater plates were similar in nature to the surface plates of the central and back-up heaters. They were 0.06096 m (2.4 in.) in overall diameter with an exposed surface having an outer diameter slightly greater than 0.0508 m (2.0 in.). Each ring had an inner diameter of 0.02624 m (1.03 in.) for enclosing the central heater. The surface of each heater plate was machined flat to a tolerance of $\pm$ 0.125 mm/m.

The copper retaining rings were used for positioning the test specimen in the apparatus. Each ring was 0.00254 m (0.1 in.) thick

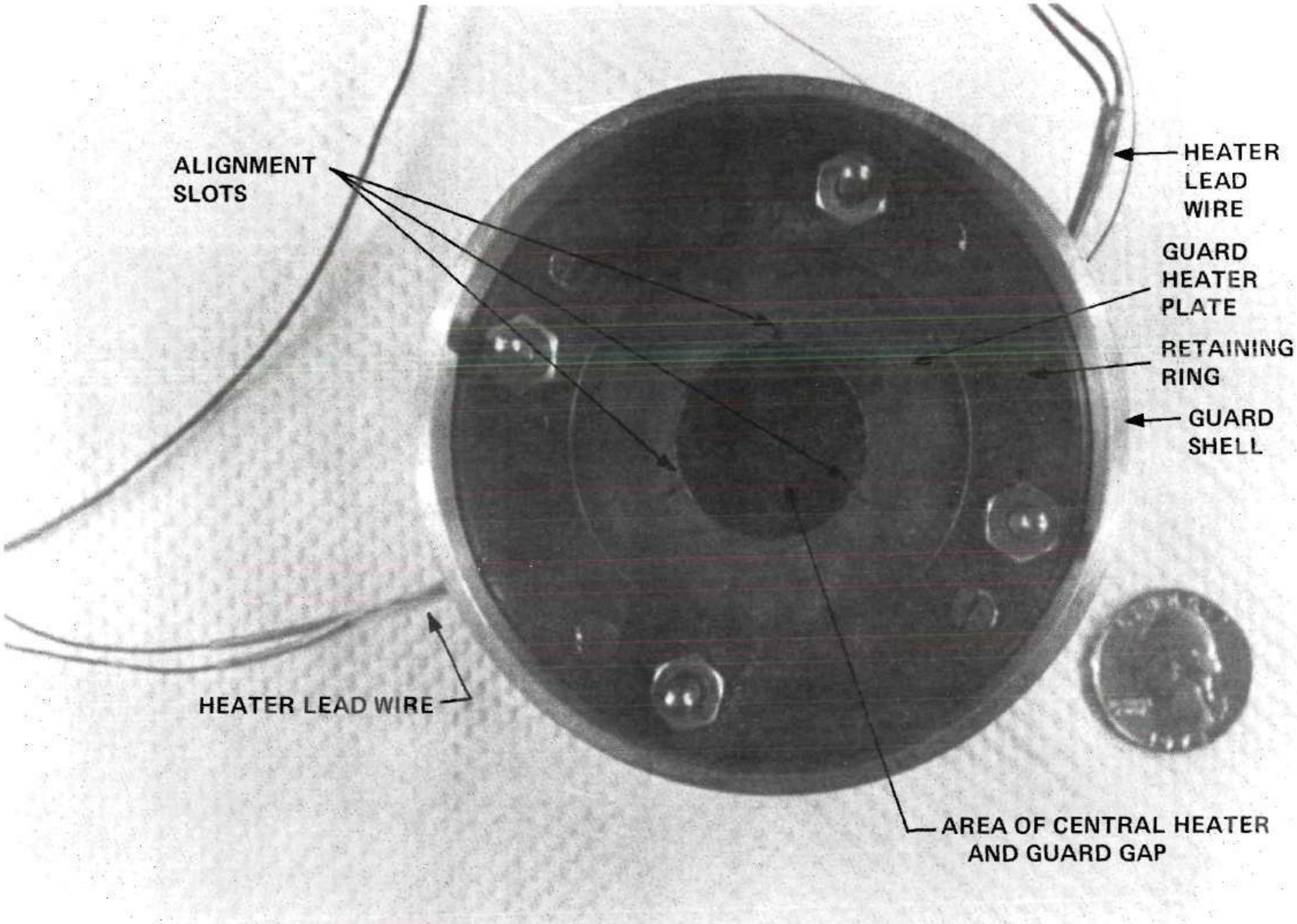

Figure 25. Guard Heater

with an outside diameter of 0.06096 m (2.4 in.) and an inner diameter of 0.05334 m (2.1 in.). Each ring was attached to a heater plate by the use of four flat-head screws symmetrically spaced about the mean diameter of the ring. This two piece assembly of the heater-retaining plates was necessary to insure the flatness of the heater surfaces.

The aluminum guard section of the heater had a cylindrical shell extending 0.03175 m (1.25 in.) from either side of its central surface. This shell enveloped the test sample and prevented heat loss from the edge of the specimen. The central surface of the guard was grooved in the same manner as the central and back-up heaters for the placement of heater wire in the guard section. The guard shell also contained access grooves for the passage of heater and thermocouple wires from the guard and central heaters to the outside of the device.

The heater wire for the guard heater was the same copper-constantan thermocouple wire used for the back-up heaters and the majority of the thermocouples in the apparatus. Although the power input for the guard heater was not monitored, the size of the heater made it desirable to insure that the power dissipated in the heater was maximized. Therefore a transition from the heater wire to 24 gage copper lead wire was made as the heater wire passed out of the heater.

There were two thermocouples placed in the guard heater, both located on the air gap between the guard and central heaters. One of these thermocouples monitored the temperature of the guard heater at the guard gap. The other thermocouple passed the same information to the guard heater ECS differential controller.

3.7. Back-up Heater

The purose of the back-up heaters was to insure an isothermal surface along one side of the test specimens. The two back-up heaters were each composed of a 0.05080 m (2.0 in.) diameter copper surface plate and a concentrically grooved base plate which contained the heater wire. The surface plates, like the central heater surface plates, were machined flat to $\pm$ 0.125 mm/m.

The heater wire was formed from 36 gage copper-constantan thermocouple wire, which was wound into the base plate. The base plate also contained a radial groove to facilitate the winding of the heater. Since the power dissipated in the back-up heaters was of no importance, there was no junction to copper lead wires made for the back-up heaters.

Thermocouple positions on the back-up heater surface plates were the same as those shown in Figure 26. Thermocouples at position A measured the temperature of the heater surface, while the thermocouples at position B provided input to the ECS differential controller.

The controllers were manually adjusted until the temperature of the two back-up heaters was held constant to within $\pm$ 0.1 C. Each back-up heater was controlled by a separate differential controller.

3.8. Coolant Chambers

The coolant chamber end-caps (Figure 27) for the guarded hot plate device were machined from aluminum. Each cap was machined in two parts -- an outer cap and a mating threaded insert. Attached to the insert was a Teflon ring which aided in positioning the specimen and the back-up heater in the device. This ring also served to insulate the

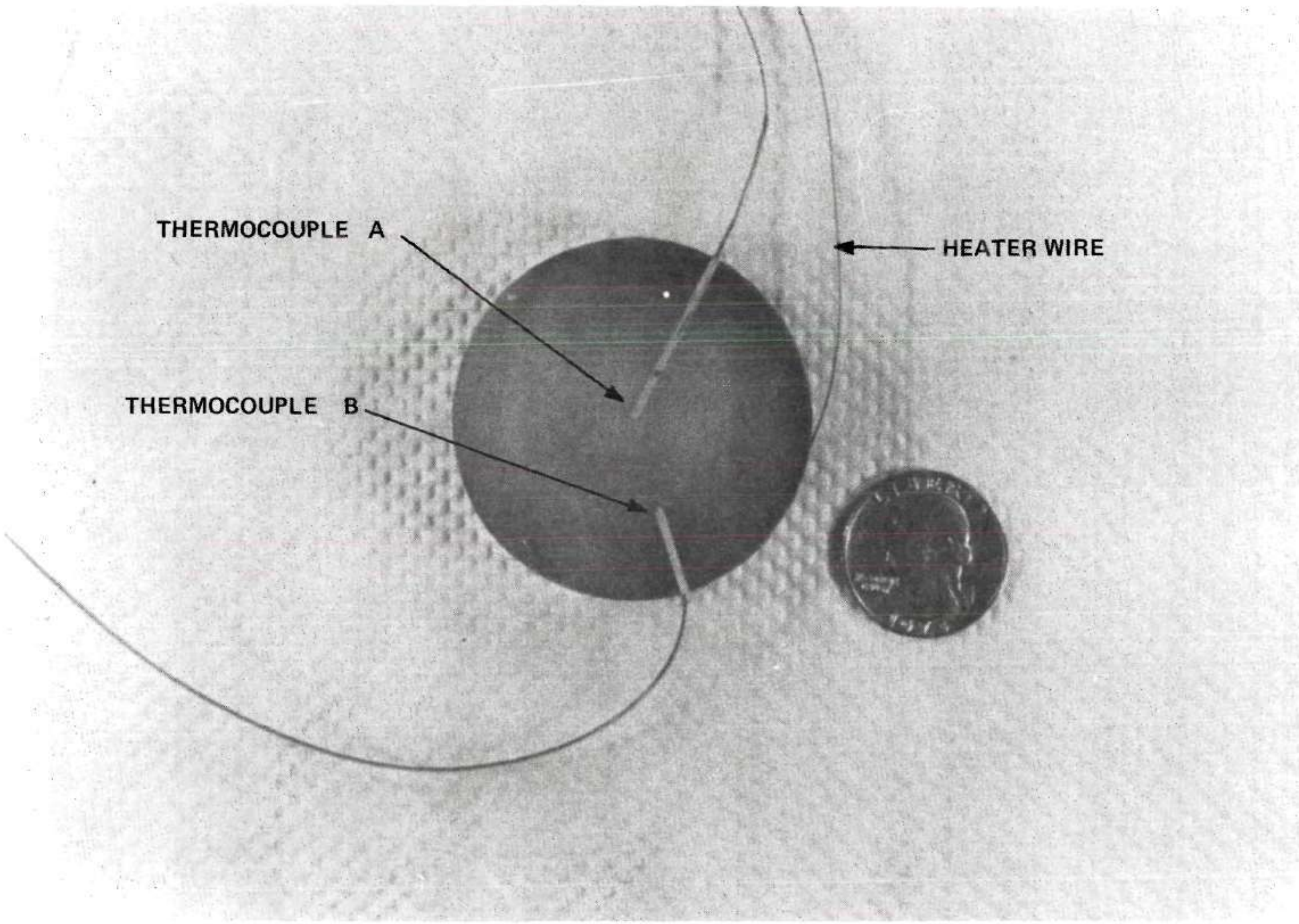

Figure 26. Back-up Heater

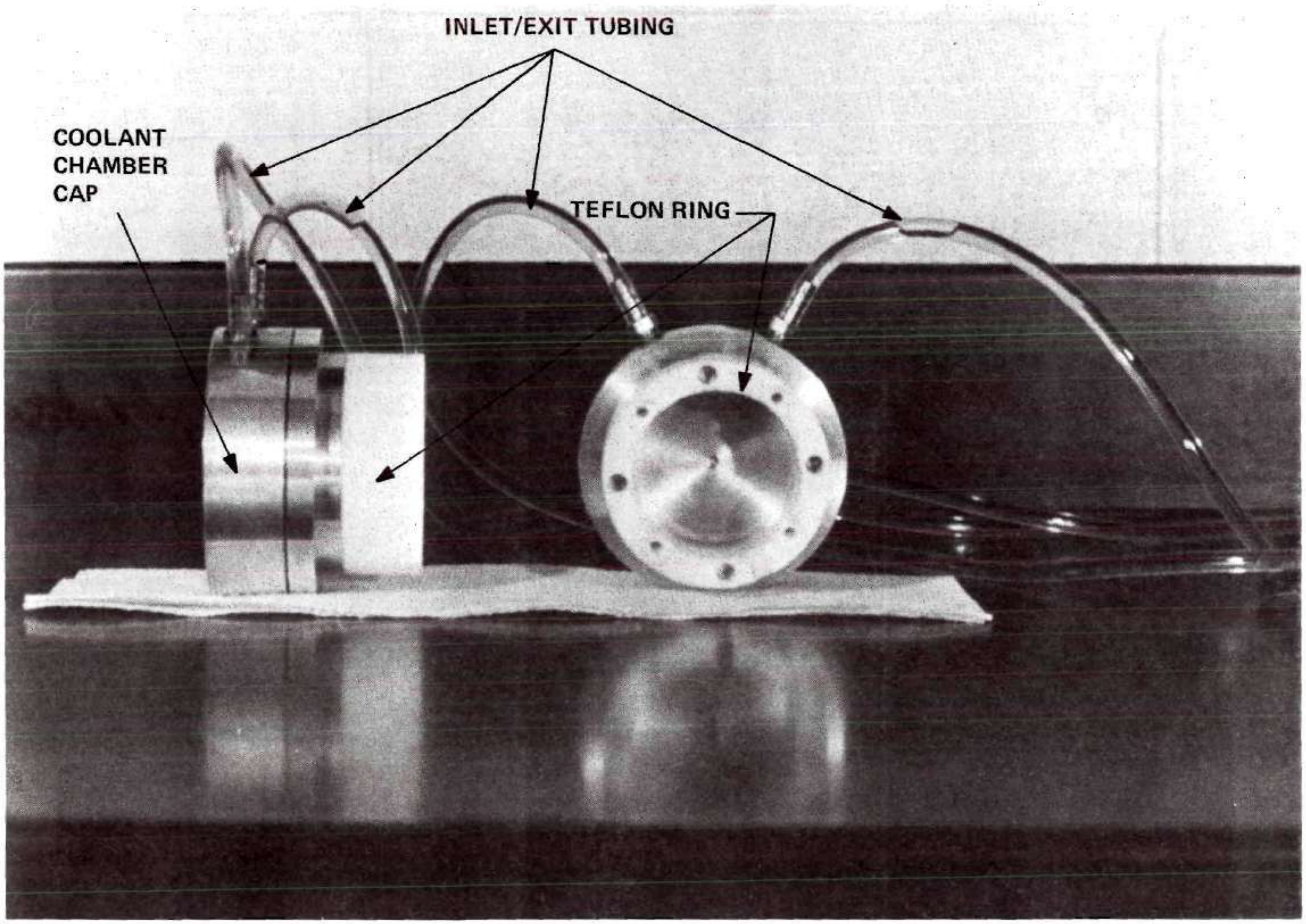

Figure 27. Coolant Chambers

back-up heater and the lower edge of the specimen from the guard ring.

The two pieces of the coolant chamber fit together to form an internal reservoir with a capacity of 0.00013 m^3 [0.092 m (3.625 in.) in diameter and 0.019 m (0.75 in.) deep] through which a coolant was circulated. The coolant temperature was monitored by a thermocouple located in the circulator reservoir.

3.9. Error Estimates

Two primary sources of error exist when the guarded hot plate method is used to measure thermal conductivity. The first source of error is associated with the flow of heat from the edge of the test specimen. The second source of error is due to the thermal imbalance which exists when there is a temperature drop across the air gap between the central heating section and the guard heater (refer to Figure 3). Jackson [9] has performed an error analysis for a cylindrical guarded hot plate device by "defining appropriate characteristic dimensions of the apparatus and utilizing the analysis for square hot plates".

By applying the same analysis to the small guarded hot plate device, it is found that (Appendix C):

1) the expected edge loss error = 1.97 percent

2) the expected thermal imbalance error = 1.73 percent

Further, the theoretical accuracy of the device, which incorporates the errors involved in the measurement of various parameters, is calculated to be no greater than 7.2 percent (See Appendix C), making the maximum total error of the guarded hot plate 10.9 percent.

CHAPTER IV

EXPERIMENTAL PROCEDURE

4.1. Specimen Fabrication

There were several considerations which required examination in the preparation of composite samples to be measured in the guarded hot plate. First, since it was desired to measure the axial thermal conductivity of the carbon fibers, they must be held with their axes perpendicular to the heater surfaces and parallel to one another. Small deviations from the required alignment should not significantly effect the measurement, since this error was a function of the cosine of the angle of misalignment. For example, for a 0.0127 m (0.5 inch) test specimen the effective thermal path length of the fiber would increase by less than one percent if the fiber were misaligned by as much as eight degrees.

Additionally, the composite test specimen must be devoid of any impurities, particularly air pockets embedded within the base matrix. The base material must provide a rigid configuration to maintain the fiber orientation, and it must be machinable to allow a smooth, flat surface for good thermal contact between the specimen and the heater plates.

Finally, due to the limited availability of the carbon fiber material, it was desirable that the specimen fabrication procedure be as conservative as possible with the amount of fiber used.

In the actual specimen fabrication process, fiber was wound onto several racks using a mechanical winding device. The number of fibers per rack was determined by a relation which was a function of the linear density of the fiber, the volume of the fiber, and the volume fraction of fiber desired in the test specimen. The fiber was then stacked into the mold in layers in order to provide even fiber distribution. The mold used in the specimen fabrication had a two inch diameter internal cross-section.

Degassed resin was then introduced into the mold under vacuum conditions and allowed to fill the mold cavity. The resin used was a low viscosity epoxy. The mold was then returned to atmospheric pressure and the resin-impregnated mold was allowed to cure on a heated-platen press. The resulting composite rod was then cut into two discs of equal thickness, and the surface of each disc was machined flat to a tolerance of $\pm$ 0.01 mm. The samples were then ready for thermal conductivity measurements.

4.2. Initial Estimate of Power Input

The initial voltage input to the central heater was estimated from the following empirical relationship which was based on the operating characteristics of the guarded hot plate.

$$V = \sqrt{\frac{0.025\ k\Delta T}{L}} \tag{31}$$

where

V = voltage input to the central heater [V]

k = anticipated thermal conductivity of the test specimen [W/mC]

L = thickness of sample [m]

ΔT = temperature drop desired [C]

For the 60 percent volume fraction carbon fiber composite specimens (the standard specimens to be supplied for further thermal conductivity analysis) the initial experimental thermal conductivity measurements suggested that a reasonable voltage input for these specimens was in the neighborhood of 4.5 volts. This input allowed for a temperature difference across the sample of 2 C.

4.3. Preliminary Procedures

4.3.1. Insulation of Hot Plate

The guarded hot plate was insultated from the environment by a layer of fiber glass insulation having a thermal conductivity of about 0.04 W/mC. The assembly was further isolated by a stainless steel shroud which fit over the test stand.

4.3.2. Sample Pressure

In order to aid in the repeatability of thermal conductivity measurements as well as to insure good contact between the specimen and the heater plates, a constant, reproducible force was applied to the device as it rested in the test stand. This force was exerted by applying a torque to a threaded rod, which in turn, forced a pressure pad against the coolant cap. The torque was measured with a torque wrench.

Theoretical analysis by Jackson [9] has shown that the torque required to produce a given compressive force may be calculated from:

$$\tau = \frac{2}{3} \mu \, Pr \tag{32}$$

where

τ = applied torque

P = compressive force

r = radius of threaded rod

μ = coefficient of kinetic friction

The ASTM standard [10] recommends a compressive stress, σ, of 2394 N/m^2 (50 lbf/ft^2), where

$$\sigma = P/A = P/\pi R^2 \tag{33}$$

and R = radius of the test specimen.

Therefore, Equation (32) may be rewritten as

$$\tau = \frac{2}{3} \mu\sigma\pi \, R^2 r \tag{34}$$

where, for the guarded hot plate,

μ = 0.47 (reference [30])

σ = 2394 N/m^2

R = 0.0254 m

r = 0.00458 m

By substituting these values into Equation (34), it was found that a torque of 0.007 N-m was required on the threaded rod in order to produce a compressive stress of 2394 N/m^2 on the test specimen.

4.3.3. Mean Temperature of Test Specimen

In order to reduce the edge loss error of the apparatus, the thermal conductivity tests were conducted at a mean specimen temperature, $\frac{T_H + T_C}{2}$, which was approximately the same as the temperature of the ambient air. Previous data [31] on carbon fiber thermal conductivity has indicated that the slope of the thermal conductivity-temperature curve in the region of interest is such that variations of several degrees in the mean specimen temperature would not significantly affect comparison of different test specimens.

4.4. Power Input to System

The power input to the central heater was measured by monitoring the current through and voltage drop across the central heater wire. The current was determined by measuring the voltage drop across the standard resistor. The voltage was measured directly at the point where the central heater copper lead wires connect with the power supply. The accuracy of the power measurement was $\pm$ 0.025 percent.

The power input measured in this way was the total power into the central heater. Since the total power was dissipated through both sides of the apparatus, the actual power used in the thermal conductivity calculations was one-half of the Vi product.

The guard heater power was supplied by the guard heater control device. At the time of the system start-up, the control settings were manipulated so as to bring the guard heater temperature to within several tenths of a degree of the central heater edge temperature. The differential control device would then maintain a sufficient power input to the guard heater to maintain the guard heater temperature within ± 0.1 C of the central heater edge temperature with only minor adjustments to the controller settings.

The power input to the back-up heaters was also controlled by the heater controllers. The controller compared the temperature of the heater plate with the controller set point. Each heater could be manipulated independently of the other. For these controllers the control settings and the set point of the controller were adjusted manually until the desired heater temperature was achieved.

The temperature of the coolant flowing through the system was controlled directly by a thermostat located on the circulator. If the coolant temperature exceeded the setting on the back-up heater controller, the coolant temperature and flow through the coolant chambers, rather than the heater controller, would control the temperature of the back-up heaters.

Once the desired temperature drop across the specimen was established, either the back-up heaters, the coolant, or both together could be used to control the mean temperature of the specimen. Using the automatic control system, equilibrium conditions could be reached in three to five hours for most test specimens.

4.5. Thermal Conductivity Measurements

All data values were obtained by following the requirements outlined in the ASTM C177 Standards [10]. The standard specifies individual observations to be taken at intervals of not less than thirty minutes, until four successive sets of measurements give thermal conductivity values differing by no more than one percent. For the relatively high conductivity carbon fiber test specimens, this requirement was not entirely reasonable. First, the temperature drop across the test specimen was on the order of 3.0 C. Thus, a change in ΔT of only 0.05 C (the smallest measurable change on the thermocouple recorder) over the 1.5 hour test period resulted in a 1.7 percent difference in the thermal conductivity calculations. Therefore, it was impractical to meet the ASTM standards which require the measurements vary by no more than one percent.

Additionally, based on the experimental measurements of the thermal conductivity, a voltage input in excess of 12 volts would be required to achieve a temperature difference of 10 C across the sample. Attempts to maintain this level of power input have given rise to various problems in the heater wiring, causing short circuiting of the central and guard heater assemblies.

As a result of the above considerations, an alternate method of data collection was required. Consequently, for those cases in which the thermal conductivity varied by more than one percent over the test period, the thermal conductivity of the test specimen was determined by taking the average value of twenty observations made at 30 minute intervals over a 10.5 hour test period.

CHAPTER V

RESULTS

5.1. Experimental Accuracy

The accuracy of the guarded hot plate device was experimentally compared with data on two different test specimens, a standard insulation material provided by the National Bureau of Standards and a Teflon specimen.

The thermal conductivity of the NBS insulation material was measured in both the small guarded hot plate and the larger device developed by Jackson. Measurement of the thermal conductivity of the material was complicated due to the fact that the specimens were easily compressed when pressure was applied to the surface of the sample. Three independent thickness measurements on the same test specimens resulted in thickness measurements which varied by 1.4 percent, whereas thickness measurements on an epoxy resin specimen varied by less than 0.1 percent. Additionally, once such a compressible sample was in the device, there was no means to check the specimen thickness when it was actually being tested.

Data from the National Bureau of Standards square guarded hot plate apparatus [32], the Jackson device and the small guarded hot plate device is compared in Figure 28. The data for the small guarded hot plate lies from 0.004 percent to 1.5 percent below the data from NBS in the temperature range 15 - 30C. Data from the device was a maximum

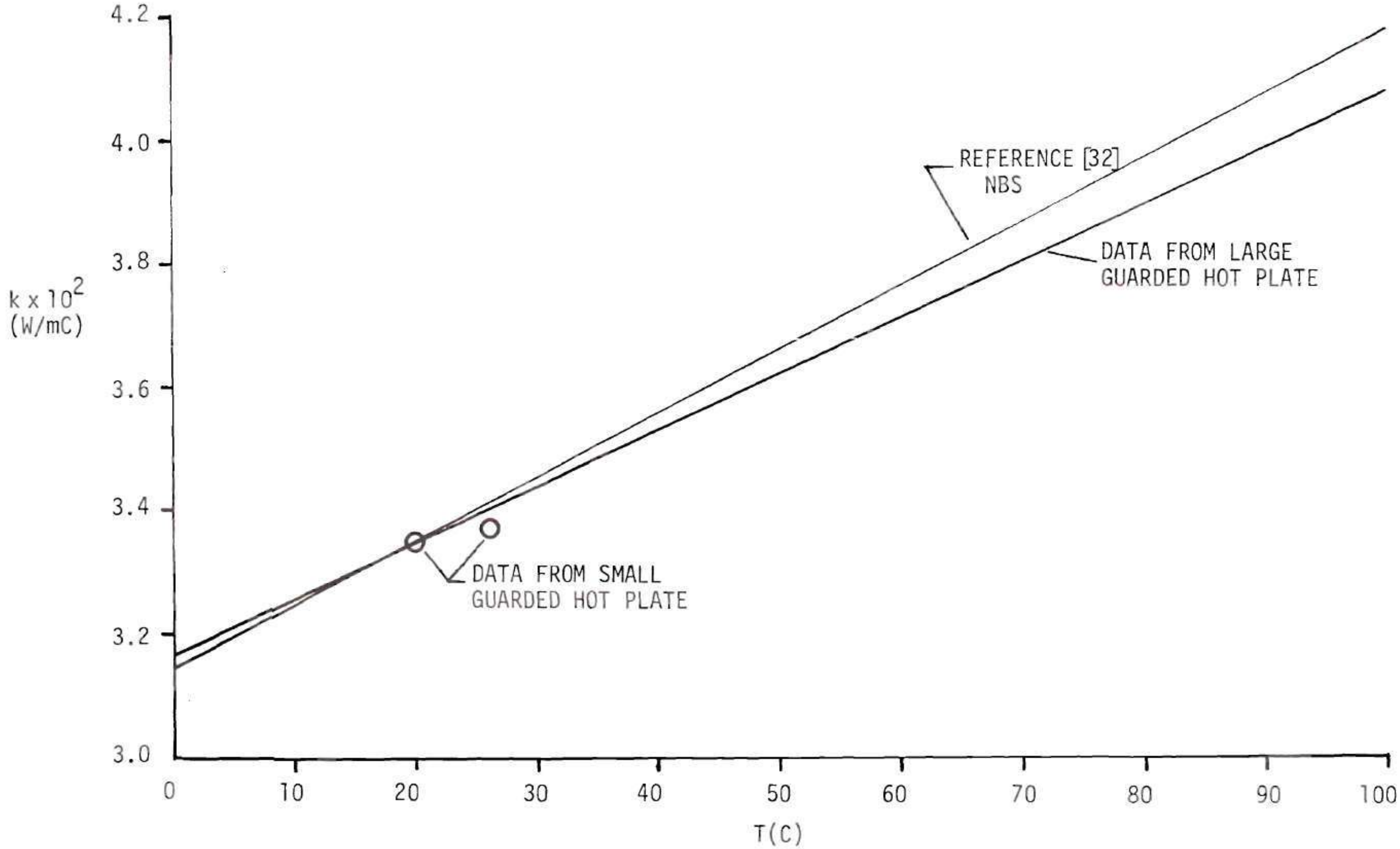

Figure 28. Thermal Conductivity of NBS Insulation.

of 1.0 percent below the measurements obtained from the Jackson guarded hot plate in the same temperature range.

The Teflon specimens were measured not only by the two guarded hot plate devices, but also by two independent laboratories using the Colora method and a thermal comparator device [9]. All test specimens were machined from the same piece of material. The latter two test methods yield thermal conductivity values of 0.195 and 0.270 W/mC respectively. Curves for the guarded hot plate data are shown in Figure 29. The data obtained from the guarded hot plate lies within 2.6 percent of the average of all available data.

5.2. Experimental Torque Analysis

A series of tests at various applied torques were run using an epoxy resin test specimen in order to determine a minimum torque necessary to insure adequate thermal contact between the specimen and the heater. The sample was measured at constant mean temperature at seven different torques beginning at 5 N·cm and terminating at a torque of 40 N·cm. The results of this series of measurements are given in Figure 30. It is seen that the thermal conductivity remains relatively constant until the applied torque is reduced below a value of approximately 10 N·cm. This value is substantially higher than the 0.7 N·cm required by the ASTM standard for minimum contact pressure.

On the basis of the experimental evidence, it was decided that all subsequent thermal conductivity measurements should be conducted at a minimum torque of 20 N·cm.

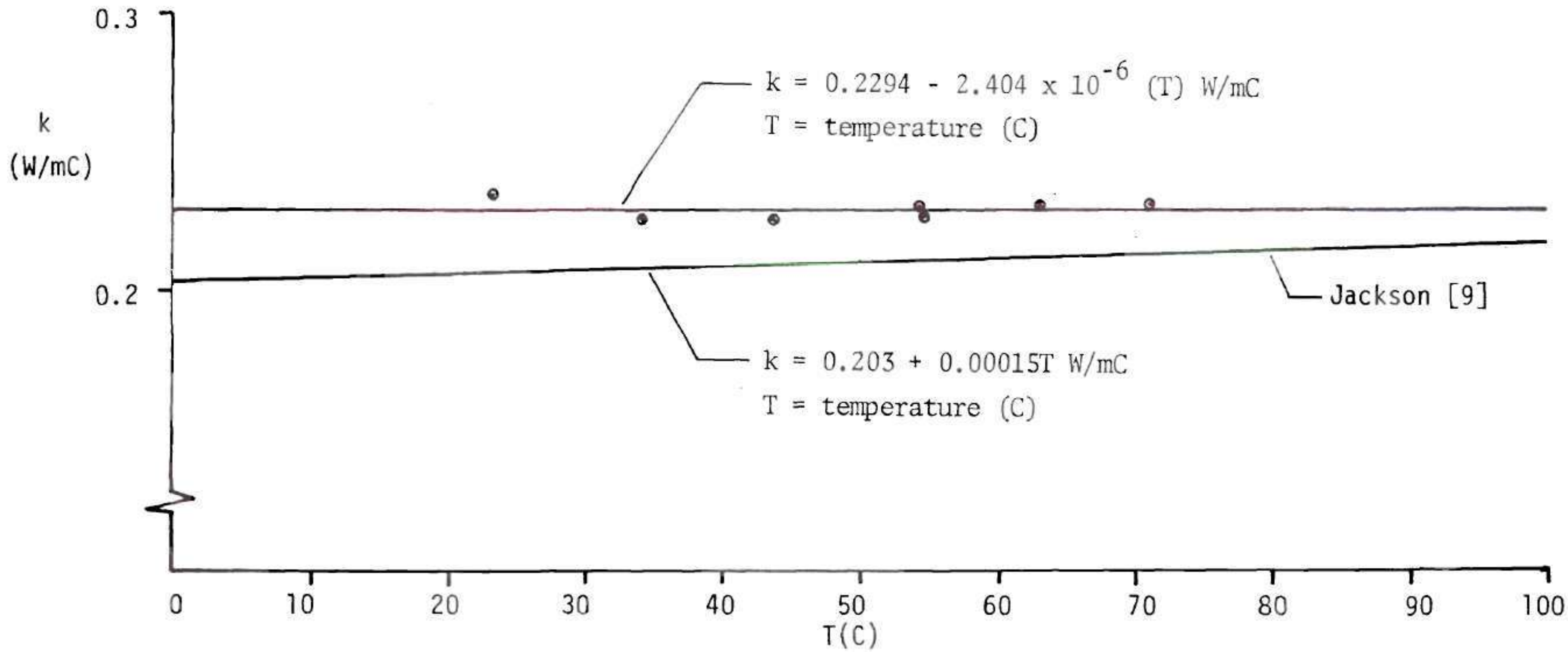

Figure 29. Thermal Conductivity of Polytetraflouroethylene (Teflon).

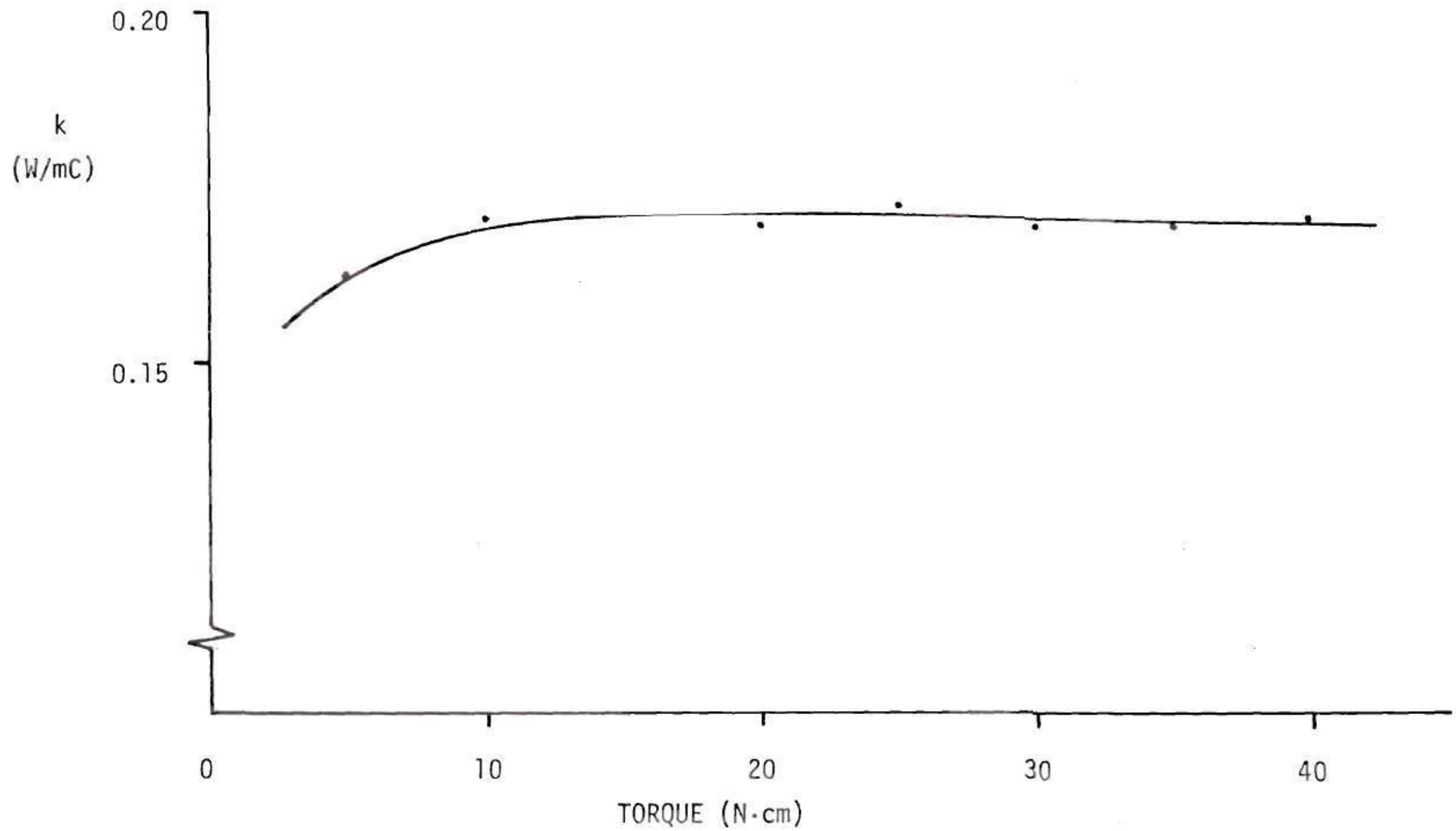

Figure 30. Results of Measurements for Thermal Conductivity as a Function of Applied Torque.

5.3 Repeatability of Measurements

Repeatability tests were conducted on various specimens at intervals ranging from several days to 2.5 months. Data within the same $\pm$ 5.0C increments was compared to insure the repeatability of the measurements. Table 1 shows the maximum percentage difference in the thermal conductivity for each specimen tested.

5.4. Carbon Fiber Thermal Conductivity

The results of the thermal conductivity of the carbon fiber/ epoxy resin composite test material are given in Figure 31. The temperature drop across each specimen and the number of observations for each test specimen are given in Table 2.

A first order least-squares fit for the data obtained results of

$$k = 7.211\ v_f + 0.170 \tag{35}$$

where v_f is dimensionless and k is in units of W/mC, which gives a thermal conductivity of 7.38 W/mC for the pure carbon fiber.

This result compares favorably with experimental data published by Kalnin [6] for other carbon fibers having a Young's modulus of about 25.3×10^6 N/m^2 (36×10^6 psi), which is the approximate value of Young's modulus of the carbon fibers measured in this thesis. Kalnin reports values of 9.4 W/mC for Union Carbide Thornel 300 fibers, 8.0 W/mC for Union Carbide Thornel 400 fibers, and 6.0 W/mC for Hercules Grafil A fibers.

Additionally, the thermal conductivity of the epoxy resin base material was determined to be 0.17 W/mC. This value also compares

Table 1. Summary of Repeatability Results

Sample	Maximum Percent Change in K	Number of Measurements
NBS Insulation	0.6	2
Epoxy Resin	3.6	9
Teflon	1.7	2

Table 2. Summary of Temperature Drop across Carbon Fiber/Epoxy Resin Composite Test Specimens.

v_f	ΔT	Number of Observations
0.0	21.40	5
0.50	2.35	5
0.60	2.80	11
0.65	5.44	8
0.70	5.15	29

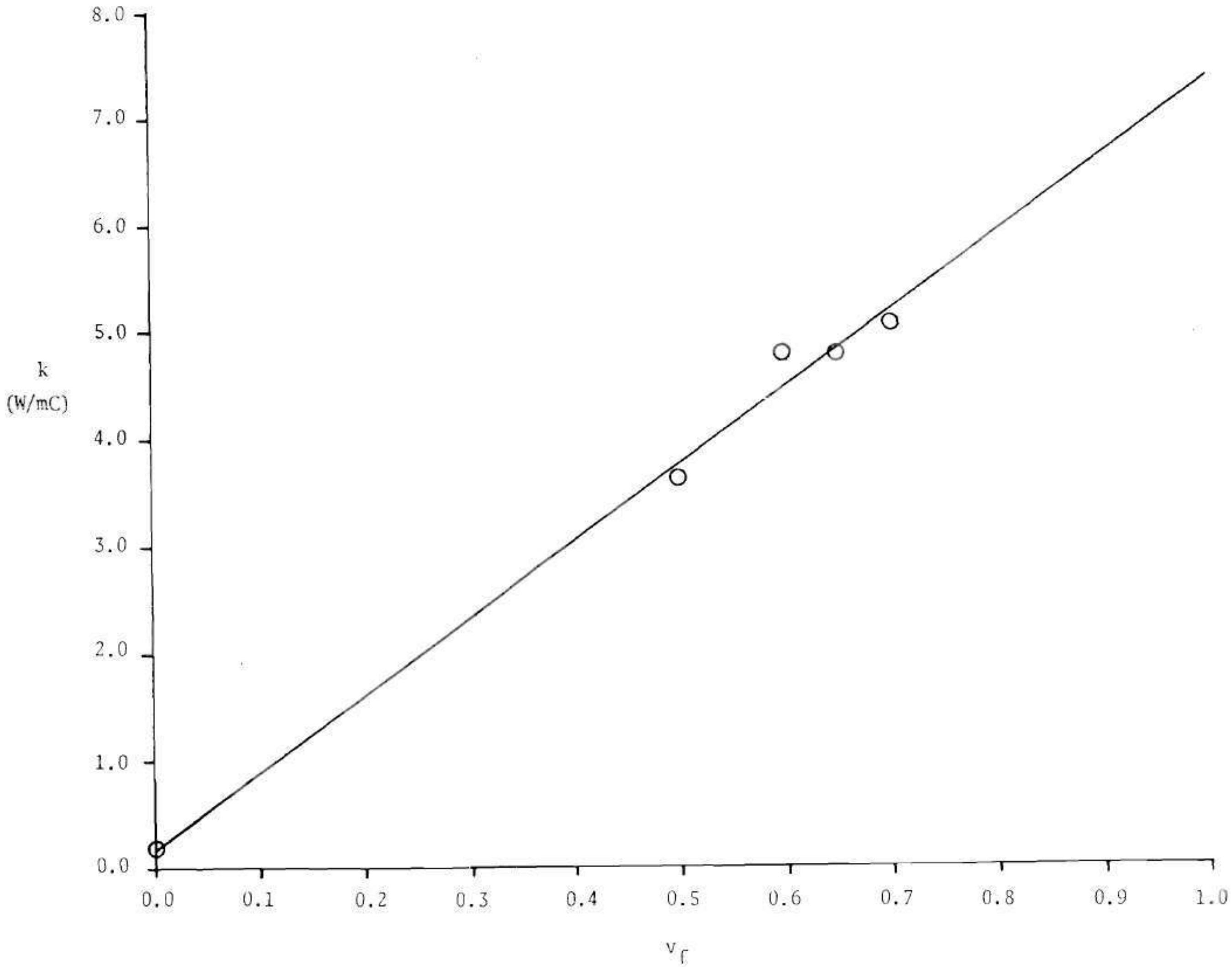

Figure 31. Carbon Fiber Thermal Conductivity.

favorably with the published values of from 0.17 to 0.23 W/mC [8, 31, 33, 34] for various types of epoxy resin materials.

CHAPTER VI

CONCLUSIONS

The results of the carbon fiber thermal conductivity tests show that good agreement was achieved with previously published data on carbon fibers having a similar Young's modulus. Furthermore, the thermal conductivity for a pure epoxy resin test specimen was also measured and compared with data available in the literature. These results suggest that the technique of measuring the thermal conductivity of the carbon fiber/epoxy resin test specimens with the guarded hot plate device is a reasonably accurate method of determining the thermal conductivity of the carbon fibers.

The data shown in Figure 31 provides a measure of the accuracy of the rule of mixtures. According to equation (9) the curve of thermal conductivity as a function of the volume fraction of the included material should be linear if the thermal model in actuality represents the geometry of the actual composite test specimens. The deviation from the straight line at higher volume fractions of carbon fiber may be attributed to two causes:

1) the low temperature differences across the test specimen which result at high carbon fiber volume contents reduced the accuracy of the test results;
2) the interaction of the carbon fibers at high volume fractions was not considered in the analog model used to predict the rule of mixtures.

An analytical error analysis was performed to estimate the maximum measurement and accuracy errors that could be expected when using the small guarded hot plate device. The results of this analysis have shown the measurement errors to be no larger than 3.695 percent and the accuracy errors to always be less than 7.184 percent.

The results of the pressure tests have shown that the torque applied to the pressure pads should not be less than 20 N·cm in order to insure good thermal contact between the test specimens and the heater surfaces.

An experimental error analysis has shown that for a polytetrafluoroethylene test specimen the data obtained with the guarded hot plate device was within 2.6 percent of the average of all data. For a standard insulation material, the guarded hot plate gave results which were within 1.5 percent of data measured on the same test specimen. Experimental repeatability tests showed that the results of the guarded hot plate were repeatable to within a maximum of 4.0 percent. These results indicate that the guarded hot plate device is a reliable and accurate method of determining thermal conductivity.

CHAPTER VII

RECOMMENDATIONS

Through the process of conducting the thermal conductivity measurements, several situations have arisen which require further investigation or attention:

1) There were no provisions in the design of the guarded hot plate to measure the sample thickness once the test specimen was inserted in the device. Therefore, when a compressible sample such as the NBS insulation material was used, the thickness of the specimen could not be accurately predicted from test to test. Measurements of the thermal conductivity on compressible specimens were therefore subject to possible large errors. A rigid spacer of known thickness and low thermal conductivity could be designed to provide a known sample thickness and prevent these errors.

The carbon fiber/epoxy resin test specimens were rigid and the thickness was accurately known so the sample thickness was never a problem.

2) It is suggested that the central heater wiring be replaced with a higher resistance wire so that higher voltage inputs to the central heater may be maintained. This modification will allow an increase in the temperature difference across the test specimen and a resulting increase in the accuracy of the measurements.

3) A statistical analysis of the experimental results may show that the 20 measurement requirement of Section 4.5 is too

restrictive and that the same results may be achieved by analyzing a smaller data base.

4) The greatest single difficulty with the measurement of the thermal conductivity of the carbon fiber/epoxy resin test specimens was the low value of ΔT obtained with the high volume fraction composite samples. It is suggested that a low volume fraction (less than 50 percent) of carbon fibers be employed in the fabrication of future samples in order to increase the temperature difference across the test specimen and thereby increase the accuracy of the thermal conductivity measurements.

5) Preliminary work indicates that the techniques used in the fabrication of the carbon fiber/epoxy resin test specimens may be used to manufacture other fiber composite samples. Thermal conductivity measurements on composite test specimens other than carbon fiber composite specimens may be used to strengthen the verification of the rule of mixtures [Equation (9)].

APPENDIX A

THERMAL CONDUCTIVITY OF A CUBIC ARRAY OF CUBIC INCLUSIONS

Appendix A presents the calculations for the determination of the thermal conductivity of a cube in a cubic array, which is discussed in Section 2.2.4. These results are derived by way of the series-parallel method of analog analysis. The basic geometry of this set of computations is shown in Figure 15 (geometry insert).

For an n by n by n matrix of cubes with each side having a length of x and an included cube of side d,

$$q = \frac{k_m (nx)^2 \Delta T}{nx} = k_m \; nx\Delta T \quad .$$

For the geometrical arrangement there are two thermal resistances in series, one for the area containing the inclusion and one for the base material.

$$R_{INCLUSION} = n \left(\frac{x-d}{k_e d^2} + \frac{d}{k_g d^2} \right) \quad ;$$

$$R_{BASE} = \frac{nx}{k_e (x^2 - d^2)} \quad .$$

For any parallel resistance of this type,

$$R = \frac{R_{INCLUSION}\ R_{BASE}}{R_{INCLUSION} + R_{BASE}} \quad .$$

Substitution for R gives:

$$R = \frac{\dfrac{n^2 x}{k_e(x^2-d^2)}\left(\dfrac{x-d}{k_e d^2} + \dfrac{d}{k_g d^2}\right)}{\dfrac{nx}{k_e(x^2-d^2)} + n\left(\dfrac{x-d}{k_e d^2} + \dfrac{d}{k_g d^2}\right)}$$

$$= \frac{\dfrac{nx}{k_e(x^2-d^2)}\left[\dfrac{(x-d)k_g + dk_e}{k_e k_g d^2}\right]}{\left[\dfrac{xk_g d^2 + (x-d)(x^2-d^2)k_g + dk_e(x^2-d^2)}{k_e k_g (x^2-d^2)d^2}\right]}$$

$$= \frac{\dfrac{nx}{k_e}\left[(x-d)k_g + dk_e\right]}{xk_g d^2 + (x-d)(x^2-d^2)k_g + dk_e(x^2-d^2)} \quad .$$

Recall

$$q = k_m nx\Delta T = \frac{n^2\Delta T}{R} = \frac{n^2\Delta T k_e[xk_g d^2 + (x-d)(x^2-d^2)k_g + dk_e(x^2-d^2)]}{nx[(x-d)k_g + dk_e]}$$

by the resistance analogy.

Therefore

$$k_m = \frac{k_e[x\,k_g d^2 + (x-d)(x^2-d^2)k_g + dk_e(x^2-d^2)]}{x^2[(x-d)k_g + dk_e]} .$$

Define $K_m = \frac{k_m}{k_e}$, $K_g = \frac{k_g}{k_e}$, and $v_f = \frac{d^3}{x^3}$.

Therefore, by substitution

$$K_m = \frac{\frac{1}{k_e}[xk_g d^2 + (x-d)(x^2-d^2)k_g + dk_e(x^2-d^2)]}{\frac{1}{k_e}x^2[(x-d)k_g + dk_e]}$$

$$= \frac{xK_g(v_f^{2/3}x^2) + (x-v_f^{1/3}x)(x^2-v_f^{2/3}x^2)K_g + (v_f^{1/3}x)(x^2-v_f^{2/3}x^2)}{x^2[(x-v_f^{1/3}x)K_g + v_f^{1/3}x]}$$

$$= \frac{x^3K_g v_f^{2/3} + (x^3-v_f^{2/3}x^3-v_f^{1/3}x^3+v_f x^3)K_g + v_f^{1/3}x^3 - v_f x^3}{x^3[(1-v_f^{1/3})K_g + v_f^{1/3}]}$$

$$= \frac{K_g v_f^{2/3} + K_g - K_g v_f^{2/3} - K_g v_f^{1/3} + K_g v_f + v_f^{1/3} - v_f}{K_g - v_f^{1/3}K_g + v_f^{1/3}}$$

$$= \frac{K_g + v_f^{1/3}(1-K_g) + v_f(K_g-1)}{K_g + v_f^{1/3}(1-K_g)}$$

so that

$$K_m = 1 + \frac{v_f(K_g-1)}{K_g + v_f^{1/3}(1-K_g)} \quad .$$

APPENDIX B

THERMAL CONDUCTIVITY OF A CUBIC ARRAY OF CYLINDRICAL INCLUSIONS

Appendix B presents the calculations for the determination of the thermal conductivity of cylindrical inclusions in a cubic array, which is discussed in section 2.2.5. These results are derived by way of the series-parallel method of analog analysis. The basic geometry for this set of computations is shown in Figure 17.

For any cylinder of length ℓ and diameter d contained in a cube of dimension x, the series resistance for the cylindrical portion of the network is given by:

$$R_{CYL} = n\left(\frac{x-\ell}{k_e \frac{\pi d^2}{4}} + \frac{\ell}{k_g \frac{\pi d^2}{4}}\right)$$

for an n by n by n array of cubic cells.

The resistance of the remaining base material is,

$$R_{BASE} = \frac{nx}{k_e\left(x^2 - \frac{\pi d^2}{4}\right)} \quad .$$

For this parallel resistance,

$$R = \frac{R_{CYL}\, R_{BASE}}{R_{CYL} + R_{BASE}} \quad ;$$

so that

$$R = \frac{\dfrac{n^2x}{k_e\, x^2 - \dfrac{\pi d^2}{4}}\left(\dfrac{x-\ell}{k_e} + \dfrac{\ell}{k_g}\right)\dfrac{4}{\pi d^2}}{\dfrac{nx}{k_e\left(x^2 - \dfrac{\pi d^2}{4}\right)} + \dfrac{4n}{\pi d^2}\left(\dfrac{x-\ell}{k_e} + \dfrac{\ell}{k_g}\right)} = \frac{\dfrac{4nx}{k_e \pi d^2\left(x^2 - \dfrac{\pi d^2}{4}\right)}\left[\dfrac{(x-\ell)k_g + k_e\ell}{k_e k_g}\right]}{\dfrac{x}{k_e\left(x^2 - \dfrac{\pi d^2}{4}\right)} + \dfrac{4}{\pi d^2}\left[\dfrac{(x-\ell)k_g + k_e\ell}{k_e k_g}\right]}$$

$$= \frac{\left\{\dfrac{4nx[(x-\ell)k_g + k_e\ell]}{k_e^2 k_g \pi d^2\left(x^2 - \dfrac{\pi d^2}{4}\right)}\right\}}{\left\{\dfrac{k_g \pi d^2 x + 4(x-\ell)k_g\left(x^2 - \dfrac{\pi d^2}{4}\right) + 4\ell k_e\left(x^2 - \dfrac{\pi d^2}{4}\right)}{k_e k_g \pi d^2\left(x^2 - \dfrac{\pi d^2}{4}\right)}\right\}} \quad .$$

Therefore

$$\frac{1}{R} = \frac{k_e\left[k_g \pi d^2 x + 4(x-\ell)k_g\left(x^2 - \dfrac{\pi d^2}{4}\right) + 4\ell k_e\left(x^2 - \dfrac{\pi d^2}{4}\right)\right]}{4nx[(x-\ell)k_g + \ell k_e]} \quad .$$

Recall, that by the resistance analogy

$$q = \frac{n^2 \Delta T}{R}$$

and by the Fourier law,

$$q = \frac{k_m (nx)^2 \Delta T}{nx} = k_m nx \Delta T \quad .$$

Therefore,

$$k_m = \frac{k_e\left[k_g \pi d^2 x + 4k_g(x-\ell)\left(x^2 - \frac{\pi d^2}{4}\right) + 4k_e\ell\left(x^2 - \frac{\pi d^2}{4}\right)\right]}{4x^2[(x-\ell)k_g + \ell k_e]} .$$

Define $K_m = \frac{k_m}{k_e}$, $K_g = \frac{k_g}{k_e}$, and $v_f = \frac{\pi d^2 \ell}{4x^3}$.

By substitution,

$$K_m = \frac{\frac{1}{k_e}\left[k_g \pi d^2 x + 4k_g(x-\ell)\left(x^2 - \frac{\pi d^2}{4}\right) + 4k_e\ell\left(x^2 - \frac{\pi d^2}{4}\right)\right]}{\frac{1}{k_e} 4x^2[(x-\ell)k_g + \ell k_e]}$$

$$= \frac{K_g \pi d^2 x + 4K_g(x-\ell)\left(x^2 - \frac{\pi d^2}{4}\right) + 4\ell\left(x^2 - \frac{\pi d^2}{4}\right)}{4x^2[(x-\ell)K_g + \ell]}$$

$$= \frac{K_g\left(\frac{4x^3 v_f}{\ell}\right)x + 4K_g(x-\ell)\left(x^2 - \frac{v_f x^3}{\ell}\right) + 4\ell\left(x^2 - \frac{v_f x^3}{\ell}\right)}{4x^2[(x-\ell)K_g + \ell]}$$

$$= \frac{4x^2 K_g\left(\frac{x^2 v_f}{\ell}\right) + 4K_g\left(x^3 - \frac{v_f x^4}{\ell} - \ell x^2 + v_f x^3\right) + 4(\ell x^2 - v_f x^3)}{4x^2[(x-\ell)K_g + \ell]}$$

$$= \frac{K_g\left(\frac{x^2 v_f}{\ell}\right) + K_g\left(x - \frac{v_f x^2}{\ell} - \ell + v_f x\right) + (\ell - v_f x)}{(x-\ell)K_g + \ell}$$

$$= \frac{K_g \frac{x v_f}{\ell} + K_g\left(1 - \frac{x v_f}{\ell} - \frac{\ell}{x} + v_f\right) + \left(\frac{\ell}{x} - v_f\right)}{\left(1 - \frac{\ell}{x}\right)K_g + \frac{\ell}{x}}$$

$$= \frac{K_g\left(1 - \frac{\ell}{x} + v_f\right) + \left(\frac{\ell}{x} - v_f\right)}{\left(1 - \frac{\ell}{x}\right)K_g + \frac{\ell}{x}} = \frac{K_g - K_g \frac{\ell}{x} + K_g v_f + \frac{\ell}{x} - v_f}{K_g - K_g \frac{\ell}{x} + \frac{\ell}{x}}$$

$$= \frac{K_g + \frac{\ell}{x}(1 - K_g) + v_f(K_g - 1)}{K_g + \frac{\ell}{x}(1 - K_g)} .$$

Finally,

$$K_m = 1 + \frac{v_f(K_g - 1)}{K_g + \frac{\ell}{x}(1 - K_g)} .$$

APPENDIX C

ERROR ANALYSIS

Appendix C presents the error and accuracy analyses based on the developments of Jackson [9]. For each of the analyses, the estimate of experimental conditions is designed to provide for a conservative estimate of the accuracy of the guarded hot plate device. Consequently, it is expected that the actual error of the device will be less than the error predicted by these calculations.

The edge loss errors are calculated from work by Jackson [9]. These errors are the result of heat flow from the edge of the test specimen to the surroundings. The edge loss error is given by

$$\varepsilon_e = \frac{k_{exp}}{k} - 1 \tag{36}$$

where

$$\left[\frac{k}{k_{exp}}\right]^{1/2} = \frac{\dfrac{\pi \ell}{L}}{e \ell n \left\{ \dfrac{\left[\text{COSH}\, \dfrac{\pi(g+\ell)}{L}\right] + 1}{\left[\text{COSH}\left(\dfrac{\pi g}{L}\right)\right] + 1} \right\} + (1-e)\, \ell n \left\{ \dfrac{\left[\text{COSH}\, \dfrac{\pi(g+\ell)}{L}\right] - 1}{\left[\text{COSH}\left(\dfrac{\pi g}{L}\right)\right] - 1} \right\}} \tag{37}$$

and

L = specimen thickness

g = guard ring width from the gap centerline (Figure 32)

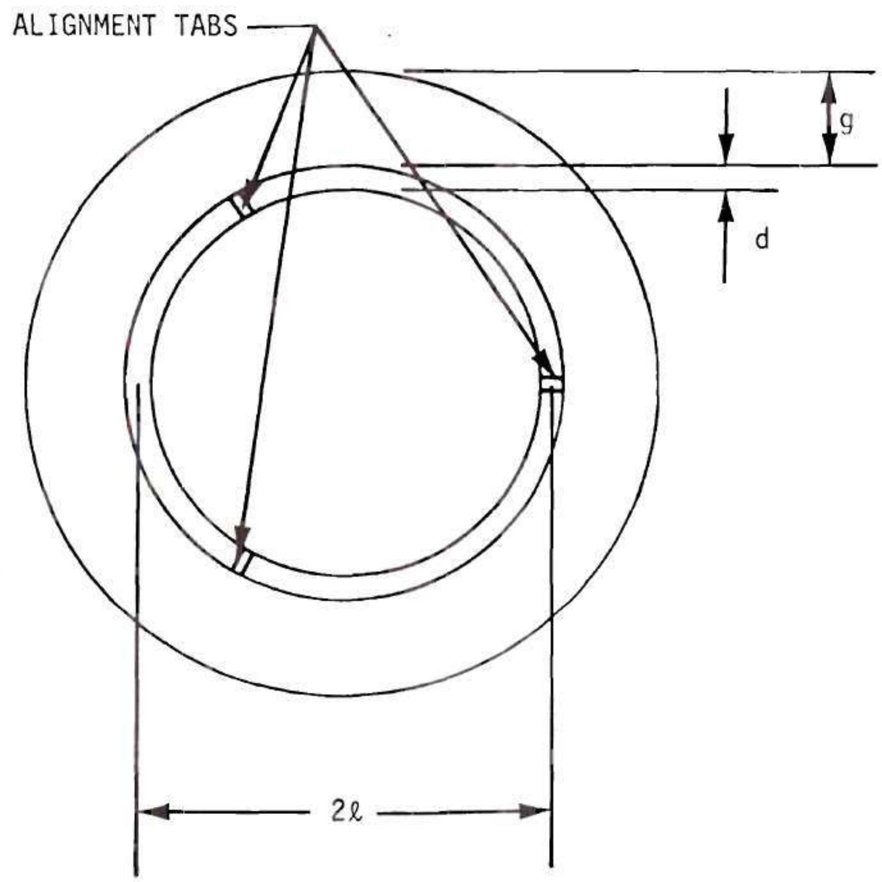

Figure 32. Central Heater Geometry.

2ℓ = diameter of the metering section from gap center to gap center (Figure 32)

k = actual specimen conductivity

k_{exp} = experimentally measured value of conductivity

e = proportionality between central heater temperature and actual specimen edge temperature, $0 < e < 1$.

For the guarded hot plate apparatus used in the carbon fiber thermal conductivity measurements:

$L \simeq 0.0127$ m

$g = 0.01405$ m

$2\ell = 0.02523$ m ($\ell = 0.01262$ m)

$e = 0.25$ (conservative estimate)

substitution of these values into Equation 37 gives

$$\left[\frac{k}{k_{exp}}\right]^{1/2} =$$

$$= \frac{0.99370\pi}{(0.25)\,\ell n\left[\frac{(\text{COSH } 2.1\pi)+1}{(\text{COSH } 1.1063\pi)+1}\right] + (0.75)\,\ell n\left[\frac{(\text{COSH } 2.1\pi)-1}{(\text{COSH } 1.1063\pi)-1}\right]}$$

$$= \frac{3.12180}{(0.25)\,\ell n\left(\frac{367.57358}{17.17313}\right) + (0.75)\,\ell n\left(\frac{365.57358}{15.17313}\right)} .$$

Therefore,

$$\frac{k}{k_{exp}} = \left[\frac{3.12180}{(0.25)(3.06358) + (0.75)(3.18194)}\right]^2 = 0.98071 \; .$$

Thus

$$\varepsilon_e = \frac{1}{0.98071} - 1 = 0.01967 \quad .$$

The thermal imbalance error due to a temperature difference between the guard and central heaters is given by Jackson [9] to be:

$$\varepsilon_g = \left[\frac{L}{2(\ell+g)}\right] \left[\frac{2(\ell+g)}{\ell}\right]^2 \left[\frac{1}{16(\ell+g)}\right] \left[\frac{T_h-T_g}{T_h-T_c}\right] \left\{\frac{q_o}{k} + \frac{\ell}{2(\ell+g)} \left[\frac{32(\ell+g)}{\pi}\right] \times \ln\left[\frac{4}{1-\exp\left(-\frac{2\pi d}{L}\right)}\right]\right\} \qquad (38)$$

where

d = guard gap width (Figure 32)

q_o = heat flow across the guard gap for a temperature imbalance of unity

$T_h - T_g$ = temperature difference between the central heater surface plates and the guard heater

$T_h - T_c$ = temperature difference across the specimen

Simplification of Equation (38) gives

$$\varepsilon_g = \left(\frac{L}{8\ell^2}\right)\left(\frac{T_h - T_g}{T_h - T_c}\right) \cdot \left\{\frac{q_o}{k} + \left(\frac{16\ell}{\pi}\right) \ell n \left[\frac{4}{1 - \exp\left(-\frac{2\pi d}{L}\right)}\right]\right\} .$$

The heat flow is a combination of all three modes of heat transfer so that

$$q_o = q_{convection} + q_{radiation} + q_{conduction} .$$

The convective heat transfer term represents the heat exchange by free convection. A correlation exists [2,9] between the Rayleigh number and the logarithm of the ratio of the equivalent thermal conductivity, k_{eq}, and the conductivity of the fluid under consideration.

The Rayleigh number for the geometry described in this theisis, based on air at 400K is 0.003, which results in $\log\left(\frac{k_{eq}}{k_f}\right) = 0$ [2]. Thus, heat transfer through the gas occurs by conduction only.

$$q_{convection} = \frac{kA}{d} \quad (T_h - T_g)$$

k = conductivity of fluid (0.03365 W/mC for air @ 400K)

$T_h - T_g$ = 0.1C for apparatus

d = 0.001 m

A = mean cross-sectional area of exchange

= thickness of central heater x parameter of metered area

= 0.00121 m^2

$q_{convection}$ = 0.00406 Watts .

The radiative heat transfer is estimated from

$$q_{radiation} = \sigma FA_1(T_h^4 - T_g^4)$$

where

σ = Stefan-Boltzmann constant = 5.729 x 10^{-8} W/m^2K^4

F = radiation shape factor between heat exchange surfaces and is equal to 1 for the case of the given geometry

A_1 = area of the emitting body = 0.00121 m^2

T_h = 400K

T_g = 399.9K .

By substitution,

$$q_{radiation} = 0.00177 \text{ Watts.}$$

The conduction term consists of heat transfer through the supports and lead wires. These are estimated as:

$$q_{conduction} = \frac{kA}{\Delta X}(T_h - T_g)$$

Wires:

Assume (conservative) 6 wires (copper) 0.0007m in diameter (k = 386 W/mK) x 0.001 m in length

$$q_{cond,wire} = \frac{6(386\ W/mk)(0.00035m)^2\pi\ (0.1K)}{0.001\ m}$$

$$= 0.08913\ W$$

ALIGNMENT TABS:

6 tabs (Teflon) 0.001 m x 0.00127m x 0.00127m

(k = 0.203 W/mK @ 0C)

$$q_{cond,tabs} = \frac{6(0.203\ W/mK)(0.00127m)^2(0.1K)}{0.001\ m} = 0.00020\ W$$

$$q_{conduction} = 0.08913\ W + 0.0002\ W = 0.08933\ W \quad .$$

Therefore,

$$q_o = q_{convection} + q_{radiation} + q_{conduction}$$

$$= 0.00406\ W + 0.00177\ W + 0.08933\ W = 0.09516\ W \quad .$$

The total thermal imbalance error is

$$\varepsilon_g = \left[\frac{0.0127m}{8(0.01262m)^2}\right]\left(\frac{0.1K}{10K}\right)\left\{\frac{0.9516\ W/K}{40\ W/mK} + \frac{16(0.01262m)}{\pi}\ \ln\left[\frac{4}{1 - \exp\left(-\dfrac{2\pi\cdot 0.001m}{0.0127m}\right)}\right]\right\}$$

$$= 0.01728.$$

Thus, making the total error,

$$\varepsilon_t = \varepsilon_e + \varepsilon_g = 0.01967 + 0.01728 = 0.03695$$

$$= 3.695\% \ .$$

The theoretical accuracy of the device, which incorporates measurements errors, is given by Jackson [9] as:

$$\Delta k = \frac{q}{(T_h - T_c)A}\,\Delta L + \frac{L\Delta q}{(T_h - T_c)A} + \frac{Lq}{A(T_h - T_c)^2}\,\Delta(T_h - T_c)$$

$$+ \frac{Lq}{A^2(T_h - T_c)}\,\Delta A \qquad (39)$$

where, for the device used,

$$q = \frac{kA\Delta T}{L} = 0.394 \quad W \simeq 0.4 \ W$$

$\Delta q = 0.000125$ W

$L = 0.01270$ m

$\Delta L = \pm\ 0.000005$ m

$(T_h - T_c) = 2.0C$

$\Delta(T_h - T_c) = \pm\ 0.10C$

$A = 0.0005\ m^2$

$\Delta A = 0.00001\ m^2$

$k = 5$ W/mC

ERROR DUE TO UNCERTAINTY IN SPECIMEN THICKNESS:

$$\frac{q\Delta L}{(T_h - T_c)A} = 0.0020 \text{ W/mC}$$

ERROR DUE TO UNCERTAINTY IN MEASUREMENT OF POWER INPUT:

$$\frac{L\Delta q}{(T_h - T_c)A} = 0.0016 \text{ W/mC}$$

ERROR DUE TO UNCERTAINTY IN MEASUREMENT OF TEMPERATURE DROP ACROSS SPECIMEN:

$$\frac{Lq\Delta(T_h - T_c)}{(T_h - T_c)^2 A} = 0.2540 \text{ W/mC}$$

ERROR IN METERING AREA:

$$\frac{Lq\Delta A}{A^2(T_h - T_c)} = 0.1016 \text{ W/mC}$$

$$\Delta k = 0.3592 \text{ W/mC}$$

$$\frac{\Delta k}{k} = 0.07184 = 7.184 \text{ percent}$$

Table 3. Summary of Error Analysis

	Percent
Edge Loss Error	1.967
Thermal Imbalance Error	1.728
Theoretical Accuracy	7.184
Total Estimated Error	10.879

APPENDIX D

SAMPLE DATA

Appendix D represents sample data taken during the experimental measurements of thermal conductivity. The numbers 1-8 on each data sheet refer to thermocouple locations in the experimental apparatus. These are:

1. central heater -- left side
2. central heater -- right side
3. central heater -- guard gap
4. guard heater -- guard gap
5. left back-up heater
6. right back-up heater
7. circulator reservoir
8. ambient air

It should be noted that the current and voltage recorded on the data sheets comprise the total input to the central heater. The specimen thickness, Δx, is the thickness of one test specimen. Therefore, since the power to the central heater is dissipated equally through both test specimens, the value of q used in the calculation of the $q\Delta x/A$ quantity is one-half of the value of the power shown on the left side of the sheet.

THERMAL CONDUCTIVITY DATA SHEET

Sample: NBS insulation

Date: 10/26/77
Observers: W. Moses

Sample Thickness 0.01174 m
Metered Area 0.0005 m^2
Current 0.04244 amps
Volts 1.0002 volts
Power 0.04245 W
Room Temperature 24.925 C
Water Temperature 5.4 C

$$k = \frac{q}{A}\frac{\Delta x}{T}$$

$\frac{q\Delta x}{A}$ = 0.49835 W/m

$\overline{k}$ = 0.0335 W/mC
$\overline{T}$ = 19.74 C

Regulated Temperature
Controller Settings:

Central/Guard Differential 10.0 | Left Cold Plate 66.0 | Right Cold Plate 68.0

Time: 8:25 pm T/C		Time: 8:55 pm T/C		Time: 9:25 pm T/C		Time: 9:55 pm T/C	
1	27.3	1	27.2	1	27.1	1	27.1
2	27.3	2	27.2	2	27.1	2	27.1
3	27.3	3	27.2	3	27.1	3	27.1
4	27.2	4	27.2	4	27.1	4	27.1
5	12.4	5	12.4	5	12.3	5	12.3
6	12.3	6	12.3	6	12.2	6	12.3
7	5.4	7	5.4	7	5.4	7	5.4
8	24.9	8	25.1	8	24.8	8	24.9

$\overline{T}_h$ = 27.30 C	$\overline{T}_h$ = 27.20 C	$\overline{T}_h$ = 27.10 C	$\overline{T}_h$ = 27.10 C
$\overline{T}_c$ = 12.35 C	$\overline{T}_c$ = 12.35 C	$\overline{T}_c$ = 12.25 C	$\overline{T}_c$ = 12.30 C
ΔT = 14.95 C	ΔT = 14.85 C	ΔT = 14.85 C	ΔT = 14.80 C
k = 0.0333 W/mC	k = 0.0336 W/mC	k = 0.0336 W/mC	k = 0.0337 W/mC
$\overline{T}$ = 19.83 C	$\overline{T}$ = 19.78 C	$\overline{T}$ = 19.68 C	$\overline{T}$ = 19.70 C

THERMAL CONDUCTIVITY DATA SHEET

Sample: Teflon

Date: 2/1/78
Observers: W. Moses

Sample Thickness 0.01036 m
Metered Area 0.0005 m^2
Current 0.08420 amps
Volts 2.012 volts
Power 0.16941 W
Room Temperature 22.58 C
Water Temperature 10.50 C

$k = \frac{q\,\Delta x}{A\,T}$ torque = 20 N-cm

$\frac{q\Delta x}{A}$ = 1.75425 W/m

$\overline{k}$ = 0.2343 W/mC
$\overline{T}$ = 23.64 C

Regulated Temperature Controller Settings:

Central/Guard Differential 481.8 Left Cold Plate 28.0 Right Cold Plate 29.9

Time: 2:40 pm T/C		Time: 3:11 pm T/C		Time: 3:45 pm T/C		Time: 4:15 pm T/C	
1	27.4	1	27.4	1	27.4	1	27.3
2	27.4	2	27.4	2	27.4	2	27.4
3	27.4	3	27.4	3	27.4	3	27.3
4	27.4	4	27.4	4	27.4	4	27.3
5	19.9	5	19.9	5	19.9	5	19.9
6	19.9	6	19.9	6	19.9	6	19.9
7	10.6	7	10.5	7	10.4	7	10.5
8	22.5	8	22.5	8	22.6	8	22.7

$\overline{T}_h$ = 27.40 C	$\overline{T}_h$ = 27.40 C	$\overline{T}_h$ = 27.40 C	$\overline{T}_h$ = 27.35 C
$\overline{T}_c$ = 19.90 C	$\overline{T}_c$ = 19.90 C	$\overline{T}_c$ = 19.90 C	$\overline{T}_c$ = 19.90 C
ΔT = 7.50 C	ΔT = 7.50 C	ΔT = 7.50 C	ΔT = 7.45 C
k = 0.2339 W/mC	k = 0.2339 W/mC	k = 0.2339 W/mC	k = 0.2355 W/mC
$\overline{T}$ = 23.65 C	$\overline{T}$ = 23.65 C	$\overline{T}$ = 23.65 C	$\overline{T}$ = 23.63 C

THERMAL CONDUCTIVITY DATA SHEET

Sample: Teflon

Date: 2/6/78 and 2/7/78
Observers: W. Moses

Sample Thickness 0.01036 m
Metered Area 0.0005 m^2
Current 0.14650 amps
Volts 3.500 volts
Power 0.51275 W
Room Temperature 24.02 C
Water Temperature 37.66 C

$k = \frac{q \Delta x}{A\ T}$ torque = 20 N-cm

$\frac{q\Delta x}{A}$ = 5.30953 W/m

$\overline{k}$ = 0.2267 W/mC
$\overline{T}$ = 54.48 C

Regulated Temperature
Controller Settings:

Central/Guard Differential 481.8 Left Cold Plate 46.0 Right Cold Plate 48.0

T/C (Time: 6:14 pm)		T/C (Time: 9:38 am)		T/C (Time: 10:08 am)		T/C (Time: 10:38 am)	
1	66.2	1	66.1	1	66.2	1	66.2
2	66.2	2	66.1	2	66.3	2	66.3
3	66.1	3	66.0	3	66.2	3	66.1
4	66.1	4	66.1	4	66.3	4	66.2
5	42.9	5	42.7	5	42.7	5	42.7
6	42.9	6	42.7	6	42.8	6	42.8
7	37.7	7	37.6	7	37.7	7	37.7
8	22.6	8	24.4	8	24.4	8	24.4

$\overline{T}_h$ = 66.20 C	$\overline{T}_h$ = 66.10 C	$\overline{T}_h$ = 66.15 C	$\overline{T}_h$ = 66.15 C
$\overline{T}_c$ = 42.90 C	$\overline{T}_c$ = 42.70 C	$\overline{T}_c$ = 42.75 C	$\overline{T}_c$ = 42.75 C
ΔT = 23.30 C	ΔT = 23.40 C	ΔT = 23.50 C	ΔT = 23.50 C
k = 0.2279 W/mC	k = 0.2269 W/mC	k = 0.2259 W/mC	k = 0.2259 W/mC
$\overline{T}$ = 54.55 C	$\overline{T}$ = 54.40 C	$\overline{T}$ = 54.50 C	$\overline{T}$ = 54.50 C

THERMAL CONDUCTIVITY DATA SHEET

Sample: Teflon

Date: 2/8/78
Observers: W. Moses

Sample Thickness	0.01036	m
Metered Area	0.0005	m^2
Current	0.16746	amps
Volts	3.998	volts
Power	0.66951	W
Room Temperature	24.22	C
Water Temperature	43.88	C

$k = \frac{q\,\Delta x}{A\,T}$ torque = 20 N-cm

$\frac{q\Delta x}{A}$ = 6.93273 W/m

$\bar{k}$ = 0.2308 W/mC

$\bar{T}$ = 62.89 C

Regulated Temperature
Controller Settings:

Central/Guard Differential 482.0 Left Cold Plate 50.2 Right Cold Plate 52.4

Time: 2:45 pm T/C		Time: 4:13 pm T/C		Time: 4:45 pm T/C		Time: 5:15 pm T/C	
1	77.8	1	77.9	1	77.9	1	77.9
2	77.9	2	77.9	2	78.0	2	78.0
3	77.7	3	77.8	3	77.8	3	77.8
4	77.6	4	77.8	4	77.8	4	77.8
5	47.9	5	47.9	5	47.9	5	47.9
6	47.8	6	47.9	6	47.8	6	47.9
7	43.8	7	43.9	7	43.9	7	43.8
8	24.3	8	24.5	8	24.2	8	24.2

$\bar{T}_h$ = 77.85 C	$\bar{T}_h$ = 77.90 C	$\bar{T}_h$ = 77.95 C	$\bar{T}_h$ = 77.95 C
$\bar{T}_c$ = 47.85 C	$\bar{T}_c$ = 47.90 C	$\bar{T}_c$ = 47.85 C	$\bar{T}_c$ = 47.90 C
ΔT = 30.00 C	ΔT = 30.00 C	ΔT = 30.10 C	ΔT = 30.05 C
k = 0.2311 W/mC	k = 0.2311 W/mC	k = 0.2302 W/mC	k = 0.2307 W/mC
$\bar{T}$ = 62.85 C	$\bar{T}$ = 62.90 C	$\bar{T}$ = 62.90 C	$\bar{T}$ = 62.93 C

THERMAL CONDUCTIVITY DATA SHEET

Sample: Teflon

Date: 2/8/78
Observers: W. Moses

Sample Thickness 0.01036 m

Metered Area 0.0005 m^2

Current 0.16746 amps

Volts 3.998 volts

Power 0.66951 W

Room Temperature 24.22 C

Water Temperature 43.88 C

$k = \frac{q}{A}\frac{\Delta x}{T}$ torque = 20 N-cm

$\frac{q\Delta x}{A}$ = 6.93273 W/m

$\overline{k}$ = 0.2308 W/mC

$\overline{T}$ = 62.89 C

Regulated Temperature Controller Settings:

Central/Guard Differential 482.0

Left Cold Plate 50.2

Right Cold Plate 52.4

Time: 5:45 pm T/C		Time: 6:42 pm T/C		Time: T/C		Time: T/C	
1	77.9	1	77.8	1		1	
2	78.0	2	77.9	2		2	
3	77.8	3	77.7	3		3	
4	77.8	4	77.7	4		4	
5	47.9	5	47.9	5		5	
6	47.9	6	47.8	6		6	
7	43.9	7	43.9	7		7	
8	24.1	8	24.0	8		8	

$\overline{T}_h$ = 77.95 C	$\overline{T}_h$ = 77.85 C	$\overline{T}_h$ = C	$\overline{T}_h$ = C
$\overline{T}_c$ = 47.9 C	$\overline{T}_c$ = 47.85 C	$\overline{T}_c$ = C	$\overline{T}_c$ = C
ΔT = 30.05 C	ΔT = 30.00 C	ΔT = C	ΔT = C
k = 0.2307 W/mC	k = 0.2311 W/mC	k = W/mC	k = W/mC
$\overline{T}$ = 62.93 C	$\overline{T}$ = 62.85 C	$\overline{T}$ = C	$\overline{T}$ = C

THERMAL CONDUCTIVITY DATA SHEET

Sample: Epoxy Resin

Date: 11/29/77
Observers: W. Moses

Sample Thickness	0.01270	m
Metered Area	0.0005	m^2
Current	0.10967	amps
Volts	2.599	volts
Power	0.28503	W
Room Temperature	22.36	C
Water Temperature	12.50	C

$k = \frac{q \Delta x}{A\ T}$ torque = 20 N-cm

$\frac{q\Delta x}{A}$ = 3.61902 W/m

$\overline{k}$ = 0.1691 W/mC

$\overline{T}$ = 25.29 C

Regulated Temperature Controller Settings:

Central/Guard Differential 483.0 | Left Cold Plate 25.0 | Right Cold Plate 26.3

T/C (Time: 3:20 pm)		T/C (Time: 3:59 pm)		T/C (Time: 4:30 pm)		T/C (Time: 5:00 pm)	
1	36.0	1	36.0	1	35.9	1	35.9
2	36.1	2	36.1	2	36.0	2	36.0
3	36.0	3	36.0	3	35.8	3	35.9
4	36.0	4	36.0	4	35.7	4	35.9
5	14.6	5	14.6	5	14.5	5	14.6
6	14.6	6	14.6	6	14.6	6	14.6
7	12.5	7	12.5	7	12.4	7	12.5
8	22.6	8	21.8	8	22.8	8	22.3

	3:20 pm	3:59 pm	4:30 pm	5:00 pm
$\overline{T}_h$ =	36.05 C	36.05 C	35.95 C	35.95 C
$\overline{T}_c$ =	14.60 C	14.60 C	14.55 C	14.60 C
ΔT =	21.45 C	21.45 C	21.40 C	21.35 C
k =	0.1687 W/mC	0.1687 W/mC	0.1691 W/mC	0.1695 W/mC
$\overline{T}$ =	25.33 C	25.33 C	25.25 C	25.28 C

THERMAL CONDUCTIVITY DATA SHEET

Sample: Epoxy Resin

Date: 11/29/77
Observers: W. Moses

Sample Thickness 0.01270 m
Metered Area 0.0005 m^2
Current 0.10967 amps
Volts 2.599 volts
Power 0.28503 W
Room Temperature 22.36 C
Water Temperature 12.50 C

$k = \frac{q\,\Delta x}{A\,T}$ torque = 20 N-cm

$\frac{q\Delta x}{A}$ = 3.61902 W/m

$\overline{k}$ = 0.1691 W/mC
$\overline{T}$ = 25.29 C

Regulated Temperature Controller Settings:

Central/Guard Differential 483.0
Left Cold Plate 25.0
Right Cold Plate 26.3

Time: 5:30 pm T/C		Time: ___ T/C		Time: ___ T/C		Time: ___ T/C	
1	35.9	1		1		1	
2	36.0	2		2		2	
3	35.9	3		3		3	
4	36.0	4		4		4	
5	14.6	5		5		5	
6	14.6	6		6		6	
7	12.6	7		7		7	
8	22.3	8		8		8	

$\overline{T}_h$ = 35.95 C	$\overline{T}_h$ = ___ C	$\overline{T}_h$ = ___ C	$\overline{T}_h$ = ___ C
$\overline{T}_c$ = 14.60 C	$\overline{T}_c$ = ___ C	$\overline{T}_c$ = ___ C	$\overline{T}_c$ = ___ C
ΔT = 21.35 C	ΔT = ___ C	ΔT = ___ C	ΔT = ___ C
k = 0.1695 W/mC	k = ___ W/mC	k = ___ W/mC	k = ___ W/mC
$\overline{T}$ = 25.28 C	$\overline{T}$ = ___ C	$\overline{T}$ = ___ C	$\overline{T}$ = ___ C

THERMAL CONDUCTIVITY DATA SHEET

Sample: Epoxy Resin

Date: 11/30/77

Observers: W. Moses

Sample Thickness	0.01270	m
Metered Area	0.0005	m^2
Current	0.10967	amps
Volts	2.600	volts
Power	0.28514	W
Room Temperature	22.88	C
Water Temperature	12.53	C

$k = \frac{q}{A}\frac{\Delta x}{T}$ torque = 25 N-cm

$\frac{q\Delta x}{A}$ = 3.62041 W/m

$\overline{k}$ = 0.1722 W/mC

$\overline{T}$ = 25.06 C

Regulated Temperature Controller Settings:

Central/Guard Differential 483.0 Left Cold Plate 25.0 Right Cold Plate 26.3

Time: 8:54 am T/C		Time: 9:26 am T/C		Time: 9:58 am T/C		Time: 10:35 am T/C	
1	35.6	1	35.5	1	35.5	1	35.5
2	35.7	2	35.6	2	35.6	2	35.6
3	35.6	3	35.5	3	35.5	3	35.5
4	35.6	4	35.5	4	35.5	4	35.4
5	14.5	5	14.5	5	14.5	5	14.5
6	14.6	6	14.6	6	14.6	6	14.6
7	12.6	7	12.5	7	12.5	7	12.5
8	22.8	8	22.9	8	22.9	8	22.9

$\overline{T}_h$ =	35.65 C	$\overline{T}_h$ =	35.55 C	$\overline{T}_h$ =	35.55 C	$\overline{T}_h$ =	35.55 C
$\overline{T}_c$ =	14.55 C	$\overline{T}_c$ =	14.55 C	$\overline{T}_c$ =	14.55 C	$\overline{T}_c$ =	14.55 C
ΔT =	21.10 C	ΔT =	21.00 C	ΔT =	21.00 C	ΔT =	21.00 C
k =	0.1716 W/mC	k =	0.1724 W/mC	k =	0.1724 W/mC	k =	0.1724 W/mC
$\overline{T}$ =	25.10 C	$\overline{T}$ =	25.05 C	$\overline{T}$ =	25.05 C	$\overline{T}$ =	25.05 C

THERMAL CONDUCTIVITY DATA SHEET

Sample: Epoxy Resin

Date: 12/1/77

Observers: W. Moses

Sample Thickness 0.01270 m

Metered Area 0.0005 m^2

Current 0.10980 amps

Volts 2.600 volts

Power 0.28548 W

Room Temperature 23.88 C

Water Temperature 12.50 C

$k = \frac{q \Delta x}{A \Delta T}$ torque = 35 N-cm

$\frac{q \Delta x}{A}$ = 3.62470 W/m

$\overline{k}$ = 0.1662 W/mC

$\overline{T}$ = 25.29 C

Regulated Temperature Controller Settings:

Central/Guard Differential 483.0

Left Cold Plate 25.0

Right Cold Plate 26.0

Time: 10:51 am T/C		Time: 11:31 am T/C		Time: 12:22 pm T/C		Time: 12:57 pm T/C	
1	36.0	1	36.1	1	36.2	1	36.2
2	36.1	2	36.2	2	36.3	2	36.3
3	36.0	3	36.1	3	36.2	3	36.2
4	36.0	4	36.2	4	36.4	4	36.3
5	14.4	5	14.4	5	14.4	5	14.4
6	14.4	6	14.4	6	14.3	6	14.4
7	12.5	7	12.5	7	12.5	7	12.5
8	23.4	8	23.0	8	24.0	8	24.3

$\overline{T}_h$ = 36.05 C	$\overline{T}_h$ = 36.15 C	$\overline{T}_h$ = 36.25 C	$\overline{T}_h$ = 36.25 C
$\overline{T}_c$ = 14.40 C	$\overline{T}_c$ = 14.40 C	$\overline{T}_c$ = 14.35 C	$\overline{T}_c$ = 14.40 C
ΔT = 21.65 C	ΔT = 21.75 C	ΔT = 21.90 C	ΔT = 21.85 C
k = 0.1674 W/mC	k = 0.1667 W/mC	k = 0.1655 W/mC	k = 0.1659 W/mC
$\overline{T}$ = 25.23 C	$\overline{T}$ = 25.28 C	$\overline{T}$ = 25.30 C	$\overline{T}$ = 25.33 C

THERMAL CONDUCTIVITY DATA SHEET

Sample: Epoxy Resin

Date: 12/1/77
Observers: W. Moses

Sample Thickness 0.01270 m
Metered Area 0.0005 m^2
Current 0.10980 amps
Volts 2.600 volts
Power 0.28548 W
Room Temperature 23.88 C
Water Temperature 12.55 C

$k = \frac{q}{A}\frac{\Delta x}{T}$ torque = 35 N-cm

$\frac{q\Delta x}{A}$ = 3.62470 W/m

$\bar{k}$ = 0.1662 W/mC
$\bar{T}$ = 25.29 C

Regulated Temperature
Controller Settings:

Central/Guard Differential 483.0 Left Cold Plate 25.0 Right Cold Plate 26.0

Time: 1:31 pm T/C		Time: 2:59 pm T/C		Time: T/C		Time: T/C	
1	36.2	1	36.2	1		1	
2	36.3	2	36.3	2		2	
3	36.2	3	36.2	3		3	
4	36.3	4	36.4	4		4	
5	14.4	5	14.4	5		5	
6	14.3	6	14.3	6		6	
7	12.5	7	12.5	7		7	
8	24.3	8	24.3	8		8	

$\bar{T}_h$ = 36.25 C	$\bar{T}_h$ = 36.25 C	$\bar{T}_h$ = C	$\bar{T}_h$ = C
$\bar{T}_c$ = 14.35 C	$\bar{T}_c$ = 14.35 C	$\bar{T}_c$ = C	$\bar{T}_c$ = C
ΔT = 21.90 C	ΔT = 21.90 C	ΔT = C	ΔT = C
k = 0.1659 W/mC	k = 0.1659 W/mC	k = W/mC	k = W/mC
$\bar{T}$ = 25.30 C	$\bar{T}$ = 25.30 C	$\bar{T}$ = C	$\bar{T}$ = C

THERMAL CONDUCTIVITY DATA SHEET

Sample: X-37 (50% carbon fiber)

Date: 11/21/77

Observers: W. Moses

Sample Thickness 0.01270 m

Metered Area 0.0005 m^2

Current 0.16838 amps

Volts 4.001 volts

Power 0.67369 W

Room Temperature 23.92 C

Water Temperature 12.78 C

$k = \frac{q \Delta x}{A\ T}$ torque = 20 N-cm

$\frac{q\Delta x}{A}$ = 8.55879 W/m

$\overline{k}$ = 3.6420 W/mC

$\overline{T}$ = 20.67 C

Regulated Temperature Controller Settings:

Central/Guard Differential 478.5

Left Cold Plate 28.7

Right Cold Plate 29.6

Time: 2:05 pm T/C		Time: 2:35 pm T/C		Time: 3:05 pm T/C		Time: 3:40 pm T/C	
1	21.7	1	21.7	1	21.7	1	21.7
2	22.0	2	21.9	2	22.0	2	22.0
3	21.7	3	21.7	3	21.7	3	21.7
4	21.7	4	21.7	4	21.7	4	21.7
5	19.5	5	19.4	5	19.5	5	19.5
6	19.5	6	19.5	6	19.5	6	19.5
7	12.8	7	12.7	7	12.8	7	12.8
8	23.9	8	23.7	8	24.0	8	24.3

2:05 pm	2:35 pm	3:05 pm	3:40 pm
$\overline{T}_h$ = 21.85 C	$\overline{T}_h$ = 21.80 C	$\overline{T}_h$ = 21.85 C	$\overline{T}_h$ = 21.85 C
$\overline{T}_c$ = 19.50 C	$\overline{T}_c$ = 19.45 C	$\overline{T}_c$ = 19.50 C	$\overline{T}_c$ = 19.50 C
ΔT = 2.35 C	ΔT = 2.35 C	ΔT = 2.35 C	ΔT = 2.35 C
k = 3.6420 W/mC	k = 3.6420 W/mC	k = 3.6420 W/mC	k = 3.6420 W/mC
$\overline{T}$ = 20.68 C	$\overline{T}$ = 20.63 C	$\overline{T}$ = 20.68 C	$\overline{T}$ = 20.68 C

THERMAL CONDUCTIVITY DATA SHEET

Sample: X-37 (50% carbon fiber)

Date: 11/21/77
Observers: W. Moses

Sample Thickness 0.01270 m
Metered Area 0.0005 m^2
Current 0.16838 amps
Volts 4.001 volts
Power 0.67369 W
Room Temperature 23.92 C
Water Temperature 12.78 C

$k = \frac{q\,\Delta x}{A\,T}$ torque = 20 N-cm

$\frac{q\Delta x}{A}$ = 8.55879 W/m

$\bar{k}$ = 3.6420 W/mC
$\bar{T}$ = 20.67 C

Regulated Temperature
Controller Settings:

Central/Guard Differential 478.5
Left Cold Plate 28.7
Right Cold Plate 29.6

Time: 4:15 pm T/C		Time: T/C		Time: T/C		Time: T/C	
1	21.7	1		1		1	
2	22.0	2		2		2	
3	21.7	3		3		3	
4	21.7	4		4		4	
5	19.5	5		5		5	
6	19.5	6		6		6	
7	12.8	7		7		7	
8	23.7	8		8		8	

$\bar{T}_h$ = 21.85 C	$\bar{T}_h$ = C	$\bar{T}_h$ = C	$\bar{T}_h$ = C
$\bar{T}_c$ = 19.50 C	$\bar{T}_c$ = C	$\bar{T}_c$ = C	$\bar{T}_c$ = C
ΔT = 2.35 C	ΔT = C	ΔT = C	ΔT = C
k = 3.6420 W/mC	k = W/mC	k = W/mC	k = W/mC
$\bar{T}$ = 20.68 C	$\bar{T}$ = C	$\bar{T}$ = C	$\bar{T}$ = C

THERMAL CONDUCTIVITY DATA SHEET

Sample: X-35 (60% carbon fiber)

Date: 11/21/77

Observers: W. Moses

Sample Thickness 0.01269 m

Metered Area 0.0005 m^2

Current 0.21070 amps

Volts 5.001 volts

Power 1.05371 W

Room Temperature 23.08 C

Water Temperature 12.10 C

$k = \frac{q\,\Delta x}{A\,T}$ torque = 20 N-cm

$\frac{q\Delta x}{A}$ = 13.3674 W/m

$\overline{k}$ = 4.7862 W/mC

$\overline{T}$ = 20.46 C

Regulated Temperature Controller Settings:

Central/Guard Differential 478.0   Left Cold Plate 28.2   Right Cold Plate 29.3

Time: 9:25 pm T/C		Time: 9:55 pm T/C		Time: 10:30 pm T/C		Time: 11:00 pm T/C	
1	21.7	1	21.7	1	21.7	1	21.7
2	22.1	2	22.1	2	22.1	2	22.1
3	21.7	3	21.7	3	21.7	3	21.7
4	21.7	4	21.8	4	21.8	4	21.7
5	19.1	5	19.1	5	19.1	5	19.0
6	19.0	6	19.1	6	19.1	6	19.0
7	12.1	7	12.1	7	12.1	7	12.1
8	22.9	8	23.1	8	23.1	8	23.2

9:25 pm	9:55 pm	10:30 pm	11:00 pm
$\overline{T}_h$ = 21.90 C	$\overline{T}_h$ = 21.90 C	$\overline{T}_h$ = 21.90 C	$\overline{T}_h$ = 21.90 C
$\overline{T}_c$ = 19.05 C	$\overline{T}_c$ = 19.10 C	$\overline{T}_c$ = 19.10 C	$\overline{T}_c$ = 19.00 C
ΔT = 2.85 C	ΔT = 2.80 C	ΔT = 2.80 C	ΔT = 2.90 C
k = 4.6903 W/mC	k = 4.7741 W/mC	k = 4.7741 W/mC	k = 4.6094 W/mC
$\overline{T}$ = 20.48 C	$\overline{T}$ = 20.50 C	$\overline{T}$ = 20.50 C	$\overline{T}$ = 20.45 C

THERMAL CONDUCTIVITY DATA SHEET

Sample: X-35 (60% carbon fiber)

Date: 11/22/77

Observers: W. Moses

Sample Thickness 0.01269 m

Metered Area 0.0005 m^2

Current 0.21070 amps

Volts 5.001 volts

Power 1.05371 W

Room Temperature 23.85 C

Water Temperature 12.10 C

$k = \frac{q \Delta x}{A T}$ torque = 20 N-cm

$\frac{q\Delta x}{A}$ = 13.3674 W/m

$\overline{k}$ = 4.7862 W/mC

$\overline{T}$ = 20.46 C

Regulated Temperature Controller Settings:

Central/Guard Differential 478.0 Left Cold Plate 28.3 Right Cold Plate 29.4

Time: 10:00 am T/C		Time: 10:30 am T/C		Time: 11:00 am T/C		Time: 11:35 am T/C	
1	21.5	1	21.6	1	21.7	1	21.7
2	21.9	2	22.0	2	22.1	2	22.1
3	21.6	3	21.7	3	21.7	3	21.7
4	21.6	4	21.6	4	21.7	4	21.8
5	19.0	5	19.1	5	19.1	5	19.0
6	19.0	6	19.1	6	19.1	6	19.0
7	12.1	7	12.2	7	12.1	7	12.0
8	24.0	8	24.0	8	23.8	8	23.6

10:00 am	10:30 am	11:00 am	11:35 am
$\overline{T}_h$ = 21.70 C	$\overline{T}_h$ = 21.80 C	$\overline{T}_h$ = 21.90 C	$\overline{T}_h$ = 21.90 C
$\overline{T}_c$ = 19.00 C	$\overline{T}_c$ = 19.10 C	$\overline{T}_c$ = 19.10 C	$\overline{T}_c$ = 19.00 C
ΔT = 2.70 C	ΔT = 2.70 C	ΔT = 2.80 C	ΔT = 2.90 C
k = 4.9509 W/mC	k = 4.9509 W/mC	k = 4.7741 W/mC	k = 4.6094 W/mC
$\overline{T}$ = 20.35 C	$\overline{T}$ = 20.45 C	$\overline{T}$ = 20.50 C	$\overline{T}$ = 20.45 C

THERMAL CONDUCTIVITY DATA SHEET

Sample: X-35 (60% carbon fiber)

Date: 11/22/77

Observers: W. Moses

Sample Thickness 0.01269 m

Metered Area 0.0005 m^2

Current 0.21070 amps

Volts 5.0001 volts

Power 1.05377 W

Room Temperature 23.90 C

Water Temperature 12.10 C

$k = \frac{q}{A}\frac{\Delta x}{T}$ torque = 20 N-cm

$\frac{q\Delta x}{A}$ = 13.3674 W/m

$\bar{k}$ = 4.7862 W/mC

$\bar{T}$ = 20.46 C

Regulated Temperature Controller Settings:

Central/Guard Differential 478.0

Left Cold Plate 28.3

Right Cold Plate 29.4

Time: 2:25 pm T/C		Time: 3:32 pm T/C		Time: 4:08 pm T/C		Time: T/C	
1	21.8	1	21.5	1	21.6	1	
2	22.1	2	21.9	2	22.0	2	
3	21.7	3	21.5	3	21.6	3	
4	21.9	4	21.4	4	21.5	4	
5	19.0	5	19.0	5	19.1	5	
6	19.1	6	19.1	6	19.0	6	
7	12.1	7	12.1	7	12.1	7	
8	23.9	8	23.8	8	24.0	8	

$\bar{T}_h$ = 21.95 C	$\bar{T}_h$ = 21.70 C	$\bar{T}_h$ = 21.80 C	$\bar{T}_h$ = C
$\bar{T}_c$ = 19.05 C	$\bar{T}_c$ = 19.05 C	$\bar{T}_c$ = 19.05 C	$\bar{T}_c$ = C
ΔT = 2.90 C	ΔT = 2.65 C	ΔT = 2.75 C	ΔT = C
k = 4.6094 W/mC	k = 5.0443 W/mC	k = 4.8609 W/mC	k = W/mC
$\bar{T}$ = 20.50 C	$\bar{T}$ = 20.38 C	$\bar{T}$ = 20.43 C	$\bar{T}$ = C

APPENDIX E

NOMENCLATURE

Latin Symbols

Symbol	Description	Typical Units
A	Cross-sectional area perpendicular to the direction of heat flow	m^2
	metered area of central heater	m^2
a	length of cube side (Section 2.2.3)	m
b	radius of sphere (Section 2.2.3)	m
c	specific heat	J/kgC
d	length of side of included square (Section 2.2.2)	m
	length of side of included cube (Section 2.2.4)	m
	diameter of included cylinder (Section 2.2.5)	m
	guard gap width (Appendix C)	m
E	controller error signal	V
e	proportionality between central heater and actual specimen edge temperature	--
Δe	electrical potential difference	V
F	radiation shape factor	--
g	guard ring width from gap centerline	m
i	electrical current	amp
K_g	k_g/k_e	--
K_m	k_m/k_e	--
k	thermal conductivity	W/mC

k_c	proportional sensitivity	--
k_e	thermal conductivity of the base material (epoxy resin)	W/mC
k_{eq}	equivalent thermal conductivity combining all modes of heat transfer	W/mC
k_{exp}	experimentally measured thermal conductivity	W/mC
k_f	thermal conductivity of a fluid	W/mC
k_g	thermal conductivity of included material (carbon fiber)	W/mC
k_i	electrical conductivity	$1/\Omega$
k_m	thermal conductivity of composite material	W/mC
k_o	thermal conductivity at T = 0	W/mC
Δk	change in thermal conductivity	W/mC
L	distance between two isothermal planes	m
	thickness of test specimen	m
ℓ	conductor length (Section 2.2.1)	m
	length of included cylinder (Section 2.2.5)	m
	radius of metering section (Appendix C)	m
M	controller output signal	V
n	number of individual cells in an analog array	--
P	compressive force	N
Q	heat of vaporization	kJ/kg
q	rate of heat transfer between isothermal surfaces	W
$q_{conduction}$	rate of heat transfer by conduction	W
$q_{convection}$	rate of heat transfer by convection	W
q_o	total rate of heat transfer	W
$q_{radiation}$	rate of heat transfer by thermal radiation	W

R	thermal resistance	mC/W
	radius of test specimen (Section 4.3.2)	m
R_{BASE}	thermal resistance of base material (epoxy resin)	mC/W
R_{CYL}	thermal resistance of cylindrical inclusion	mC/W
R_e	electrical resistivity	Ω
$R_{INCLUSION}$	thermal resistance of cubic inclusions	mC/W
R_{PS}	thermal resistance determined by the parallel-series method	mC/W
R_{SP}	thermal resistance determined by the series-parallel method	mC/W
r	radius of threaded rod on pressure pad	m
s	any selected complex variable	--
T	temperature	C
T_a	end temperature of Kohlrausch test specimen	C
T_c	temperature of low temperature isothermal plane	C
T_D	rate time	S
T_g	temperature of guard heater	C
T_h	temperature of high temperature isothermal plane	C
T_I	reciprocal of reset control	s
T_m	center temperature of Kohlrausch test specimen	C
$\bar{T}$	mean temperature $\frac{T_H + T_C}{2}$	C
ΔT	temperature difference between isothermal planes	C
t	time	s
V	voltage drop across central heater	V
v_f	volume fraction of included material	--
x	length of side of cube	m

Greek Symbols

Symbol	Description	Typical Units
α	thermal diffusivity	m^2/s
β	temperature coefficient of thermal conductivity	1/C
γ	$\frac{1}{Kg - 1}\left(\frac{4\pi}{3v_f}\right)^{2/3}\frac{1}{\pi}$	--
ε_e	edge loss error	--
ε_g	thermal imbalance error	--
ε_t	$\varepsilon_e + \varepsilon_g$	--
η	outward drawn normal to a surface	m
θ	reference angle (Figure 12)	rad
μ	coefficient of kinetic friction	--
ρ	volumetric density	Kg/m^3
σ	compressive stress	N/m^2
	Stefan-Boltzmann constant	W/m^2K^4
τ	torque	$N \cdot cm$

REFERENCES

1. Chambers, William E., "Low-Cost High-Performance Carbon Fibers", Mechanical Engineering, 97, no. 12, December 1975, p. 37.

2. Eckert, E. R. G., and Robert M. Drake, Analysis of Heat and Mass Transfer, New York, McGraw-Hill Book Co., 1972.

3. Carslaw, H. S., and J. C. Jaeger, Conduction of Heat in Solids, 2nd ed., Oxford, Clarendon Press, 1959.

4. Jakob, Max, Heat Transfer, 1, New York, John Wiley and Sons, Inc., 1949.

5. Kreith, Frank, Principles of Heat Transfer, 3rd ed., New York, Intext Educational Publishers, 1973.

6. Kalnin, I. L., "Thermal Conductivity of High-Modulus Carbon Fibers", Composite Reliability, ASTM STP 580, American Society for Testing and Materials, 1975, p. 560.

7. Schroder, J., "Apparatus for Determining the Thermal Conductivity of Solids in the Temperature Range from 20 to 200C", The Review of Scientific Instruments, 34, no. 6, 1963, p. 615.

8. Lee, H. J., and R. E. Taylor, "Thermophysical Properties of Carbon Graphite Fibers and Mod-3 Fiber-Reinforced Graphite", Carbon 1187.

9. Jackson, Kenneth W., Development of a Guarded Hot Plate Thermal Conductivity Measuring Apparatus for Thermoplastic Materials, M. S. Thesis, Georgia Institute of Technology, Atlanta, 1976.

10. American Society for Testing and Materials, "Standard Method of Test for Thermal Conductivity of Materials by Means of the Guarded Hot Plate", ASTM Standard C-177-71, 1971.

11. Springer, G. S., and J. W. Tsai, "Thermal Conductivities of Unidirectional Materials", Journal of Composite Materials, 1, 1967, p. 166.

12. Behrens, Ernst, "Thermal Conductivities of Composite Materials", Journal of Composite Materials, 2, no. 1, 1968, p. 2.

13. Lord Rayleigh, "On the Influence of Obstacles Arranged in Rectangular Order upon the Properties of a Medium", Philosophical Magazine, 34, 1892, p. 481.

14. Meredith, Robert E., and Charles W. Tobias, "Resistance to Potential Flow through a Cubic Array of Spheres", Journal of Applied Physics, 31, no. 2, 1960, p. 1270.

15. Maxwell, J. C., A Treatise on Electricity and Magnetism, 2nd ed., 1, Oxford, The Clarendon Press, 1881.

16. Garrett, K. W., and H. M. Rosenburg, "The Thermal Conductivity of Epoxy Resin/Powder Composite Materials", Journal of Physics: D Applied Physics, 7, 1974, p. 1247.

17. Kingery, W. D., "Thermal Conductivity: XIV, Conductivity of Multicomponent Systems", Journal of the American Ceramic Society, 42, no. 12, 1959, p. 617.

18. Gorring, Robert L., and Stuart W. Churchill, "Thermal Conductivity of Heterogeneous Materials", Chemical Engineering Progress, 57, no. 7, 1961, p. 53.

19. Godbee, H. W., and W. T. Ziegler, "Thermal Conductivities of M_gO, Al_2O_3, and ZrO_2 Powders to 850°C", Journal of Applied Physics, 37, no. 1, 1966, p. 56.

20. Schumann, T. E. W., and V. Voss, "Heat Flow Through Granulated Material", Fuel in Science and Practice, 13, no. 8, p. 249.

21. Fricke, Hugo, "A Mathematical Treatment of the Electric Conductivity and Capacity of Disperse Systems", Physics Review, 24, 1924, p. 575.

22. Duga, Jules J., "Electrical and Thermal Transport Models for Analysis of Reinforced Composites", Battelle Memorial Institute ONR TR No. 1, 1966.

23. Brewer, John W., Control Systems: Analysis, Design, and Simulation, Englewood Cliffs, New Jersey, Prentice-Hall, Inc., 1974.

24. Elonka, Stephen M., and Alonzo R. Parsons, Standard Instrumentation Questions and Answers, 2, New York, McGraw-Hill Book Co., 1962.

25. Webb, C. R., Automatic Control: An Introduction, London, McGraw-Hill Publishing Co., Ltd., 1964.

26. Holzbock, Werner G., Automatic Control: Principles and Practice, New York, Reinhold Publishing Corp., 1958.

27. Murphy, Gordon J., Basic Automatic Control Theory, Princeton, New Jersey, D. Van Nostrand Co., Inc., 1957.

28. Ku, Y. H., Analysis and Control of Linear Systems, Scranton, Pennsylvania, International Textbook Company, 1962.

29. Dorf, R. C., Modern Control Systems, Reading, Massachusetts, Addison-Wesley Publishing Co., 1974.

30. Baumeister, Theodore, ed., Standard Handbook for Mechanical Engineers, New York, McGraw-Hill Book Company, 1967.

31. Thermophysical Properties of Matter, Purdue University, Thermophysical Properties Research Center.

32. Correspondence with Mr. Tamami Kusuda, Chief, Thermal Engineering Section, National Bureau of Standards, June, 1977.

33. Lee, H. J., and R. E. Taylor, "Determination of Thermophysical Properties of Layered Composites by Flash Method", Proceedings of the 14th International Conference on Thermal Conductivity, (Thermal Conductivity 14, Klemens and Chu, ed.,) New York, Plenum Press, 1976.

34. Harper, C. A., ed., Handbook of Plastics and Elastomers, New York, McGraw-Hill Book Company.